

DYNAMICS ON COMPLEX NETWORKS WITH
APPLICATION TO POWER GRIDS

by

SAKSHI PAHWA

B.E., University of Mumbai, India, 2007

M.S., Kansas State University, 2010

AN ABSTRACT OF A DISSERTATION

submitted in partial fulfillment of the
requirements for the degree

DOCTOR OF PHILOSOPHY

Department of Electrical and Computer Engineering
College of Engineering

KANSAS STATE UNIVERSITY

Manhattan, Kansas

2013

Abstract

The science of complex networks has significantly advanced in the last decade and has provided valuable insights into the properties of real world systems by evaluating their structure and construction. Several phenomena occurring in real technological and social systems can be studied, evaluated, quantified, and remedied with the help of network science. The electric power grid is one such real technological system that can be studied through the science of complex networks. The electric grid consists of three basic sub-systems: Generation, Transmission, and Distribution. The transmission sub-system is of particular interest in this work because its mesh-like structure offers challenging problems to complex networks researchers. Cascading dynamics of power grids is one of the problems that can be studied through complex networks. The North American Electric Reliability Corporation (NERC) defines a cascading failure as the uncontrolled successive loss of system elements triggered by an incident at any location.

In this dissertation, we primarily discuss the dynamics of cascading failures in the power transmission grid, from a complex networks perspective, and propose possible solutions for mitigating their effects. We evaluate the grid dynamics for two specific scenarios, load growth and random fluctuations in the grid, to study the behavior of the grid under critical conditions. Further, we propose three mitigation strategies for reducing the damage caused by cascading failures. The first strategy is intentional islanding in the power transmission grid. The aim of this method is to intentionally split the grid into two or more separate self-sustaining components such that the initial failure is isolated and the separated components can function independently, with minimum load shedding. The second mitigation strategy involves controlled placement of distributed generation (DG) in the transmission system in order to enhance robustness of the grid. The third strategy requires the addition of a link in

the transmission grid by reduction of the average spectral distance, utilizing the Y_{bus} matrix of the grid and a novel algorithm.

Through this dissertation, we aim to successfully cover the gap present in the complex networks domain, with respect to the vulnerability analysis of power grid networks.

DYNAMICS ON COMPLEX NETWORKS WITH
APPLICATIONS TO POWER GRIDS

by

SAKSHI PAHWA

B.E., University of Mumbai, India, 2007

M.S., Kansas State University, 2010

A DISSERTATION

submitted in partial fulfillment of the
requirements for the degree

DOCTOR OF PHILOSOPHY

Department of Electrical and Computer Engineering
College of Engineering

KANSAS STATE UNIVERSITY

Manhattan, Kansas

2013

Approved by:

Major Professor
Caterina Scoglio

Copyright

Sakshi Pahwa

2013

Abstract

The science of complex networks has significantly advanced in the last decade and has provided valuable insights into the properties of real world systems by evaluating their structure and construction. Several phenomena occurring in real technological and social systems can be studied, evaluated, quantified, and remedied with the help of network science. The electric power grid is one such real technological system that can be studied through the science of complex networks. The electric grid consists of three basic sub-systems: Generation, Transmission, and Distribution. The transmission sub-system is of particular interest in this work because its mesh-like structure offers challenging problems to complex networks researchers. Cascading dynamics of power grids is one of the problems that can be studied through complex networks. The North American Electric Reliability Corporation (NERC) defines a cascading failure as the uncontrolled successive loss of system elements triggered by an incident at any location.

In this dissertation, we primarily discuss the dynamics of cascading failures in the power transmission grid, from a complex networks perspective, and propose possible solutions for mitigating their effects. We evaluate the grid dynamics for two specific scenarios, load growth and random fluctuations in the grid, to study the behavior of the grid under critical conditions. Further, we propose three mitigation strategies for reducing the damage caused by cascading failures. The first strategy is intentional islanding in the power transmission grid. The aim of this method is to intentionally split the grid into two or more separate self-sustaining components such that the initial failure is isolated and the separated components can function independently, with minimum load shedding. The second mitigation strategy involves controlled placement of distributed generation (DG) in the transmission system in order to enhance robustness of the grid. The third strategy requires the addition of a link in

the transmission grid by reduction of the average spectral distance, utilizing the Y_{bus} matrix of the grid and a novel algorithm.

Through this dissertation, we aim to successfully cover the gap present in the complex networks domain, with respect to the vulnerability analysis of power grid networks.

Table of Contents

Table of Contents	viii
List of Figures	xi
List of Tables	xiii
Acknowledgements	xv
Dedication	xvi
Preface	xviii
1 Introduction	1
1.1 Background	2
1.2 Motivation	2
1.3 Contribution	4
1.4 Organization	8
2 Literature Review	10
2.1 Overview	10
2.2 Vulnerability Analysis	12
2.3 Mitigation Strategies	15
2.4 Vulnerability Indices or Robustness Metrics	16
2.5 Interconnected Networks and Grid of the Future	19
3 Dynamics of Cascading Failures in Power Transmission Grids	22
3.1 Introduction and Related Work	22
3.2 Model	24
3.3 Cascading Failures in Power Grids	26
3.3.1 Effect of Load Growth on the Dynamics of the Power Grid	26
3.3.2 Effect of Random Fluctuations on the Dynamics of the Power Grid	29
3.3.3 Effects of load growth and random fluctuations on large networks - Polish grid	32
3.4 Discussion	35
4 Mitigation Strategies - Intentional Islanding	38
4.1 Introduction	38
4.2 Related Work	40

4.3	Optimal Intentional Islanding	42
4.4	Complex Networks based Methods for Islanding	43
4.4.1	Islanding using Modified Fast Greedy Method	44
4.4.2	Islanding using Modified Bloom Method	45
4.5	Results and Comparison of the Different Methods of Intentional Islanding	47
4.5.1	Island Characterization - Modified Fast Greedy and Modified Bloom Methods	54
4.6	Discussion	55
5	Mitigation Strategies - Controlled Distributed Generator Placement in Transmission Grid based on Electrical Measures	57
5.1	Introduction	57
5.2	Related Work	58
5.3	Topological and Electrical Structure of Power Grids	59
5.3.1	Electrical Centrality	60
5.3.2	Electrical Node Significance	65
5.3.3	Method for Placement of DG in the Transmission System	65
5.4	Comparison with Method II	69
5.5	Results	70
5.6	Discussion	82
6	Mitigation Strategies - Addition of a Link in the Transmission Grid based on Spectral Distance Method	83
6.1	Introduction	83
6.2	Related Work	84
6.3	Y_{bus} matrix and Laplacian	86
6.4	Procedure to Find the Location of the New Link	88
6.5	Results	89
6.6	Discussion	100
7	Conclusions and Future Work	104
7.1	Conclusions	104
7.2	Future Work	107
	Bibliography	124
A	Power Flow Models	125
A.1	AC Power Flow Model	125
A.2	DC Power Flow Model	126
B	Optimal Islanding Algorithm	128
B.1	Given:	128
B.2	Objective function:	129
B.3	To Find:	129

B.4	Constraints:	129
B.4.1	Topological constraints	129
B.4.2	Power flow model constraints	132
C	Algorithms for Modularity Based Islanding Methods - Modified Fast Greedy and Modified Bloom	134

List of Figures

1.1	A block schematic of an electrical network	3
1.2	A complex networks representation of an electrical network	3
3.1	Effect of load growth on the IEEE grids	27
3.2	Effect of load growth on the synthetic networks.	30
3.3	Effect of random fluctuations on IEEE grids	33
3.4	Effect of random fluctuations on synthetic networks	34
3.5	Effect of load growth and random fluctuations on the 2746-node Polish grid .	36
4.1	An example of intentional islanding on a small test network	40
4.2	Optimal islanding for the 14-node network	48
4.3	Optimal islanding solution for the 30-node network	50
4.4	The 5-island scenario for the 30-node system using the three methods	51
4.5	The 6-island scenario for the 118-node network using modified Bloom method	53
4.6	The 6-island scenario for the 118-node network using modified Fast Greedy method	53
5.1	Physical structure of the 57-node network	61
5.2	Electrical structure of the 57-node network	62
5.3	Physical structure of the 118-node network	63
5.4	Electrical structure of the 118-node network	64
5.5	Electrical node significance for the 57-node network	66
5.6	Electrical node significance for the 118-node network	67
5.7	Vulnerability analysis of 57-node network without DG	71
5.8	Vulnerability analysis of 57-node network with DGs placed using electrical centrality and electrical node significance	72
5.9	Vulnerability analysis of 57-node network with DGs placed using Method II .	73
5.10	Histogram showing the distribution of links (initial failure) for 57-node net- work in different load ranges without DG	74
5.11	Histogram showing the distribution of links (initial failure) for 57-node net- work in different load ranges with DG using electrical measures	75
5.12	Histogram showing the distribution of links (initial failure) for 57-node net- work in different load ranges with DG using Method II	76
5.13	Vulnerability analysis of 118-node network without DGs	78
5.14	Vulnerability analysis of 118-node network with DGs placed using electrical measures	79
5.15	Histogram showing the distribution of links (initial failure) for 118-node net- work in different load ranges without DG	80

5.16	Histogram showing the distribution of links (initial failure) for 118-node network in different load ranges with DG using electrical measures	81
6.1	Location of the additional link on the physical topology of the 57-node network	91
6.2	Location of the additional link on the physical topology of the 118-node network	92
6.3	Vulnerability analysis of the 118-node network without the additional link .	94
6.4	Vulnerability analysis of the 118-node network with link addition by spectral distance method	95
6.5	Vulnerability analysis of the 118-node network with link addition by algebraic connectivity method	96
6.6	Histogram showing the distribution of links (initial failure) for 118-node network in different load ranges without additional link	97
6.7	Histogram showing the distribution of links (initial failure) for 118-node network in different load ranges with addition of link using Spectral Distance Method	98
6.8	Histogram showing the distribution of links (initial failure) for 118-node network in different load ranges with addition of link using Algebraic Connectivity Method	99
6.9	Vulnerability analysis of the original and new 118-node networks, considering failure of a single link (link 20)	101
6.10	Vulnerability analysis of the original and new 118-node networks, considering failure of a single link (link 113)	102

List of Tables

3.1	Average value of α_c for the synthetic networks	29
4.1	Average percentage per island of total load remaining in the 14-node system by optimization and the two modularity approaches for 2 islands	48
4.2	Average percentage per island of total load remaining in the 30-node system by optimization and the two modularity approaches for 5 islands	49
4.3	Average percentage per island of total load remaining in the 57-node system by the two modularity approaches for 2 islands	51
4.4	Average percentage per island of total load remaining in the 118-node system by the two modularity approaches for different number of islands	52
4.5	Average percentage per island of total load remaining in the 247-node system by the two modularity approaches for different number of islands	52
4.6	Characteristics of islands created by modified Fast Greedy method for the 118-node network	54
4.7	Characteristics of islands created by modified Bloom method for the 118-node network	54
5.1	Comparison of the results of vulnerability assessment of the 57-node network without DGs, with DGs based on electrical measures, and with DGs based on Method II	77
5.2	Comparison of the results of vulnerability assessment of the 118-node network without DGs, and with DG placement based on electrical measures	77
6.1	Characteristics of the 57-node network before and after the addition of long link	93
6.2	Characteristics of the 118-node network before and after the addition of long link	94
6.3	Average load remaining on the 57- and 118-node network (in %) by link addition based on different methods	100

Acknowledgments

I would like to express my deepest gratitude towards Dr. Caterina Scoglio, who has not only been the major advisor for my PhD, but has also been a mentor, guide, friend, and confidante along the way. She has always celebrated success and has been encouraging in difficulties times. She has truly supported me in the ups and down of life as a PhD student and has helped me develop an individual thought process.

I would like to thank my other committee members, Dr. Noel Schulz, Dr. Ruth Miller, and Dr. Antonio Scala, who have made major contributions to the completion of this dissertation. Dr. Schulz has played an important role in my professional development by opening up a plethora of opportunities for me to be a part of and give my contributions to. Dr. Ruth Miller's persistence and demand for perfection kept pushing me to do better. Her patience helped me to keep the pressure away and yet enabled me to achieve my goals. Dr. Scala's research guidance during my visit to his university in Rome, and collaboration with him on research projects opened up new aspects of research before me.

I would like to especially thank Dr. Bruce Law, who agreed to be the external chair for my defense. Also, special thanks to Tamara Robinson, the technical editor for the Engineering Research and Graduate Programs, for providing valuable suggestions to help me improve the quality of my dissertation.

Sunflower Networking Group (SNG) has been an important part of my life in the United States. I can never forget the impact on my professional and personal life by all the past and present members of SNG: Mina Youssef, Yunzhao Li, Ali Sydney, Phillip Schumm (and his family), Ling Xue, Faryad Darabi Sahneh, and all the others. I have made friends for life in this wonderful research group.

Faculty and staff of Electrical and Computer Engineering, especially, Dr. Gruenbacher, Dr. Rys, and Dr. Morcos, have been helpful, encouraging, and supportive all these years. I would also like to thank the Electrical Power Affiliates Program (EPAP), Department of

Energy (DOE), and the Department of Electrical and Computer Engineering (ECE), for providing financial support during the course of my graduate studies.

I would like to extend special thanks to all my family, friends, and well-wishers in India, Manhattan, other parts of Kansas, Tennessee, and in the other parts of the United States, for the wonderful support and encouragement that they have always provided. I cannot be thankful enough to my Art of Living family in Kansas and beyond.

My love and thankfulness to Mrs. Mukta Pahwa and Dr. Anil Pahwa, better known to me as Mukta aunty and Anil uncle, and their sons (my cousins), Samir and Mrinal. I have been very lucky to have a family and home away from home. My transition to a new place and culture was very easy because of the love and care provided by my family here.

Last, but not the least, I would like to express my deepest gratitude to my loving parents, Mrs. Priti Pahwa and Mr. Sunil Pahwa, and my younger brother, Saksham Pahwa, who encouraged me to dream and to find ways to realize the dream. They have been by my side in all situations, in spite of the great physical distance between us. It will be an extremely proud moment for them to see this dissertation.

Dedication

To my loving parents, Mrs. Priti Pahwa and Mr. Sunil Pahwa.
Mummy and papa, this dissertation would not have been possible
without your support, love, and care.

Preface

This dissertation is submitted as a requirement for the degree of Doctor of Philosophy in the Department of Electrical and Computer Engineering at Kansas State University. The dissertation is entitled “Dynamics of Complex Networks with Applications to Power Grids”, and the research has been performed under the supervision and guidance of Prof. Caterina Scoglio.

The following list of published and submitted journal articles and the book chapter describe, in short, all the research work used for this dissertation:

Book Chapter

Pahwa, S., Youssef, M., and Scoglio, C., **Electrical Networks - An Introduction**, Network of Networks, Springer Publications, 2013. In Print.

Journal articles

Published:

- Pahwa, S., Youssef, M., Schumm, P., Scoglio, C., and Schulz, N., **Optimal Intentional Islanding to Improve the Robustness of Power Grid Networks**, Physica A, Vol. 392, no. 17, pp. 3741-3754, 2013.
- Pahwa, S., Scoglio, C., Das, S., and Schulz, N., **Load Shedding Strategies for Preventing Cascading Failures in Power Grid**, Electric Power Components and Systems, Vol. 41, no. 9, pp. 879-895, 2013.
- Scala, A., Pahwa, S., and Scoglio, C., **Cascade failures from distributed generation in power grids**, International Journal of Critical Infrastructure, 2013. In Production.

Submitted:

- Pahwa, S., Scoglio, C., and Scala, A., **Abruptness of Cascade Failures in Power Grids.**
- Manzano, M., Calle, E., Ripoll, J., Manolova Fagertun, A., Torres-Padrosa, V., and Pahwa, S., **Epidemic and Cascading Survivability of Complex Networks.**

In Preparation:

- Pahwa, S., Scoglio, C., **Improving the Robustness of the Power Grid Network by Addition of a Link using Spectral Methods.**
- Pahwa, S., Scoglio, C., **Placement of Distributed Generation using Electrical Measures to Improve the Robustness of Power Grid Networks.**

This dissertation primarily focuses on cascading failures in the power grid network and strategies to mitigate the effects of such disturbances to the network, from the perspective of complex networks. This dissertation is a contribution to the complex networks community and the researchers in this community working on general complex networks, other critical infrastructure, or the power grid specifically.

Since August 2010, this research has been supported by grants from various sources. A portion of the work has been supported by the Electrical Power Affiliates Program (EPAP), originally comprised of Burns & McDonnell, Westar Energy, Nebraska Public Power District (NPPD), and Omaha Public Power District (OPPD). A majority of this work has been supported by the Department of Energy through two individual grants - “Resourceful Kansas DE-EE0003812” and “Kansas Wind Consortium DE-EE0000555”

The results and conclusions obtained through these publications and dissertation are the views of the authors and do not necessarily reflect the opinions of the sponsoring sources.

Chapter 1

Introduction

In the times of the early man, fire obtained by rubbing flint stones together was the only source of heat and light. Life was simple because only basic needs such as food, clothing, and shelter needed to be fulfilled. In the 18th century, electricity was invented and life completely changed. Many years have passed and the modern day world of morning coffee, cell phones, and air conditioners is now a reality. Not a day goes by in which a TV, computer, or music player is not utilized. Electricity has become so commonplace and necessary that it is often taken for granted, until it is no longer available because of a disruption. In this dissertation, we extend the science of complex networks to a real-world system - the power grid. The power grid is one of the greatest man-made engineering wonders. However, most of the times we fail to realize what goes on in the background when we turn on our devices, and the long distances traversed by the electricity to reach our homes and offices, as and when demanded. The stress on the grid keeps increasing with the ever increasing number of devices operating on electricity, introduction of new kinds of generation sources, and so on.

Few theories about the different dynamic effects of the power grid have been proposed in the past. Through this dissertation, we bring forth, not only a few other challenges that the modern electric grid faces, but also some methods by which a small change in the infrastructure can go a long way to strengthen the grid.

1.1 Background

A world without electricity is beyond our imagination. Starting from the prehistoric times, man has made much progress in every walk of life. We have become accustomed to getting everything at the flick of a switch, touch of a button, or turn of a knob. While we have become so used to enjoying the benefits of electricity, it is not easy to imagine how electricity travels from its source to our homes and offices. It sometimes has to cover large distances through a complex network of transmission lines and power substations to provide us the facilities and entertainment that we take for granted. This network which transports electricity from the source to the consumers is called the electrical network. The electrical network is a collective term for different components such as transformers, transmission lines, substations, and different stages and sub-networks devoted to generation, transmission, and distribution. Sometimes, there may be sub-transmission and secondary distribution networks too. A simple schematic of an electric network is shown in Figure 1.1. In the past decade, analysis of the electrical power system as a complex network has been evolving as a challenging topic of research. A power grid can be represented as a network of buses connected to each other by transmission lines. The flow dynamics of the network accounts for the power flow through the electrical grid. The Figure 1.2 shows a complex networks representation of a power grid through nodes and links. The generators, loads, as well as the other buses are all represented as homogeneous nodes in this picture. However, they can be distinguished from each other depending on the type of analysis.

1.2 Motivation

Critical infrastructure, in general, refers to the assets that an economy and a society cannot function without. The electrical power grid is one such asset. Our dependence on electricity has increased so much, that even small periods of absence of electricity can cause a huge chaos. The aging grid is not just handling excessive stress in the modern years, but also a threat of attacks. As a result, it becomes necessary to study the dynamics occurring in the

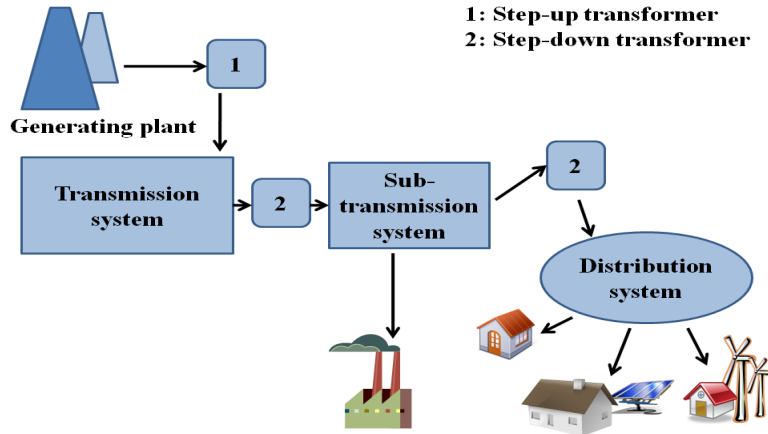


Figure 1.1: This figure shows a simple block schematic of an electrical network. The electrical network is generally divided into three sub-networks: Generation, Transmission, and Distribution. Additionally, sub-transmission and secondary distribution systems may be present. The transmission system operates at the highest voltage. The sub-transmission operates on medium voltage levels, while the distribution system operates on low voltage.

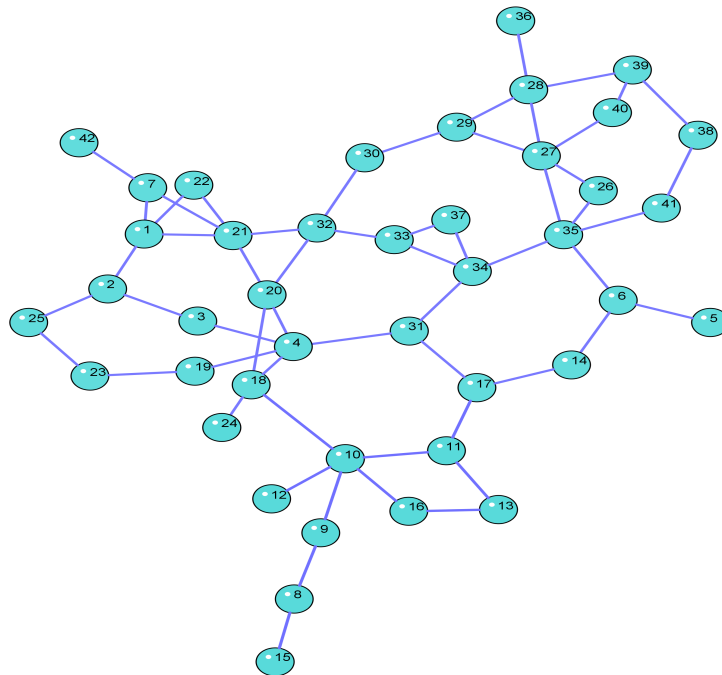


Figure 1.2: The picture shows the modeling of an electrical grid as a complex network. The buses are represented as nodes, and the transmission lines as the links connecting these nodes. The picture typically depicts a transmission system, with a mesh-like structure.

power grid due to the modern practices, and find a solution to the problem before it turns into a crisis.

While power system researchers are working their way towards the upgrading and safety of the grid, the research on power grid is an interdisciplinary problem, crossing over several disciplines. The structure of the network of transmission lines and buses stores a huge amount of useful information that can be unraveled and used for the benefit of the society through the science of complex networks. It is with this goal that we have modeled the power grid as a complex network, in this work, to analyze the dynamics of the grid from a networks perspective, and suggest some strategies that can help to strengthen the grid. In this dissertation, we have mainly focused on the cascading phenomenon of the grids through simple models and used techniques from the network science domain to suggest methods to mitigate such disturbances. According to the most recently approved definitions by the North American Electric Reliability Corporation (NERC)⁹³, a cascading failure is the uncontrolled successive loss of system elements triggered by an incident at any location, and results in widespread electric service interruption that cannot be restrained from spreading beyond an area predetermined by studies. Blackouts resulting from a cascading failure can cause inconvenience to customers and financial losses to the electric utilities. Cascading failures can occur due to several reasons or combination of reasons, such as excessive demand on the system, weather conditions, or human error. It is not only important to study the cause and effect of cascading failures, but also ways to mitigate them. As a result, this dissertation is mainly directed towards examining the causes of cascading failures through a simulative approach, and proposing small structural changes through which the grid can regain the capability to handle increasing stress.

1.3 Contribution

This dissertation is primarily focused on the power transmission grid. The transmission grid has a mesh-like structure, and hence presents very interesting challenges to the complex

networks researchers. One of the things that we study in this work is the dynamics of the power transmission grid under two different scenarios, load growth, and presence of random load fluctuations, and how these scenarios affect the normal functioning of the grid. These scenarios show interesting results pertaining to the complex dynamics of the power grid network. The load growth scenario indicates the presence of a threshold phenomenon, while the random load fluctuations show smoother transition. The results also indicate that the fragility of the network may increase with increasing size. However, as mentioned, the power grid is an extremely complex system and several different scenarios must be tested to get a deeper insight into the dynamics of power grids.

Considering the ever increasing demand and the changes coming in the electrical power grid, it is very important to find solutions to the existing problems, that will be on par with the current, as well as the future status of the grid. With this consideration, we propose three mitigation strategies for cascading failures in power grids.

The first strategy is based on intentional islanding in the transmission grid, to separate the grid into self-sustaining parts, so that an initial failure, which could lead to a cascade of overload failures, is isolated from the remaining part of the grid. We propose two methods for intentional islanding, derived from a complex networks based quality function called modularity. Modularity has been widely used in social and other networks for community detection. We have chosen two popular modularity based algorithms, called the Fast Greedy algorithm, and the Bloom algorithm, out of the many available algorithms because these two methods have given promising results for the other kinds of complex networks that they have been used for. In this work, we have have modified these modularity based algorithms to include a power flow model and a load shedding model, in order to make them suitable for a power grid network. The results of islanding obtained by these two methods are then compared with an optimal islanding scheme and we find that these strategies provide a good balance between the complexity of the algorithm and the accuracy of the results. The accuracy of the results is tested by comparing the amount of load shedding performed by each

method whenever an islanding scenario occurred, with the optimal load shedding scenario. The intentional islanding using Modified Fast Greedy and Modified Bloom methods have been performed on the IEEE 14-, 30-, 57-, 118-, and 300-node systems³¹. The optimal islanding method has high complexity and can be used only for the 14-node and the 30-node network. However, the other two algorithms can solve the islanding problem for networks up to thousands of nodes in a matter of few seconds or minutes, depending on the network size. Moreover, Modified Bloom algorithm is faster in execution than Modified Fast Greedy and also causes less load shedding than Modified Fast Greedy during island creation. We also compare the two algorithms, in terms of execution time and load shedding for different number of islands. Modified Bloom performs better for all cases, but the best number of islands for different networks is different for the two algorithms. These algorithms are described in detail in Appendix C.

The second mitigation strategy discusses the controlled placement of distributed generators in the transmission grid as a way to enhance the robustness of the grid. In this work, distributed generators refer to conventional sources. The presence of distributed generators allows power to be supplied to the nodes locally or through shorter distances. Also, presence of several small generators in the system allows power to be supplied to loads by more than one sources, thus reducing the risk of leaving a few nodes without power in case of a generator failure. The determination of correct locations for the placement of DG is crucial to achieve the the best benefit of the strategy, in terms of load retention in the grid in case of a failure. Improper placement in incorrect amount can actually have an opposite effect on the robustness of the grid, making it more vulnerable. We used two electrical measures to determine the location of DG - electrical centrality and electrical node significance. These measures are used together to determine the set of candidate locations for the placement of DG. The amount of DG that must be placed in the selected nodes from the candidate set depends on the relative significance of the node, and is done exhaustively. Vulnerability analysis is performed before and after DG placement, and the results prove that correct

placement of DG can really help improve the robustness of the power grid network. We used the IEEE 30-, 57-, and 118-node networks for the analysis. The 14-node network is too small of a test system and is not flexible enough to test the above mentioned technique. We also compare our results of vulnerability analysis with that of another method for DG placement, recently proposed in literature. We find that the results obtained by our method improve the robustness of the grid much more than the other method.

The third mitigation strategy considers the strategic addition of a link in the transmission network, using a spectral method. The spectrum of a graph, or in this case, network, holds important information about the characteristics of the network. We utilized this information to determine the location of an additional link. The presence of an additional long link can provide a new path for connecting the distant nodes in the network and new routes for redirecting the power flow, if required. We call our method the spectral distance method and utilize the eigenvectors corresponding to the second, third, and fourth smallest eigenvalues of the Y_{bus} matrix of the power grid to compute the spectral distance between all pairs of nodes in the network. The computation of spectral distances gives an indication of the nodes that are spectrally distant from most other nodes. Using this information, the location of the link is selected. This is done based on a method that we describe in Chapter 6. We perform vulnerability analysis of the system before and after placement of the link, and the results clearly show an improvement in the robustness of the network in terms of load retention in the network after the failure. We compare our results with a popular method in the complex networks, known as algebraic connectivity method, and find that the results by the spectral distance method are better than those obtained by the algebraic connectivity method. We also test several cases of random link addition and conclude that our method provides a substantial enhancement in robustness of the grid. We, finally, compare the characteristics of the networks, such as characteristic path length, diameter, clustering coefficient, and average degree, before and after link placement to test if changes in the spectral characteristics have an effect on the physical characteristics, and

find that structural changes do occur in some cases. This method was tested on the IEEE 30-, 57-, and 118-node networks.

Although we have not used optimization strategies for the above methods, these methods provide substantial improvement in the robustness of the grid, and are also low in complexity. The results obtained by all the above methods clearly show an improvement in the robustness of the system than without any strategy, and hence they show the merit of the strategies.

1.4 Organization

The dissertation is organized as follows:

In Chapter 2, we give, in detail, a review of the work previously done in the vulnerability analysis of power grids from a complex networks perspective, the details that are missing in these previous studies, and how the inclusion of these missing details would make them much more useful in the vulnerability analysis of power grids. It is these gaps in the literature that have motivated us to continue the work done by previous researchers and present the results in the form of this dissertation.

The first part of this dissertation - dynamics on power transmission grids with respect to cascading failures - has been discussed in Chapter 3. In this chapter, we show, through simulative analysis, how the grid dynamics are affected, using two different scenarios. We discuss the different mitigation methods Chapter 4 onwards. In Chapter 4, we propose two intentional islanding methods as a way to enhance the robustness of the grid. These are complex networks based methods, using the quality function called modularity, to partition the grid into islands. We compare the results of the islands obtained by these methods, with an MILP based optimal islanding scheme. In Chapter 5, we discuss the controlled placement of DG in the transmission grid, based on two electrical measures: electrical centrality and electrical node significance. The results of this work have been compared with another complex networks based methods, recently proposed in literature, and the vulnerability

analysis before and after placement of DGs is performed. Chapter 6 discusses the method to place an additional long link in the transmission system, followed by vulnerability analysis of the grid, to show that the addition of the link indeed improves the robustness of the grid. Conclusions, and scope for future work are finally discussed in Chapter 7.

Chapter 2

Literature Review

The electrical network has been introduced in Chapter 1. In this chapter, the electrical grid as a complex network will be discussed in more detail, starting with an overview, followed by the development of this field of study, the relevance of these studies with respect to the scope of the dissertation, and the improvements in the methods discussed in the dissertation, as compared to the previous work.

2.1 Overview

As mentioned in the previous chapter, a general electrical network consists of three main parts: Generation, Transmission, and Distribution. The aim of the electrical network is to transport electricity from the source to the consumers. The transmission sub-system is the backbone of the complete electrical network and connects all the main load centers in the system to the main generating plants, while operating at the highest voltage level. Sometimes, there is no clear distinction between the transmission and sub-transmission networks and sometimes they are distinctly separated from each other. The generation and transmission sub-systems together constitute the bulk power system. The distribution sub-system consists of the final stage of power transfer to the individual consumers⁷⁰.

The transmission sub-system has been the most studied of the sub-networks of the electrical network. The mesh structure of the transmission network makes it particularly interesting to study different problems on this network. The distribution sub-network usu-

ally has simple topologies such as a tree or a ring. Most radial networks are meshed networks initially. However, for a better analysis of their protection schemes and losses, they are always represented and analyzed as an equivalent radial or ring network¹¹⁵.

All real systems can be modeled into graphs with the individual entities of the system as the nodes and the connections between these entities as the links. The types of connections help us to classify these graphs as random, scale-free, hybrid, or some other kind of topology. When dynamics are considered on these graphs, either on nodes or links, they are referred to as networks. It is the particular dynamic and the models considered for the analysis of these dynamics which distinguish different networks from each other. The study of power grid as a complex network started a little before the beginning of the last decade, and gained more importance and momentum after the North American blackout of 2003⁴⁶ and other European blackouts that followed in the same year^{73, 65, 35}. A basic electrical network can be regarded as a connection of buses through transmission lines, where every bus carries a load or demand that must be satisfied by the power flowing through these lines. Every electrical network must follow the basic laws of Physics called the Kirchoff's equations. These are equalities that deal with the conservation of charge and energy in electrical circuits.

Most of the complex network analysis has been carried out on high voltage transmission grids because their structure is mesh-like and it projects a complexity that is very interesting in the study of different characteristics of electrical networks. In general, power grid networks tend to be sparse networks, as indicated by the IEEE power grid data available at³¹. The average node degree of the transmission grid is small. There is a common agreement among the researchers that the average degree of the transmission grid is between 2.5 and 5 (for both, American and European grids). It is important to note, from a security point of view, that a power grid should not have topological hubs. There are some nodes which are "critical" since they carry a high load, yet their degree is not large relative to the size of the grid.

Every node in the electrical network is characterized by a finite capacity, described

by the maximum load that the node can carry. Similarly, every link is characterized by a capacity which indicates the maximum amount of power flow that the link can carry, without overheating or melting. The capacity of the link is one of the factors governing the flow of power on the link. It is important to incorporate the flow dynamics into the topological model of the electrical network through power flow models. A simple approximation of the complete AC power flow model is the linearized DC model⁴⁹. The set of equations of this model not only incorporate the Kirchoff's laws but also give a rule for the flow of power through each link based on its reactance and the phase angles of the nodes at the two ends of the link. The model is discussed in detail in Appendix A.

This field has constantly evolved and continues to evolve. There are many more challenges that the electrical network of the future offers and the answers are hidden, at least partly, in the structure and design of the networks. The field of complex networks has a big responsibility of understanding these challenges and bringing forth the answers.

2.2 Vulnerability Analysis

Much work has been done in the area of robustness studies of electrical networks, considering the increasing occurrences of power grid blackouts all over the world, in the last decade. Cascading failures used to be a rare phenomenon, but with the unprecedented dependence on the electricity infrastructure, bad practices, and the lack of restructuring of the system, it is now becoming an occurrence that can be heard of several times a year^{46, 102, 32, 12, 45, 92, 76, 133, 91, 57, 68, 130, 33}. Many times, these cascading failures are triggered by small local disturbances which spread throughout the network due to the complex flow dynamics of the electrical system.

At the very beginning, a study of the cascade spread models, as adapted to power grids was emerging. One of the first studies in this area was presented in¹¹⁰, in which a very simple model for spread of disturbances in power transmission grid was proposed. This model considered a network of nodes, each representing a power generation or transmission

element and the connections between these nodes were not transmission lines, but coupling between the nodes, which was a way to simulate the circuit equations in a real power network. Every node was characterized by a load and a threshold of the load that it could handle. Whenever a node reached its load threshold, load was randomly transferred to the neighboring nodes. The power grid networks considered for evaluation were either well-defined simple ring networks or ring-like structures with some randomness to add a paradigm of complexity as compared to the simple ring structures. The ring-type random power grid networks considered in this work were characterized by their path lengths and clustering co-efficient.

Another model, known as the “capacity” model, was proposed in⁸⁴ and was supposedly the first “dynamic” model suggested for the power grid. This model considered the flow of a quantity between two nodes through a shortest path and the load on a node was the total number of shortest paths through that node, or in other words, the betweenness of the node, as mentioned in⁶¹. The capacity of the node was the maximum load it could handle and it was assigned to each node in proportion to the initial load carried by the node. If there was an overload failure in a node, there was a load redistribution among the neighboring nodes of the failed node, or in other words, the redistribution of the shortest paths in the neighboring nodes. The results indicated that this redistribution can lead to a cascade of overload failures in networks with a heterogeneous distribution of loads.

In the “efficiency” model for dynamic complex networks, presented in³⁸, the focus was also on cascades caused by overloading of nodes and the subsequent redistribution of the flow on the network but this model was different from the other models because it did not remove the overloaded nodes from the network but simply reduced the efficiency of the flow through this node. As a result, it caused a redistribution of flows through other nodes, indirectly redistributing the shortest paths and the damage to the network was quantified as the decrease in global efficiency, as described in⁷⁴. This work mentioned that the degree distribution of an electrical power grid is exponential but it is heterogeneous in

the distribution of loads in the network.

The same model has also been used, specifically for the Italian electric power grid in³⁹ with the result that the grid is very vulnerable to those failures that occur on the nodes with the highest betweenness. This model distinguished between the nodes as generators and distribution stations, similar to⁷ in which the structural vulnerabilities of the North American power grid were evaluated. The authors of this work also agree with⁹ in noting that the degree distribution of the North American grid, similar to the Western power grid, is exponential. It is a single-scale network and there is a cost involved with addition of each edge. They also showed the vulnerability of the North American grid based on the edge range approach, discussed in⁸⁵, which was one of the first few works to consider attacks on links. They further go on to discuss a connectivity loss measure to find the number of generator nodes that are connected to any given substation node. The authors of¹⁰¹ formulate a bi-level mixed integer nonlinear programming problem to identify the small groups of lines, which if removed, can cause a severe blackout.

In⁶², two real power grid networks, the Nordic grid and the Western States US grid have been studied, their topological characteristics with respect to cascading failures have been compared and these results are further compared with networks from two theoretical models, the Erdos-Renyi random network model⁴² and the Barabasi-Albert scale-free network model¹⁶. These comparisons show clearly the similarities and differences of the two real power grids with respect to the theoretical models, as well as with respect to each other. Some important topological characteristics of the two real grids are highlighted in this study. The robustness of the European power grids under intentional attack has been tested in¹¹⁴ by selective node removal process. A mean field analysis of the fragility is also presented.

In²⁴, the authors have presented an initial evidence of the electrical network possessing a self-organized criticality and have studied the global dynamics related to the cascading failures using time-series correlation data of power system blackout sizes. Two types of

transitions in the cascading failure blackouts were suggested in²². They show that the probability distribution of the blackout size of the North American blackout data has a power tail. This work was followed up in²⁵, where it was established that the power system is indeed a self-organized critical system. The total number of transmission lines tripped and the total amount of load shed were the measures used to quantify the size of the cascade in⁶⁷. Load shed is the amount of load intentionally removed from the system to bring the system back to a stable state from the disturbed state. When there are failures, especially those which lead to the loss of the system elements causing a large redistribution of load, load shedding becomes necessary to curtail the excess load in the disturbed system, which can be restored after system stability is achieved. Load shedding, although a last resort measure, can be useful to prevent a total blackout of the system. In the above work, the authors use a Galton-Watson branching process to approximate the cascading process of load shed in blackouts.

2.3 Mitigation Strategies

Proposing mitigation strategies for preventing the spread of cascades has become the need of the hour and is a way to suggest solutions to the problem at hand. The work in⁸³ discusses a method to reduce the size of a cascade in complex networks with a heterogeneous degree distribution, after the initial failure has taken place, but before it begins to spread throughout the network. This method has been applied to the electric power network and involves making costless modifications to the network in a time less than that would take the initial failure to spread. It talks about strategies for intentional removal of nodes or links that would significantly reduce the size of cascades.

The probabilistic hidden failure model, which throws light on the protective system failures, was proposed in¹¹⁷. Hidden failures in the elements of protection systems were considered to be one of the leading causes of cascading failures in electrical power grids, after the 1996 blackout of the Western grid of the United States. More work on such

reliability study was undertaken soon after, as seen in^{14, 122}, and²⁸. This hidden failure model was further adopted in blackout propagation and mitigation studies in^{29, 27, 23}. These works included the linearized DC power flow model, to account for the underlying dynamics.

In⁹⁶, three mitigation strategies have been discussed for mitigating cascading failures in power grids. Two of the proposed strategies are load shedding strategies while the third one is intentional islanding using distributed sources. Intentional islanding is the intentional splitting of the power grid into sub-parts with their own generation so that these sub-parts can sustain on their own when separated from the remaining network. In this work, islanding is performed using modularity. If all the islands do not have a generator after the first step of islanding, a second step called super-islanding is performed. A polynomial time optimal load shedding algorithm is presented in¹⁷ to control cascading failures occurring due to deterministic failures. The author also proposes another algorithm for stochastic failures. All these models justify the use of DC power flows for the reason that during emergency situations, a faster and always converging solution is needed, especially if the network size is large.

2.4 Vulnerability Indices or Robustness Metrics

Several metrics and vulnerability indices have been suggested as a way to identify nodes and links which play an important role in the spread of the cascade. A vulnerability index based on identification of vulnerable links by weighted betweenness of the links is proposed in³⁰. The weights on the links are represented by the reactances of the links and the shortest electric distance is represented as the sum of the weights along the shortest electric path, where the shortest electric path between two nodes is the path whose sum of the weights is the smallest among all possible paths between the two nodes. They also do time domain simulations which verify that their vulnerability metric can not only identify the most critical lines in the system but also those lines which may be vulnerable due to their position in the system, even though they are lightly loaded. They tested their results on the IEEE 39-bus

test system and the Huazhong-Chuanyu power grid.

The concept of random-walk betweenness was introduced in⁸⁸ where an example of an electric circuit was used to show the effectiveness of the method. It is based on random walks, counting how often a node is traversed by a random walk between two other nodes. It is a generalized technique that may be used for the analysis of power grid networks.

Attention shifted towards the use of power flow model along with the topological models since it was being realized that all the information about power grids was not being captured by purely topological models, although they provided useful information about the structure of the system. The work in⁵⁸ talks about the electrical centrality measure for power networks considering the electrical topology rather than the physical topology. They mention the use of the standard AC power flow model for this work⁴⁹, without going into the details of the model. The flow propagates through the path of least resistance, and this flow distribution is governed by the relative complex impedance of each path. Also, there can be several paths through which power can flow between two nodes. They use the bus impedance matrix or the inverse of the admittance matrix to define electrical distance between nodes and use this information to represent an electrical topology. They present a conclusion that electrically, the power grid is a scale-free network, although a lot of topological studies indicate a single-scale structure^{7, 9, 87, 8, 106}, while a few show a scale-free structure^{16, 26}. Similar work has been done in¹²⁸, without the use of any power flow model. Other centrality measures, based on not only the topology but also the electrical parameters of the grid are investigated in¹²⁹. “Efficiency” of the network, as mentioned in previous works was replaced by “net-ability” in¹¹. The results obtained using efficiency and net-ability were compared with the reference DC power flow model and net-ability emerged to be a better metric than efficiency. Another metric called “entropic degree” was presented in¹⁸, along with net-ability. These findings were further strengthened by the work presented in⁵⁹, in which the authors use the DC power flow model with the IEEE 300-bus system³¹. The results of this work indicate that although topological models can provide the general vulnerability trend, they may not be

realistic to suggest any risk mitigation resources without the help of physics-based models.

A metric, η , to measure the robustness of a power grid network with respect to cascading failures was discussed in ¹³⁸, based on probability of link survival as well as the average rank of the link. Probability of link survival is calculated as the ratio of the number of times a particular link failed due to the removal of an initial link to the total number of links in the network, while the average link rank is calculated depending on the stage of cascade that the link fails at, considering different initial failures. The average depth of cascade is then the product of the link survival probability and the average link rank and it is used to determine η .

The long-term reliability effects for an electric transmission grid, evolving over time, are explored in ¹⁰⁵. The authors take into account policies such as N-1 criterion as well as direct response policy to quantify the reliability of the evolving transmission grid with respect to cascading line overloads and outages as well as slow load growth. The N-1 policy is the standard policy which ensures the upgrade of the transmission lines to satisfy the requirement that a single outage does not lead to overloading of the other transmission lines. The direct response policy leads to an upgrade of the transmission lines involved in the cascading outage that led to some load-shedding. The authors have compared the long-term effect of these policies on the probability distribution of outage size with different number of contingencies.

An electrical power system can be considered as robust only if it can operate in a state of equilibrium, not just in normal but also in perturbed conditions. This was a possibility until a few years ago, but in the current state of affairs, an upgrade in the electrical infrastructure is definitely called for. The stability study of electrical networks, in general, is a topic of multi-disciplinary research, involving fields like electrical and computer engineering, physics, networks, controls, and others. It depends on many natural and human factors which lead to one or more of the events such as load or generation change, short circuit of transmission lines, which is regarded as a link failure in network theory, and other behavioral changes.

2.5 Interconnected Networks and Grid of the Future

Restructuring the electrical network would be an important step in the planning and design of the future electrical network. However, implementation and operation also need to be changed and this realization has driven us towards the Smart Grid. The Smart Grid would lead to many changes in the current infrastructure of the electrical power system, including heavy incorporation of decentralized distributed generators (DGs), renewable energy resources, energy storage, bidirectional flows, improved communications, higher security, climate change mitigation, an increased degree of interconnections³⁷ and above all, the need for systemic governance.

Interconnections are an inherent part of electrical systems, whether it is the interconnection of several electrical grids or the interconnection of electrical grids with other complex systems such as communication networks. A recent report by the World Energy Council discusses the importance of interconnecting different grids, even across the borders, to fulfill the increasing energy demands of the world³⁶. At the same time, it also talks about the challenges that would be faced for such interconnections. Several approaches to model the interdependence between the telecommunication network and the electrical network are discussed in⁵⁴, including the use of Bayesian networks and “precedence graphs”. A simulative approach has been used to evaluate the interdependence between the communication and power grid networks in⁶⁹ using MPLS. The results show how a fault in the communication network may propagate to the connected power grid and lead to failures in the latter.

As studied in²⁰, interconnected networks behave very differently with respect to failures in comparison to single networks. When there is a failure in one network, the dependent nodes in the other network also fail and this may result in a cascade of failures in the interdependent networks. They study the percolation threshold for interconnected networks which is much larger than that of a single network. This study is continued in⁹⁹ and⁴⁸. In order to understand how interdependence among systems affect the cascading behaviors, the authors in¹⁹ study a sandpile model on modular random graphs as well as graphs based

on interdependent power grids. They show both, the advantages and disadvantages of interdependent systems and conclude that some interdependence is beneficial but too much interdependence opens up new possibilities of cascading failures.

In general, electrical networks usually do not operate in isolation. There is usually some kind of loose tie between the electrical systems owned by different utilities, within a region, a country or even between neighboring countries. Whenever failures take place, there is always a risk that the initial failure that occurred in one part of the interconnected power grid might spread to the other parts. This is what happened in the very recent blackout in India, where the Northern, Eastern, and the North Eastern grids were affected due to the failure that occurred in one location³³. Power grid intentional islanding is gaining a lot of importance as a mitigation strategy for cascading failures in interconnected power grids. However, it is also necessary that the island creation does not lead to further failures in the system and cause excessive load-shedding. Multiple approaches to intentional islanding have been suggested to find the optimal set of lines to be disconnected, including modularity, mixed-integer non-linear programming, spectral matrix methods, simulated annealing, slow-coherency based methods and many others^{96, 44, 118, 55, 56, 107, 100, 136, 125}.

Some of the basic quantities that are usually monitored in case of an electrical network using an AC model are voltages, currents, power, and phase angles. In case of a DC model, the number of quantities to be monitored reduces to real power and phase angles, which are closely related to each other. The two power flow models are explained in Appendix A.

Electrical power grids as critical infrastructures continue to evolve and pose newer challenges. While topological models give important information about the structure of the grids, the electrical models add information about the complex flow dynamics. It is very important that the topological and electrical models are incorporated into each other and work hand in hand for the planning and restructuring of the grid, and for the implementation of proper measures to make it robust to all kinds of failures. Also, further investigation into the design of interconnected networks, such that the pros are higher than the cons, is

essential. In the present times when the demand for electricity is ever increasing, a proper restructuring could be the key to more robust and stable interconnected electrical grids.

Chapter 3

Dynamics of Cascading Failures in Power Transmission Grids

3.1 Introduction and Related Work

The need for electric power is becoming indispensable in almost every situation, and life seems to come to a standstill even with a small disruption. Blackouts were rare, but the frequency of large blackouts has increased in the last 10 years. Power grids are non-linear systems, and many researchers have used chaos theory^{43, 22, 41, 63} to analyze the complex dynamics of the power flowing through the grid. The chaos theory analysis predicts that the frequency of occurrence of massive cascading failures is related to their magnitude. In mathematics, a popular model called the ‘sand pile’ model¹⁵ states that when sand is continuously piled in a heap, a point occurs when a portion of the pile suddenly begins to subside. If an attempt is made to prevent the breakdown by adding more sand, the pile just collapses. Drawing analogy with this model, the researchers in¹⁵ have mentioned that as a power grid approaches a critical point, the possibility of a collapse increases. With the addition of new elements to the grid, increasing demand, interconnections, and increase in power flows, the grid may be quickly approaching its critical point. At such a point, it becomes necessary to study the complex dynamics arising in the grid and to find possible solutions to problems that may arise because of these dynamics.

Research has been done on power grids as complex networks, including vulnerability

analysis and quantification of damage to the grids through robustness metrics. However, most cascade models for power grids are exclusively topology-based models^{38, 123, 124} of local redistribution of load upon failure, and these models disregard the flow dynamics of electricity. The load is measured in terms of topological metrics such as betweenness centrality in these topological models. The authors of⁵⁹ assert that the combination of topological and power flow models is necessary for network science to provide meaningful solutions for the power grid. One of the simplest models for cascading failures was proposed in⁸⁴ and was popularly known as the “capacity” model because each node and link had a finite capacity in this model. The capacity was proportional to the initial load on each node, and the initial load was the betweenness centrality of the node when the network was normally functioning. When a failure occurs, all the shortest paths change, thus changing the betweenness centrality or load of the nodes. This model was followed by the “efficiency” model proposed in³⁸ and⁷⁴. Another model, known as the OPA model, was presented in¹³ and²⁴. This model is most similar to the model used in this dissertation, as described in the further sections.

The lack of a complex networks based model for the analysis of power grid was a major drawback of the studies conducted some years ago. We adapted the above models to include the power flow equations with actual load and impedance information³¹, and we named this model as the Overload Cascade model. This model assigns capacity to the links in the network proportional to the initial power flowing through them, in the absence of any disturbance. When a disturbance occurs, these power flows are redistributed and the flow dynamics of the network are observed. The model is described in detail in the next section.

In this work, we subject the grid to two scenarios, load growth and random fluctuations, and observe the effects of these individual scenarios on the dynamics of the grid, through extensive simulations, using the Overload Cascade model. These two scenarios simulate real world conditions: The increasing power demand represents the load growth scenario, and one of the possible examples of random fluctuations is the inclusion of distributed generation in the grid. The results of these two situations give insights into the behavior of the grid under

different stress conditions and a distinct behavior is observed in each case. More detail and discussion on these behaviors follow further in the chapter. This simulative analysis lays the foundation for the following chapters of this dissertation, in which we describe three different methods to alleviate the undesired effects occurring as a result of the dynamic behavior of the grid under different stress conditions.

3.2 Model

As mentioned before, many models used for power grid analysis in complex networks domain have been entirely topological^{38, 123, 124, 84, 74}. However, in order to make the work realistic, the underlying dynamics must be considered and used with the model to achieve meaningful results. This research considers a model introduced in our previous work^{96, 111, 95} to simulate a cascading failure scenario and we call it the Overload Cascade model. In this model, the initial load and generation on the nodes represent the initial state of the system. Power flows are calculated using the DC Power Flow model explained in Appendix A, and every link has a capacity which determines the maximum amount of power that can be carried by that link. During normal operation, the system is stable and all power flows are within limit. If a disturbance, such as failure of an element, sudden increase in demand, or load fluctuations, takes place in the system, all power flows are recalculated using flow equations and utilization of all links is checked to see whether or not they are within their capacity. If any link exceeds its capacity, it is removed from the system, and its power is redistributed among other links, depending on impedances of the other links. Even though the model is simple, the presence of the flow equations guarantees that Kirchoff's and Ohm's laws are properly considered, thus making the model more realistic for use with the power grid. The reduced complexity of this method allows its use even with large systems and provides a reasonable balance between complexity of the method and accuracy of the results. Moreover, the accuracy of the method and results depends on the type of analysis. The analysis in this dissertation mainly concerns monitoring the amount of real power flow in every line and the

direction of power flow. As a result, the accuracy provided by the Overload Cascade model along with the DC Power Flow model is adequate for the purpose. Also, as mentioned in studies conducted in^{94, 103}, the accuracy of DC models with respect to active power flows is very close to that of the complete AC model.

The main equation of the Overload Cascading model is:

$$C_{ij} = \beta * P_{ij}^0 \quad (3.1)$$

where C_{ij} is the capacity of link $i - j$, β is a constant, usually 0.5, and P_{ij}^0 is the initial power flow through link $i - j$. This equation says that the capacity of a link is proportional to the initial power it carries, which in turn, is a function of the inductance of the link, as seen from the equations of the DC Power Flow model. It will be observed in the next equations that the power flow in a link is determined by the total load on the node.

The main equation of the DC Power Flow model is as follows:

$$P_{ij} = \frac{\delta_{ij}}{x_{ij}} \quad (3.2)$$

where P_{ij} is the power flow in the link $i - j$, δ_{ij} is the difference in phase angles between the voltages at the sending bus (i) and receiving bus (j), and x_{ij} is the inductance of the transmission line. The voltages are considered as 1 p.u. for the DC Power Flow model.

Kirchoff's law is expressed by the equation:

$$P_i = \sum_{j=1}^N P_{ij} \quad (3.3)$$

where P_i is the total load on a node and it is equal to the algebraic sum of the power flowing through the node. If the demand on the node increases, the flow of power through the links connected to that node also changes.

3.3 Cascading Failures in Power Grids

In this work, we subject the power grid to two scenarios. First, a case is considered in which increasing demand on a power grid leads to line overloads and outages, corresponding to a scenario in which the power grid is operated to its limit. Second, we consider the presence of random fluctuations in the network and analyze the behavior of the grid in response to random changes in load. With the results of these two scenarios, we provide insights into the dynamic behavior of the grid.

For the analysis of cascading failures, the IEEE test networks³¹, as well as the Polish grid obtained from MATPOWER¹⁴¹ have been used.

3.3.1 Effect of Load Growth on the Dynamics of the Power Grid

As previously stated in the above references, if the power grid reaches its critical point, the possibility of a breakdown is apparent. Thus, one way to study cascading behavior of the grid is to stress it to its critical point. This is a realistic situation because the demand for electrical energy is constantly increasing in the modern society. This load growth is modeled by increasing all loads simultaneously by a factor of α , between 0 and 1, in steps of 0.1. Every time the loads are increased, the Overload Cascade model is run to calculate the power flow in the network. The increase in the demand causes increased power flows through the links. Since each link is bound by a finite capacity, some of the links exceed their capacity and get overloaded in order to supply the increased demand. These overloaded links fail and the power that was being carried by them is redistributed among the other links in the network. As a result of this redistribution, some more links may reach their capacity and fail. This may lead to a cascade of overload failures. This simulation is performed for different values of α between 0 and 1, in steps of 0.1, and the fraction f of links that failed at the end of each simulation is recorded. The final fraction of links lost is plotted against the corresponding α as shown in Figure 3.1. The sub-figures 3.1(a), 3.1(b), 3.1(c) and 3.1(d) show results of simultaneous load growth in the 14-, 30-, 57-, and 300-node IEEE networks.

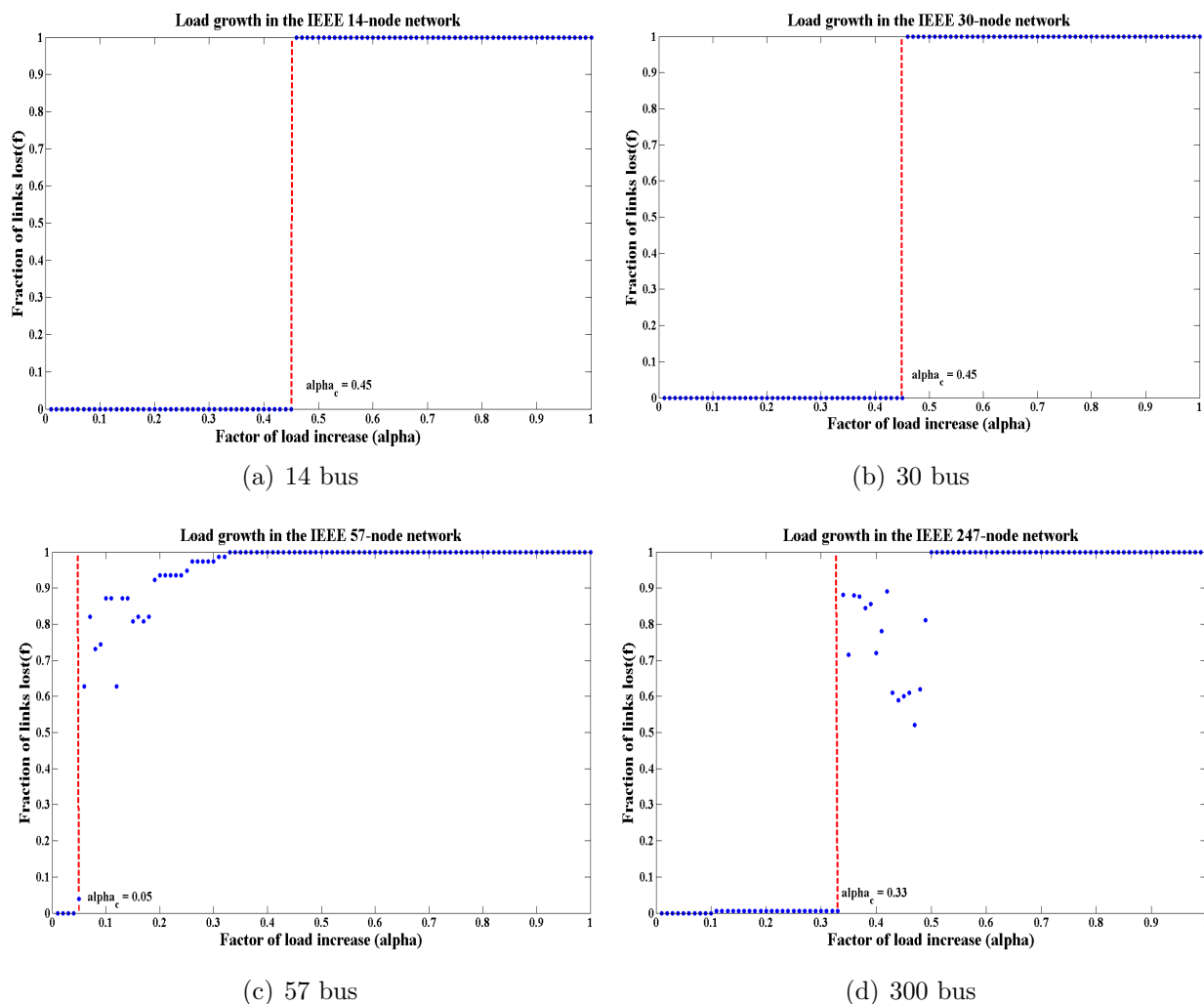


Figure 3.1: The effect of load growth can be seen on IEEE 14-, 30-, 57-, and 300-node networks. The load is increased by an amount α between 0 and 1 as represented on the x-axis. The fraction f of tripped links corresponding to each α is plotted on the y-axis. It is seen that there exists a threshold of load growth, below which the network is intact or undergoes very few failures, and beyond which it approaches a complete breakdown. A sharp transition is seen for the 14-node and 30-node network. The networks go through an intermediate stage before complete breakdown in case of the 57-node and 300-node networks.

As seen from Figure 3.1, the networks remain intact or have a very small number of link failures up to an increase in load by a critical value of load growth α_c , after which the network approaches a breakdown state. The state in which there are no failures or few failures (less than 5%) is termed as the operational state or normal working state, and the state in which the grid undergoes failure of more than 95% of the links is considered as the complete breakdown state. The state of the network between 5% - 95% failures is termed as the intermediate state. For the 14-node network, the transition is sudden, in the sense, that the network is intact up to the value of α approximately equal to 0.45 (corresponding to 45% increase in load on all the nodes), and then completely disintegrates as the load is increased beyond this value of α . Similarly, the transition for the 30-node network is abrupt. In case of both, 14-node and 30-node networks, the transition occurs close to 45% of load increase. The occurrence of the point of transition depends, to a certain extent, on the topology of the network and its size. For the 57-node network, a transition phenomenon is seen, but at an earlier stage than the 14-node and 30-node networks. For the 300-node network, transition occurs around 34% of simultaneous load increase. Thus, the common characteristic observed in these results is the threshold phenomenon. A transition threshold is present for each network below which the network is intact or in the normal working state, and beyond which a considerable damage to the network is seen in terms of the fraction of links remaining.

To further test the occurrence of the threshold phenomenon, we generated synthetic power grid networks, using the properties of the real grids, and the algorithm used in⁹⁶. Power grids are critical infrastructure, and hence little data is publicly available. Synthetic networks of 50-, 100-, 200-, and 400-nodes were generated to complete the tests. The synthetic networks are randomly generated, and hence, it is necessary to perform the tests on many instances of every network. As a result, we generated 100 instances of each of the synthetic networks. Similar to the procedure for the IEEE test networks, the synthetic networks were also subjected to continuously increasing load, by a factor of α . The simulations,

using the Overload Cascade model, were repeated for different values of α between 0 and 1 in steps of 0.1, and the results were plotted in the graph shown in Figure 3.2. Similar to the case of IEEE networks, a threshold phenomenon is observed in the case of synthetic networks also. Since these generated networks are random, the point of transition for each network of the same size will change. As a result, the final fraction f of failed links for every α is recorded by averaging over the values of f obtained for the each of the 100 instances of a particular network under consideration. Table 3.1 indicates the average value of α_c , at which the transition occurs, for each of the synthetic networks. Figure 3.2 shows results of the cascading effects in the synthetic networks, thus confirming the presence of the threshold phenomenon.

Table 3.1: *Average value of α_c for the synthetic networks*

<i>Network(N)</i>	<i>Transition point α_c</i>
50	0.19
100	0.17
200	0.195
400	0.160

3.3.2 Effect of Random Fluctuations on the Dynamics of the Power Grid

Random perturbations can occur in the grid for several reasons. If these random fluctuations are small, their effect may not be felt. However, if the fluctuations are considerable in magnitude, they can cause many undesirable effects on the functioning of the grid, including the initiation of a cascading failure. As an example, random perturbations can occur due to the incorporation of renewable distributed generators (DGs), such as wind turbines and solar panels, in the grid.

In order to implement a random load variation, a two-step procedure is followed: a random variable vector X_i is generated for each node i of the network under consideration, and a value σ between 0 and 1 is selected to be used with the random variable vector to produce

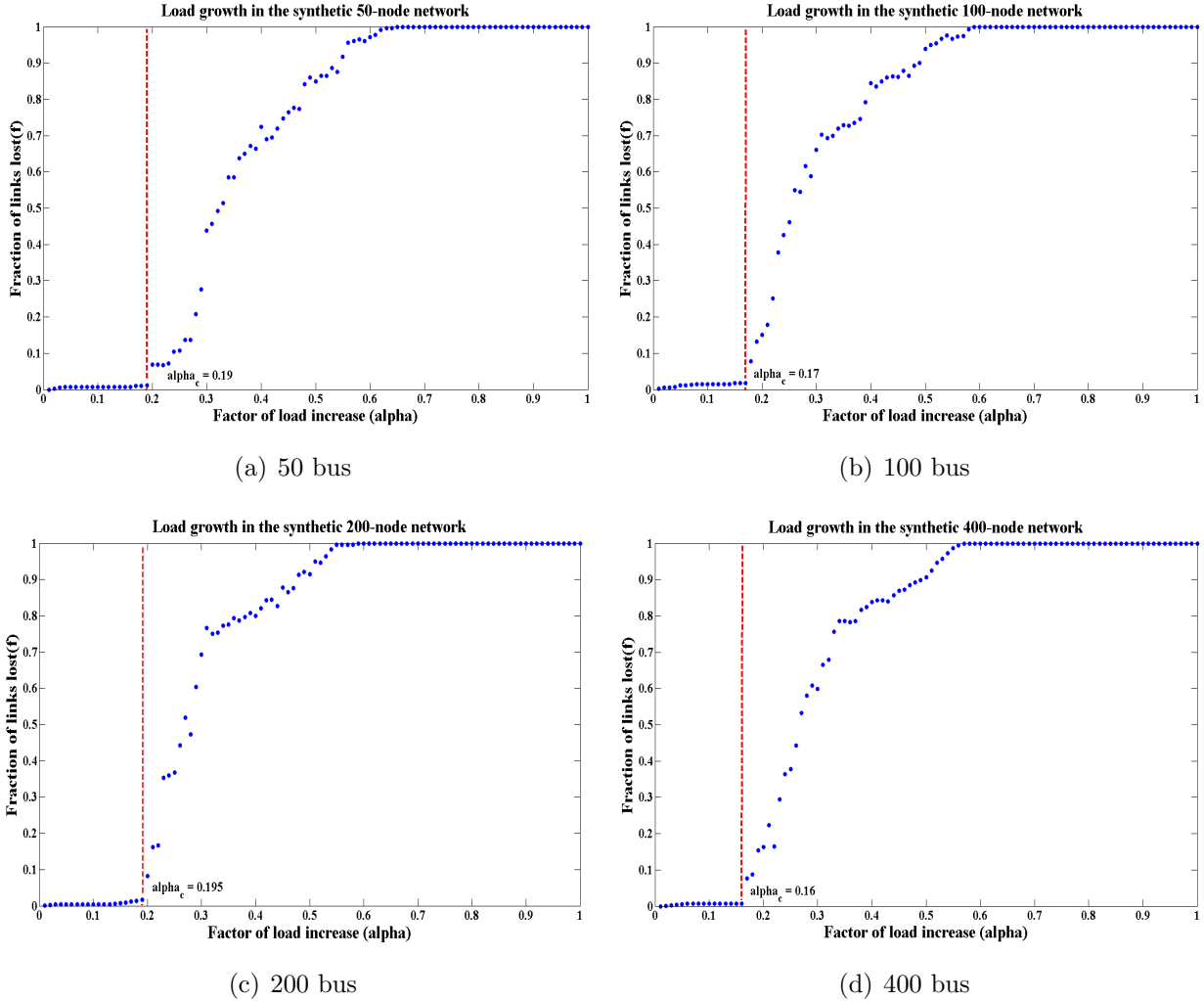


Figure 3.2: The effect of load growth on the synthetic networks of sizes 50, 100, 200, and 400 nodes, is represented in this figure. The networks are randomly generated, therefore, 100 instances of each network are considered and the results shown in the figure are averaged over the 100 instances of the network under consideration. The load is increased by an amount α between 0 and 1 as represented on the x-axis. The average fraction f of tripped links corresponding to each α is plotted on the y-axis. It is seen that a threshold exists at the critical point, in this case also, below which the network is intact or in normal working condition, and beyond which it approaches a breakdown state. All the networks go through an intermediate state before complete breakdown.

the fluctuations, as shown in equation 3.4. If L_{new}^i is the new value of load/generation for each node i of the network under consideration, and L_i is the corresponding original value, the new value, after the introduction of random fluctuation is calculated using the following equation:

$$L_{new}^i = L_i * [1 + (\sigma * X_i)], \quad i = 1, 2, \dots, N \quad (3.4)$$

where N is the number of nodes in the network and σ changes in steps of 0.1.

As an example, consider the IEEE 14-node network. A random variable vector X for this network would be of size 14, to match with the number of nodes in the network, one random variable for each node. We generate 100 such vectors of random variables for each of the IEEE networks of size 14, 30, 57, and 300 nodes. The value of σ ranges between 0 and 1, and changes in steps of 0.1. For each network, random variable vector, and sigma, the fraction of links tripped, f , is recorded. The flow dynamics are regulated by the Overload Cascade model in conjunction with the DC Power Flow model, and a link is tripped if it exceeds the capacity assigned to it. For the IEEE networks, the fraction of failed links corresponding to each σ is obtained by averaging over the number of random variable vectors, which is 100 in this case. Figure 3.3 shows the results of the simulations for the different IEEE test networks. It can be noticed from the figure that the transition becomes much smoother, as compared to the load growth scenario, and no obvious threshold is seen. Moreover, for the random fluctuation case, it can be seen that the value of f for $\sigma = 1$ does not reach complete breakdown in the examined range of σ . The graphs show an increasing trend and if the range of σ is expanded, it may be possible to see the networks approaching a breakdown state. In the case of random fluctuations, f depends not only on σ , but also on the selected random variable vector. In general, the introduction of random fluctuations smooths out the transition, thus causing a gradual change in the operational state of the network.

Similarly, in Figure 3.4, results for introduction of random load fluctuations in the

synthetic networks of sizes 50, 100, 200, and 400 nodes are shown. In this case, the networks are randomly generated and 20 instances of each network are used. Each of these instances is subjected to 20 generated random variable vectors and final results of f corresponding to each σ are computed by averaging over the number of instances of the network as well as the number of random variable vectors. It can be observed in Figure 3.4 also that the networks do not reach complete breakdown in the examined range of σ . They show an increasing trend, in general, and may reach a state of complete breakdown if the range of σ is extended. These graphs illustrate that the transition for random fluctuations is smoother, unlike the transition for load growth, for the IEEE and the synthetic networks.

3.3.3 Effects of load growth and random fluctuations on large networks - Polish grid

The Polish grid has been used to test the effect of load growth and random fluctuations, in order to observe the qualitative behavior of a large network under different scenarios. The Polish winter-off-peak grid, available at¹⁴¹, is a large grid with 2746 nodes and 3505 links. The Polish grid is an example of a real network, with realistic values of loads and impedances. This network is part of the national high-voltage power grid of Poland, and the data is collected and used by Polish transmission system operators. This network is used to test the effect that its large size can have on its behavior, with respect to load growth and random fluctuations. The results of applying the two scenarios on the Polish grid are shown through the graphs in Figure 3.5.

Figure 3.5(a) shows that, as expected, increasing all loads in the grid causes an abrupt breakdown, indicating the presence of a threshold. All the loads in the grid were increased by a factor α ranging between 0 and 1, and changing in steps of 0.001. It can be seen that the critical transition point for load growth scenario arrives much sooner for the Polish grid, as compared to both, IEEE test networks and synthetic networks. One of the possible reasons for the early transition is the large size of the network. Figure 3.5(b) shows results of introducing random fluctuations in the Polish grid. Random fluctuations were generated

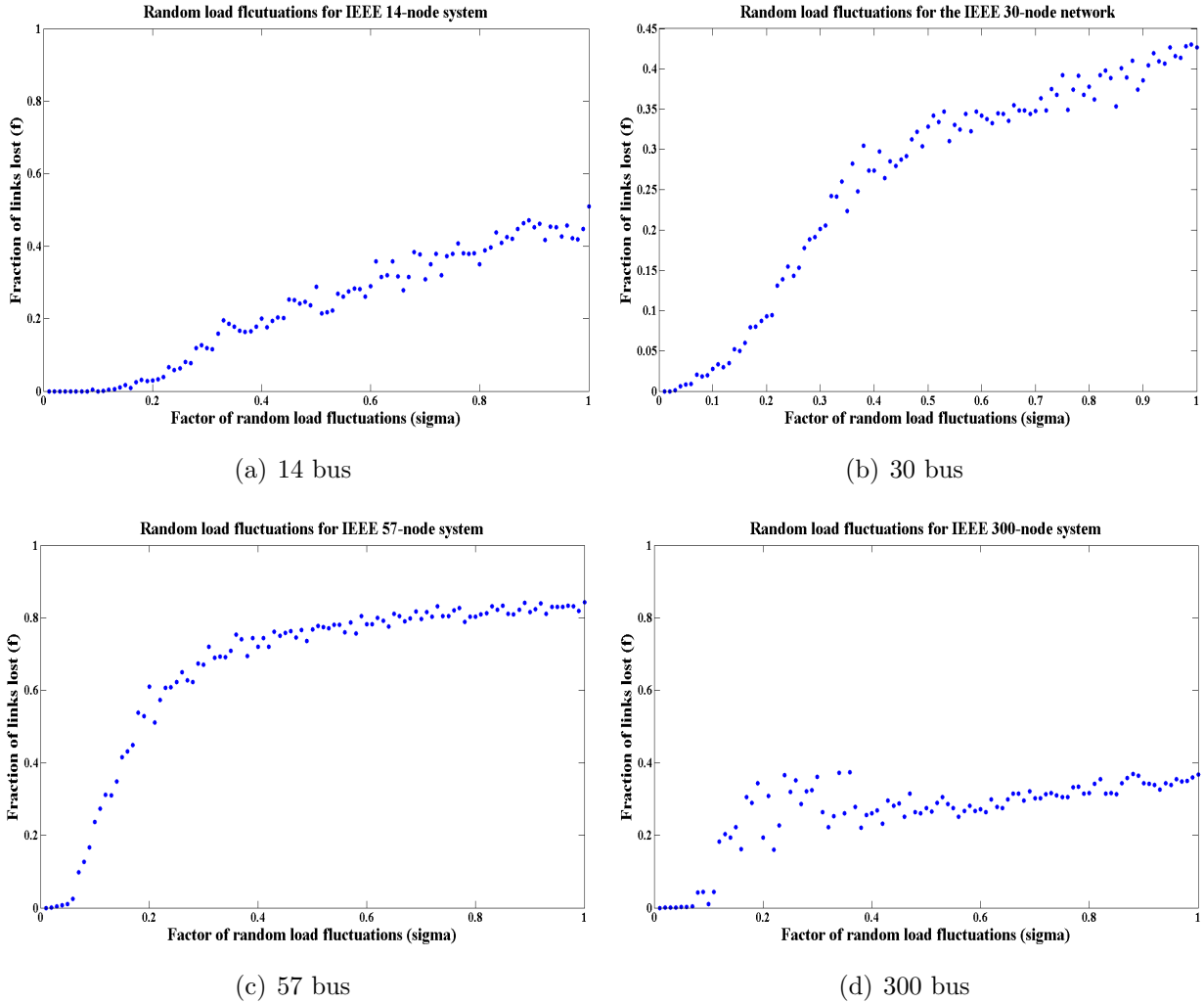
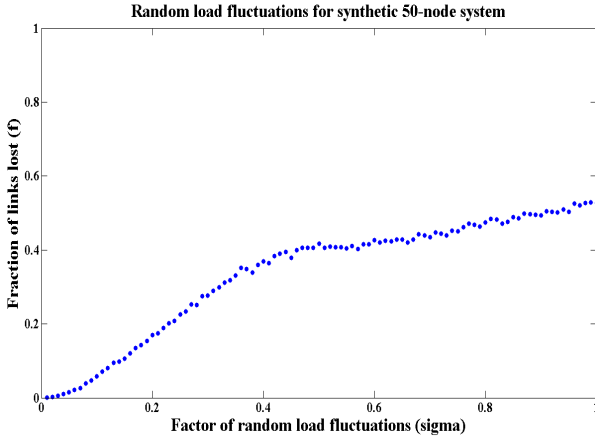
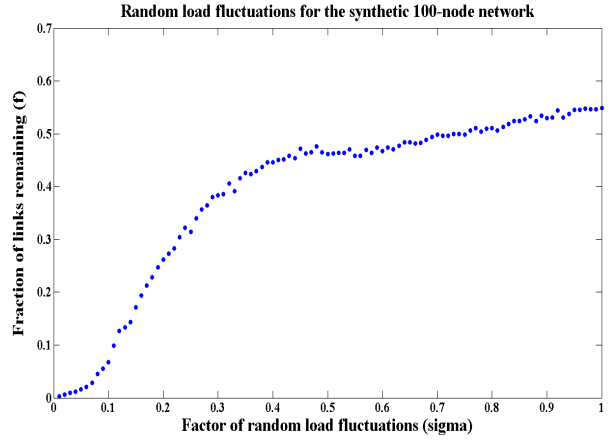


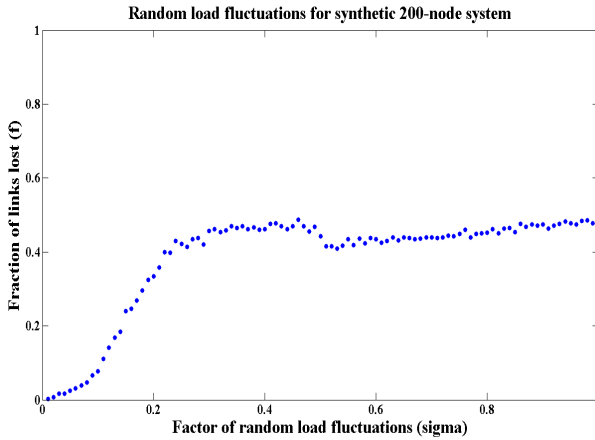
Figure 3.3: *The effect of random fluctuations on the IEEE 14-, 30-, 57-, and 300-node networks is shown in this figure. The relative strength of the random fluctuation depends on the random variable vector and the value of σ used. A set of 100 different noise configurations are used with σ ranging between 0 and 1. The number of links failed must be averaged to account for each of the 100 random variable vectors, and hence, the figure represents the average value of f for each value of σ . An important characteristic of this figure is the vanishing threshold. The transition in this case becomes much smoother, as compared to the case of load growth. Also, a complete breakdown is not reached for the examined range of σ . The graphs show an increasing trend and if the range of σ is expanded beyond 1, it may be possible to see the networks approaching a breakdown state.*



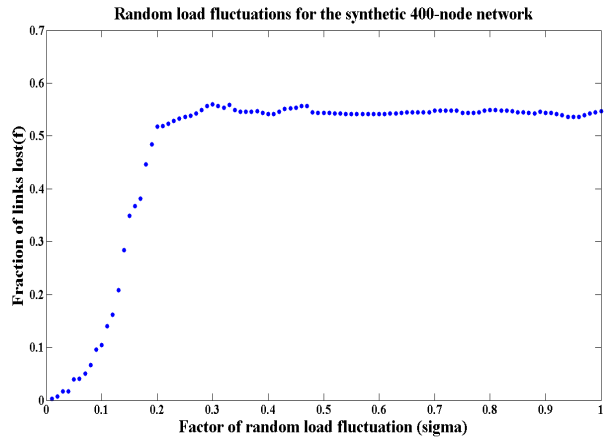
(a) 50 bus



(b) 100 bus



(c) 200 bus



(d) 400 bus

Figure 3.4: *The effect of random fluctuations in synthetic networks of size 50, 100, 200, and 400 nodes is shown in this figure. In this case, in addition to the random variable vectors, there is randomness in the networks also. Hence, the final fraction of links failed, f is averaged, not only based on the 20 instances of the network under consideration, but also, on the 20 random variable vectors. In this figure also, it can be seen that the transition is smoother, no definite threshold is visible, and f is less than 1 for the examined range of σ , with the graphs showing an increasing trend, in general.*

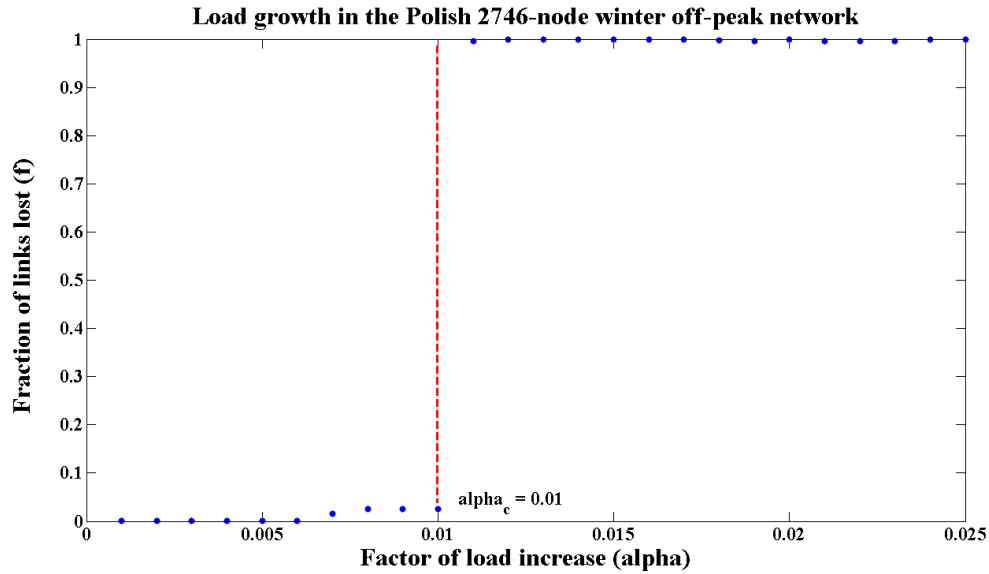
using the same procedure as described previously, using 100 different realizations of random variable vectors with different values of σ ranging between 0 and 1 and increasing in steps of 0.01.

It can be observed from Figure 3.5(b) that the transition is abrupt even in the case of random fluctuations for the Polish grid, with 2746 nodes. In this case, a threshold phenomenon can be seen. One main difference between this network and the previous networks that were subjected to random load fluctuations, is the size of the network. This leads us to the understanding that the fragility of the grid may increase with increasing size. In previous scenarios, a threshold was not seen for random fluctuations, but it is evident in the case of the 2746-node Polish grid.

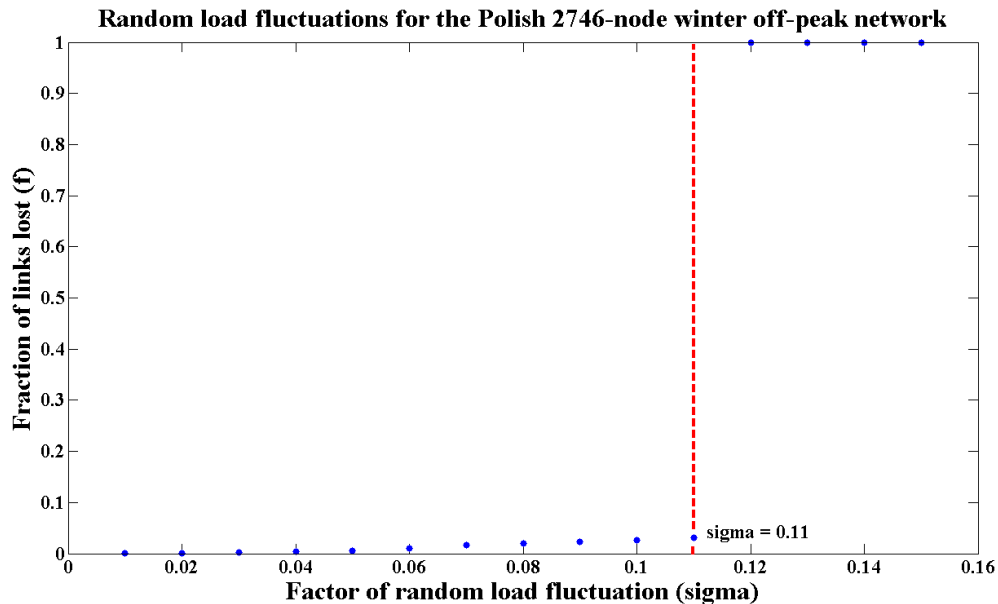
3.4 Discussion

The work in this chapter analyzes the effect of load growth and random fluctuations on IEEE test networks, synthetic networks, and the large Polish grid. The analysis indicates that blackouts due to line overloads may follow a threshold phenomenon. A specific transition point is evident in case of load growth for all the networks. Such a transition becomes smoother for random fluctuations and no specific threshold can be seen. However, for large systems such as the Polish grid, a threshold is observed even in the case of random fluctuations, indicating that large systems may be more fragile. This result implies that, although it is beneficial to create large systems by interconnection of grids, these interconnected networks^{1,2} experience a risk of cascading failures, as the fragility of a system may increase with its size.

Further more, the system does not reach a complete breakdown in the case of random fluctuations, for any of the networks, besides the Polish grid, in the examined range of random fluctuations. The graphs show an increasing trend, in general, and if the range of σ is expanded beyond the examined range, the networks would probably experience complete breakdown at a later stage. Both the situations, load growth and random fluctuations, can



(a) Polish grid load growth



(b) Polish grid random load fluctuations

Figure 3.5: The effect of load growth and random fluctuations for a large network, the 2746 bus Polish grid (off-peak configuration, winter 2003-2004) is shown in this figure. Fig. 3.5(a): Continuous load growth by a factor of α causes the network to break down completely after a threshold. This threshold arrives very early, as compared to the other networks which underwent the same experiment, and this early breakdown is possibly a characteristic of large networks. Fig. 3.5(b): Every point in the graph corresponds to 100 different realizations of random variable vectors that were used to produce the random fluctuations, in combination with σ . The transition is abrupt, unlike the occurrence of a smooth transition for the other networks subject to random fluctuations. Again, the large size of the network is a possible reason for the presence of a threshold in the case of random fluctuations in the Polish grid. This experiment indicates that the fragility of the grid may increase with size.

be regarded as realistic situations, the former indicating continuous increase in demand, and the latter suggesting an instance such as presence of renewable distributed generation in the network. However, the power grid is a complex system with complex flow dynamics. Several other scenarios are possible and can be modeled besides the two scenarios, load growth and random fluctuations, that were considered in this chapter. The power grid exhibits different critical behaviors under different conditions and it is not easy to predict or conclude the type of behavior the grid would exhibit under a particular condition. More scenarios must be simulated and tests must be conducted in order to get a deeper understanding of the dynamic behavior of power grid networks under different stress conditions.

Chapter 4

Mitigation Strategies - Intentional Islanding

4.1 Introduction

Power grids were designed for the purpose of transfer of electricity from the generators to the consumers, and were engineered keeping in mind the ever-increasing demand for electricity. However, in modern times the grid has reached a point where it has become very important to allow for its expansion in terms of technology and intelligence. Since the last few years, power grids have become increasingly interconnected. There are exchanges of large amounts of power over very long distances among different utilities to satisfy the increasing demand from the customers. The current setup is making the grid less stable and more vulnerable to intentional and unintentional failures. The system reliability and stability has been affected. As a matter of fact, there have been many occurrences of cascading failures in the recent past. Defined by the North American Electric Reliability Corporation (NERC), a cascading failure is “the uncontrolled loss of any system facilities or load, whether because of thermal overload, voltage collapse, or loss of synchronism, except those occurring as a result of fault isolation” as mentioned in³⁴. In simple words, when one failure leads to successive failure of other elements of the grid, leading to huge losses, the process is called a cascading failure. Some strategies such as reciprocal altruism⁶⁰, changing the dynamic equilibrium of the system to a point of self-organized criticality^{13, 64},

and different load shedding schemes^{96, 134, 10, 50} have been suggested in the past for reducing the effects of cascading failures.

Intentional islanding of the power system is one such strategy. Intentional islanding can be defined as the intentional splitting of the grid into separate controllable parts or islands, each with its own independent generation. Intentional islanding may be accompanied by some load shedding in order to balance the generation and load in the sub-systems. Intentional islanding can be very helpful in isolating failures or localizing them within the region where they occurred and preventing them from spreading throughout the system. Several techniques have been proposed previously for islanding in power systems, such as those based on spectral analysis, slow coherency, ordered binary decision trees as well as optimization.

Intentional islanding does not take place every time there is a failure. We maintain a list of vulnerable links, the links which if disconnected, can cause a huge damage to the system. If any of these vulnerable links happen to be the initial failure, islanding must be initiated. Using the vulnerability index proposed in¹³⁸, we also know the order in which the links fail. Hence, whenever a vulnerable link fails as a secondary failure to a non-vulnerable link, the islanding scheme must be activated. An example of an islanding scheme for a small test network with 12 nodes and 21 links is shown in Figure 4.1.

In this dissertation, we propose two methods for intentional islanding, based on network partitioning, and derived from the Fast Greedy algorithm⁸⁶ and the Bloom algorithm¹¹³. The original Fast Greedy and Bloom algorithms are based on the community detection quality function called modularity^{3, 89, 47, 90}. Since the concept of islanding is similar to that of detecting communities, by integrating the power flow model, we can make these algorithms realistic for islanding in power grids. We call these new algorithms as Modified Bloom and Modified Fast Greedy methods. Both the methods have a polynomial running time, but the Modified Bloom approach is faster. In general, these methods are an efficient balance between the amount of load shedding and the algorithm scalability. Both have been

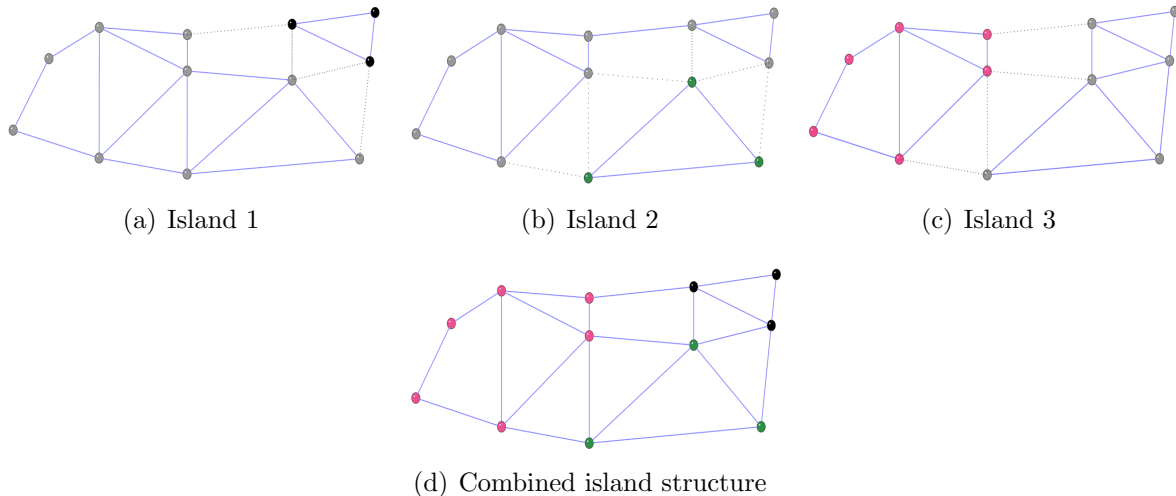


Figure 4.1: *The structure of three islands that belong to an example power grid with 12 nodes and 21 lines. Sub-figures 4.1(a)-4.1(c) show individual islands in different colors. These islands are connected with their topological complements by the dotted lines. Sub-figure 4.1(d) shows the combined island structure with each island represented by the corresponding color of the islands shown in sub-figures 4.1(a)-4.1(c) at the top.*

tested on the IEEE 57-, 118- and 247-node networks, besides the 14-node and the 30-node networks. The 247-node network is a modification of the IEEE 300-node network and has been obtained as discussed in⁹⁶.

The island boundaries can be computed offline for both the techniques and can be known to the operators in advance. Whenever a failure occurs, the predetermined set of transmission lines in the region where the island is needed, can be disconnected. Hence, the strategies can be implemented in real time. The results of islanding of the two methods is compared with the results of an optimal islanding scheme presented in¹³⁷.

4.2 Related Work

Since the past few years, the problem of intentional islanding is being studied as an important approach for isolating failures in the power grid^{108, 77, 125, 136, 104, 44, 55}. It has been proposed by some researchers as an appropriate control action to protect the system when

large disturbances take place. It is also considered to be an effective method to contain disturbances within a smaller area. Islanding leads to a faster restoration of the system to its initial state, as shown in^{108, 77}. Different methods have been suggested to define islanding based on slow coherency generator grouping combined with graph theory, ordered binary decision diagrams (OBDD), linear and non-linear optimization as well as spectral methods. While slow coherency methods are among the first few methods proposed for islanding, spectral methods are fairly new.

The slow coherency methods are based on grouping the generators according to slow coherency and then trying to find the minimum cut-set from the interface network between the generator groups using some search techniques^{108, 52, 125, 53, 136, 139}. The other category of methods deals with the ordered binary decision diagrams approach^{104, 66}. For large-scale power networks, islanding using OBDD is an NP-hard problem. Hence, different two and three phase variants of this strategy have been suggested.

The authors of⁴⁴ and¹¹⁸ present a mixed integer programming approach for optimal power grid islanding, both with the objective of minimizing load shedding only within the island. The authors of⁴⁴ also discuss connectivity constraints so that the nodes within each island are connected. As opposed to the techniques mentioned before, these two optimization techniques can form multiple islands at the same time.

The authors of⁵⁵ have used spectral matrix methods for islanding. They used successive bisection techniques based on the signs of the Laplacian eigenvalues to partition the grid. Cluster optimization using simulated annealing is suggested in⁵⁶. In⁸², separation of a power system into islands based on the second largest eigenvalue of the graph of the power system, also known as the algebraic connectivity, is presented. The authors have also shown that the computation time of this method has a linear relationship with number of transmission lines used for partitioning. However, these methods suffer from the drawback of the absence of a power flow model which makes them unrealistic for use within a power system.

While the above are the more common approaches for islanding in power grid, some

researchers have also proposed the use of global search meta-heuristics such as genetic algorithm⁷⁷ and particle swarm optimization⁷⁵ for islanding as computationally efficient methods. A few of the above methods can form only two islands at a time, although the procedure can be repeated to obtain more islands.

4.3 Optimal Intentional Islanding

The authors of⁹⁷ have presented an MILP formulation to find the optimal islands when a failure takes place in any part of the grid. The number of islands is represented by n_{isl} , and the island index is k such that $k = 1 \dots n_{isl}$. The number of islands is given as an input to the formulation and is mainly limited by the number of generators present in the network. The power grid topology is denoted to be G , the island topology to be g_k , the group of links that interconnects the island with its topological complement to be l_k , and the topological complement of the island to be $T_k = G \setminus \{l_k \cup g_k\}$. They denote s to be the index that distinguishes between the two partitions of the power grid due to the existence of an island k i.e. for island k , $s = 1$ denotes the island topology (g_k) and $s = 2$ denotes the island topological complement (T_k). For a given power grid, islands are constructed such that the amount of generation/load change from normal operation and the island size are minimized as follows

$$\begin{aligned} \text{Minimize } & A \sum_{i=1}^{i=N} \sum_{k=1}^{k=n_{isl}} |power_i - d_i^k| \\ & + B \sum_{i=1}^{i=N} \sum_{j=1}^{j=N} \sum_{k=1}^{k=n_{isl}} \mu_{i,j}^{k,1} \end{aligned} \quad (4.1)$$

where N is the number of nodes, A and B are optimization parameters.

The first part of the objective function aims at minimizing the load shedding in the island and the complement with $power_i$ being the original load of each node i and d_i^k being the new load after partitioning the grid, whose value is decided based on the formulation and

the constraints. The smaller the difference between the original and the new values, the better is the result of islanding. The links which interconnect the different islands are chosen by the optimization such that the removal of those links does not cause additional damage to the network in terms of load loss. The second part of the objective function aims at minimizing the size of the island to limit the failure to a small region of the network. The variable μ counts the size of the island in terms of number of links. The subscript i, j refers to the link $i - j$ and the superscript $k, 1$ refers to the presence of the links within ($s = 1$) the island k . The values of parameters A and B can be used to decide the dominant part in the optimization

The islanding topology and power flow constraints are discussed in detail in Appendix B. Optimal islanding is computationally expensive for larger systems. The running time to solve the constraint programming problem for IEEE 14-node and 30-node networks is 45 minutes and 3.5 hours, respectively. To overcome this problem of scalability, we propose two methods based on modularity for islanding of power grids.

4.4 Complex Networks based Methods for Islanding

A community is usually a set of well connected nodes that are less connected to the remaining network. If we think of a power grid to be a network of nodes connected by transmission lines, we can use the power flow model incorporated into a community detection algorithm to “partition” the grid or to form islands such that this island formation leads to minimum load shedding in the system. Out of the numerous community detection algorithms, we select two among the faster and more efficient algorithms for island formation: Fast Greedy⁸⁶ and Bloom¹¹³. We modify these two algorithms by incorporating the power flow model and imposing some conditions to adapt them to a power grid.

In general, modularity is a quality function that determines the quality of the partitions on a scale of 0 to 1, with 1 being the best value. For a general network, modularity can be

defined as:

$$Q(P, G) = \frac{1}{2L} \sum_{i=1}^N \sum_{j=1}^N (a_{ij} - \frac{d_i d_j}{2L}) \delta_{c_i c_j}, \quad (4.2)$$

where N is the number of nodes and L is the number of edges in the graph G ; a_{ij} represents the existence of an edge between nodes i and j , d_i represents the degree of node i or the number of nodes connected to node i . P is the partition of the graph that divides it into communities by the quality measure Q . The communities of nodes i and j are represented as c_i and c_j respectively. The δ -function is 1 if nodes i and j are in the same community ($c_i = c_j$), otherwise it is 0.

The objective of the two methods presented in this chapter is to minimize the amount of load shedding in the system (both island and complement) and is given as:

$$J = \text{Minimize} \sum_{i=1}^N \sum_{k=1}^{n_{isl}} | \text{power}_i - d_i^k | \quad (4.3)$$

This objective is the same as the first part of the objective function of the optimization, as shown in Equation B.1. However, we do not impose any restrictions on the size of the islands as described in the second part of Equation B.1 because any such restriction would only reduce the quality of the islands and result in higher load shedding. Thus, the size of the islands is decided by the partitioning methods themselves. Similar to the optimization, the number of islands is limited by the number of generators in the network and the modified partitioning methods make sure that every island has at least one generator. Both methods are polynomial in complexity, but the Bloom method is faster than the Fast Greedy.

4.4.1 Islanding using Modified Fast Greedy Method

The original Fast Greedy algorithm is an example of an agglomerative algorithm that begins with a number of partitions equal to the number of nodes in the network and merges these partitions depending on the benefit to the objective. For a power grid with N nodes, we begin with $n'_{isl} = N$ islands and a $n'_{isl} \times n'_{isl}$ benefit matrix ΔJ from Equation C.1. Thus, at the beginning, each node is an individual island. According to the algorithm, the pairwise

benefit $\Delta J_{r,s} = J_{new} - J_{old}$ is computed for every pair of islands Isl_r and Isl_s . J_{new} is the value of the objective after combination of islands and J_{old} is the value of the objective in the current state. This benefit is computed for each potential pair of islands by a linear programming problem for minimal load shedding, which is basically the objective of the problem. Thus, the pair of islands that gives the largest decrease in the objective value or in other words, the minimal load shedding, is merged. This merged pair is now an individual island and can be merged with any other islands to continue the process. After every merge, the benefit matrix ΔJ shrinks in size and must be recomputed. One of the requirements that this method must meet is the presence of at least one generator in every island. The required number of islands, $n_{isl} \leq n_{gen}$, where n_{gen} is the number of generators in the system, is given as an input. Once there are n_{gen} islands, if $n_{isl} = n_{gen}$, the process stops. However, if $n_{isl} < n_{gen}$, the process of “superislanding” begins by combining two or more of these n_{gen} islands to reach the final goal of attaining n_{isl} islands after which the process stops. The process of superislanding also happens in the same way as above. The size of ΔJ is the same as the final number of islands n_{isl} at the end of the process.

The original Fast Greedy approach has a running time complexity of $O(N^2 \log N)$ and the incorporated linear programming load shedding scheme adds a complexity of $O(N^3)$. Thus, this method is polynomial in complexity with a running time of $O(N^5 \log N)$. The algorithm for this method is shown in Appendix C.

4.4.2 Islanding using Modified Bloom Method

The Bloom type method begins with a few seed nodes and the islands grow from these seeds by adding adjacent nodes one at a time. In the original Bloom algorithm, the selection of the initial seeds is a stochastic process. However, in the case of islanding, we imposed all the generators in the network to be the initial seeds so that the number of islands at the beginning is equal to n_{gen} . This step is to make sure that every island has at least one generator. The nodes which are covered by the islands are said to be in the “covered” set

and the other nodes are said to be in the “*uncovered*” set. Thus, at the beginning, all the generator nodes are a part of *covered*. We maintain a set of “*boundary*” nodes for each island. These boundary nodes have at least one connection to the island they are boundary nodes for, and they may become a part of that island. Again, the required number of islands, n_{isl} should be less than or equal to n_{gen} . All the islands are grown in parallel from the initial seeds, as opposed to growing one community at a time in the original Bloom. This is because the original Bloom has only one stochastically chosen seed node at a time whereas the modified Bloom for islanding has multiple seeds nodes determined right at the beginning. Similar to the Fast Greedy approach, this approach also computes a benefit matrix $\Delta J_{N \times n_{gen}}$ after every merge which expresses the change to the objective value if any adjacent node merges into an island, using the linear programming problem for minimal load shedding. The node that adds the maximum benefit to the objective function (or the minimal load shedding) is chosen to merge with the island and moves from the *boundary* set to the *covered* set and its adjacent nodes move to the *boundary* set from the *uncovered* set. The nodes that already are a part of one island cannot be a part of any other island to avoid any overlapping of islands. The algorithm continues until all the nodes of the system are covered.

The original Bloom approach has an average running time of roughly $O(N)$ and a worst case running time of roughly $O(N^2)$. The linear programming contributes $O(N^3)$. Thus, the average running time of this approach is roughly $O(N^4)$ and the worst case running time is roughly $O(N^5)$. Bloom type approach is computationally more efficient than the Fast Greedy approach and in general, gives better results for load shedding. The algorithm for this method is described in Appendix C.

Few different partitioning methods have been described in literature for partitioning of power grids as mentioned before. However, to the best of our knowledge, no other network partitioning algorithms using modularity have been applied previously for this purpose.

The two approaches - Fast Greedy and Bloom, are very promising algorithms for network partitioning, in terms of complexity and are among the faster and highly efficient algorithms.

4.5 Results and Comparison of the Different Methods of Intentional Islanding

Optimal islanding has been tested on the IEEE 14-node and the 30-node networks and the two modularity-based methods have additionally been tested on the 57-, 118- and 247-node networks³¹. Results and comparisons are shown through tables and graphs. The original 30-node network has only 2 generators, but to make it more suitable for islanding, 7 other generators were introduced in the system and the generation was equally divided among these 9 generators. Those nodes in the 30-node network that were carrying no load were converted into the 7 additional generator nodes. Similarly, the original 247-node system has 1 large generator and 7 other small distributed generators. The generation was equally divided among all these 8 generators and then island formation was carried out. These islanding techniques would be very suitable for the future grid which would have the incorporation of more distributed generation.

Table 4.1 shows the average percentage of total load that remains after islanding in the 14-node network, using each of the three strategies. There are 2 generators in the system and hence, there are 2 islands. The number of islands is represented by n_{isl} . The results show that the islands formed by each of the two modularity-based methods are exactly matching with the islands formed by the optimization. Also, as indicated in the table, the techniques can preserve around 86% of the load on average per island, in the system. The island structure is shown in Figure 4.2. The circles represent the nodes and the connections between them are the transmission lines. The big circles represent the generator nodes and the small circles are the load nodes. Every island is represented by a separate color and nodes belonging to the same island have the same color.

Optimal islanding on the 30-node system, with 9 generators and 5 islands, is a more

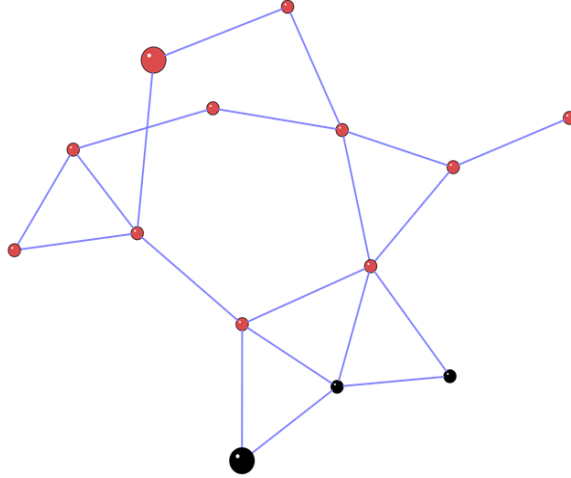


Figure 4.2: Optimal islands for the 14 node system. The two islands are represented in a separate color and all nodes having the same color belong to the same island. The big circles represent the generators and small circles represent the load nodes.

Table 4.1: Average percentage per island of total load remaining in the 14-node system by optimization and the two modularity approaches for 2 islands

Average percentage of total load remaining			
n_{isl}	Optimal	Bloom type	Fast Greedy type
2	86.28	86.28	86.28

challenging case. Hence, we explain this case in detail. We apply the optimal islanding strategy on the IEEE 30-node system with 5 islands as the input. The topology of the islands and their topological complements are shown in Figure 4.3. The dotted lines (- -) are the transmission lines that interconnect every island with its topological complement. Sub-figures [a]-[e] represent individual islands connected to their topological complement and sub-figure [f] represents the complete 5-island structure. Every island is represented by a separate color and all nodes of the same color belong to an island. The gray colored nodes belong to the topological complement of the island in each sub-figure. The big circles represent the generators and the small circles represent the load nodes.

As shown in Figure 4.3, every island has at least one generator and two transmission lines to guarantee the island connectivity. In addition, the test results show that due to line

capacities, a few nodes experience load shedding but majority of the loads do not need any load shedding. Hence, the power generation is reduced at some generators. Another reason that a generator reduces its output power is that the total load in the island becomes less than its normal output generation. Table 4.2 shows the results for the 30-node system with 9 generators and 5 islands. The optimization can converge up to at most 5 islands. The table indicates that the optimization performs better than the modularity-based methods in this case. Each merging decision made by these two methods is irreversible such that the local improvement at one step might not prove to be the best choice eventually and might lead to situations such as the one with the 30-node system where these methods give solutions which are below the optimal. Refinements to these methods might help to improve their performance to give results closer to optimal solution. Nevertheless, still approximately 60% of the load is maintained using these approaches which is a substantial gain when compared to the collapse of the entire system. Figure 4.4 represents the different islanding structures for the optimal, Bloom type and, the Fast Greedy type approach respectively. This difference in the islanding structures is an indication of the difference in the amount of load shedding by the different methods.

Table 4.2: *Average percentage per island of total load remaining in the 30-node system by optimization and the two modularity approaches for 5 islands*

Average percentage per island of total load remaining			
n_{isl}	Optimal	Bloom type	Fast Greedy type
5	93.84	60.65	59.94

In Tables 4.3, 4.4, 4.5, we show the results for the 57-,118- and the 247-node systems for the two modularity-based methods. Since the optimization is not scalable for networks much larger than 30-nodes, further tests are done using only the Fast Greedy and Bloom approaches.

For the 57-node network, both the methods perform very well and preserve 95-96% of the load in the network. There are 2 generators in this network and so the tests were

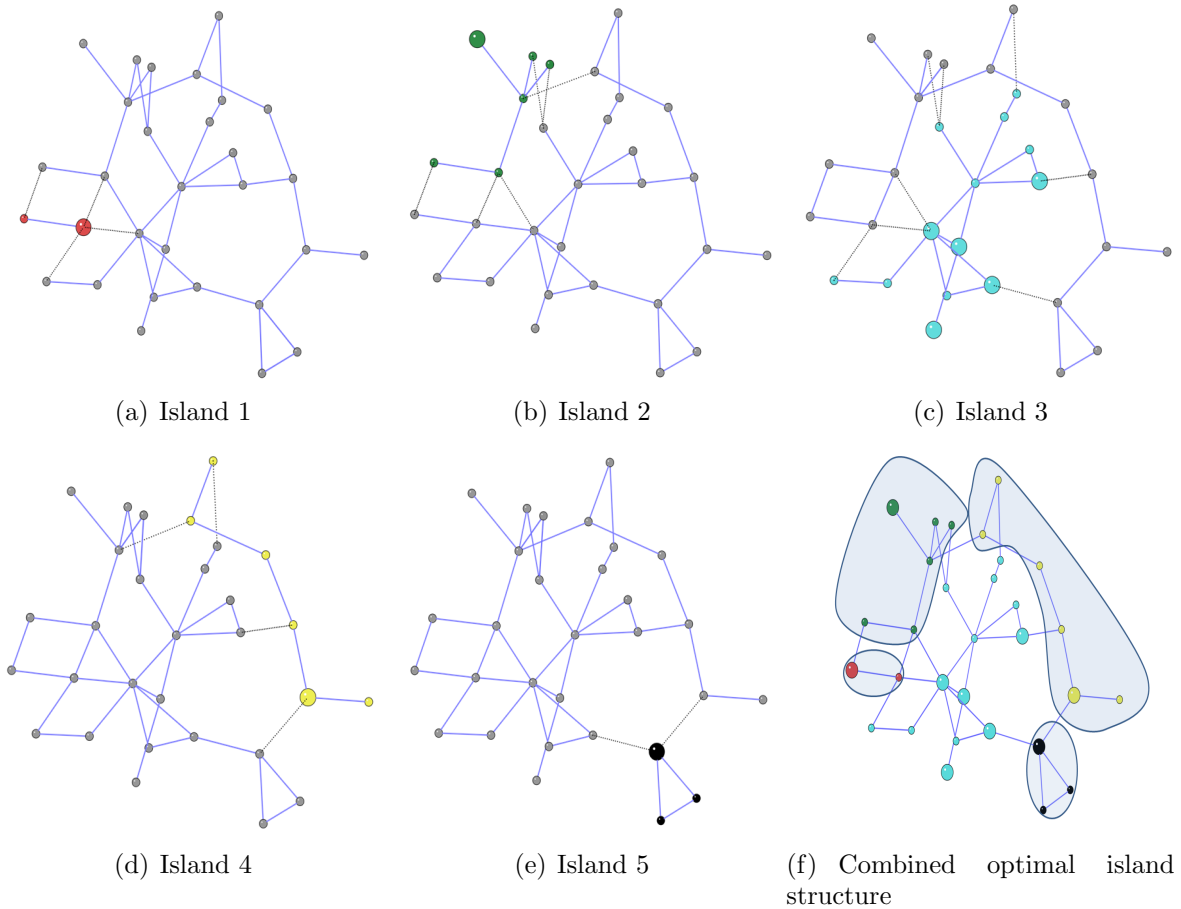


Figure 4.3: *The optimal islanding solution for the 30-node system. The system has 9 generators and 21 load nodes. Every island is represented by a separate color and all nodes having the same color belong to the same island. The big circles represent the generators and small circles represent the load nodes. The sub-figures 4.3(a)-4.3(e) represent the 5 individual islands and the sub-figure 4.3(f) represents the combined optimal islanding solution. The generators are only shown in the respective island in sub-figures 4.3(a)-4.3(e).*

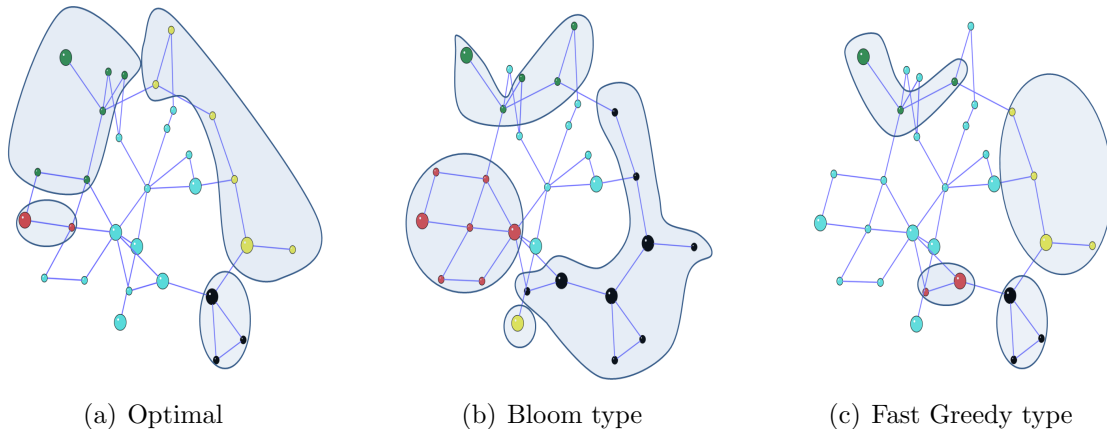


Figure 4.4: *The 5-island scenario for the 30-node system using optimization (a), Bloom type approach (b) and the Fast Greedy type approach (c). The difference in the island structure from these three approaches leads to different amounts of load shedding in the system.*

carried out for 2 islands. We did not add more generators to this network as in the earlier case of the 30-node network because we wanted to test the approaches on the original network, without altering the existing generation and load. In the previous case of the 30-node network, modifications were made to fully exploit the possibilities with the optimization problem and to see the limits to which it may be used.

Table 4.3: *Average percentage per island of total load remaining in the 57-node system by the two modularity approaches for 2 islands*

Average percentage per island of total load remaining		
n_{isl}	Bloom type	Fast Greedy type
2	95.42	95.91

For the 118-node system, we tested the two approaches for different number of islands from 2 to 6. For each case, we see that the Bloom type approach performed better than the Fast Greedy type and the two approaches, in general, showed a good performance. We also see that the Bloom type method has the minimum load shedding with 3 islands whereas the

Fast Greedy type has its best results with 6 islands. Figures 4.5 and 4.6 show the 6 island structures for the 118-node system with the Bloom and the Fast Greedy type approaches respectively. Again, different islands are represented by different colors and the big circles represent the generator nodes.

For the 247-node system, once again, in general, Bloom type method performs better than the Fast Greedy type. The best case for the Bloom type approach is the one with 2 islands in which it preserves about 68% of the system load. On the other hand, the Fast Greedy type performs the best with higher number of islands with about 59% system load preserved for 5 and 6 islands.

Table 4.4: *Average percentage per island of total load remaining in the 118-node system by the two modularity approaches for different number of islands*

Average percentage per island of total load remaining		
n_{isl}	Bloom type	Fast Greedy type
2	83.98	77.52
3	86.36	77.43
4	84.81	78.31
5	83.76	78.76
6	83.03	78.81

Table 4.5: *Average percentage per island of total load remaining in the 247-node system by the two modularity approaches for different number of islands*

Average percentage per island of total load remaining		
n_{isl}	Bloom type	Fast Greedy type
2	68.44	55.74
3	63.36	43.87
4	59.89	56.93
5	57.92	59.56
6	56.65	59.33

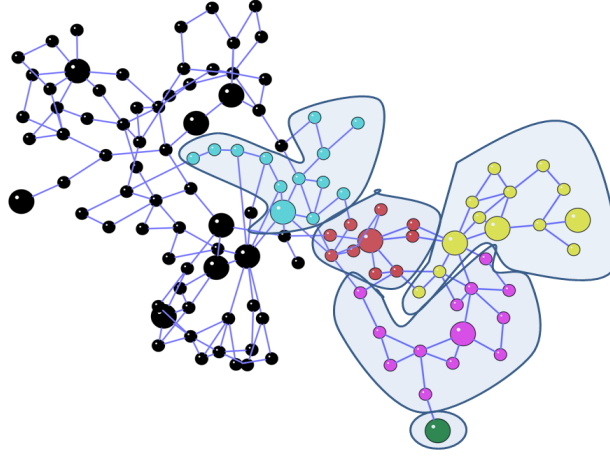


Figure 4.5: *The 6-island scenario for the 118-node system using Bloom type approach. Every island is represented by a separate color and all nodes having the same color belong to the same island. The big circles represent the generators and small circles represent the load nodes.*

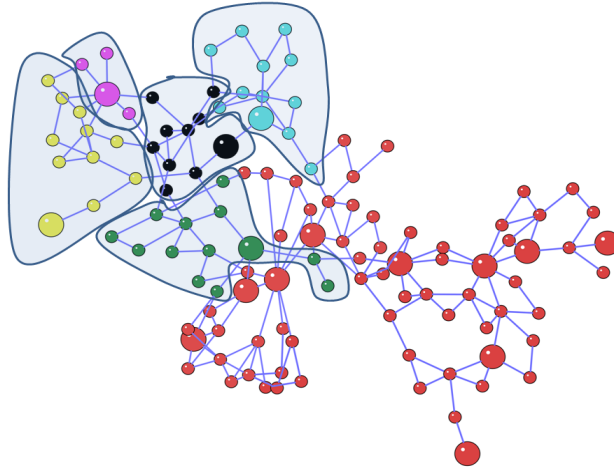


Figure 4.6: *The 6-island scenario for the 118-node system using Fast Greedy type approach. Every island is represented by a separate color and all nodes having the same color belong to the same island. The big circles represent the generators and small circles represent the load nodes.*

4.5.1 Island Characterization - Modified Fast Greedy and Modified Bloom Methods

As can be seen from the results above, the modified Bloom algorithm gives a better solution for the islanding structure than the modified Fast Greedy algorithm. This can be said because it not only is less complex and gives results in shorter time, but also the amount of load shedding that is needed with the modified Bloom is less than that needed with modified Fast Greedy. However, it may be possible to obtain much more useful information about the effectiveness of the methods and the stability of the islands through their structural properties. Tables 4.6 and 4.7 show the characteristics of the different islands of the 118-node network with the modified Fast Greedy and modified Bloom, respectively. The 118-node network has 6 islands with both the methods. However, with the modified Bloom method, one of the islands is an individual node, which is both a generator as well as a load. The characteristics of this island have not been considered in this analysis.

Table 4.6: *Characteristics of islands created by modified Fast Greedy method for the 118-node network*

	I1	I2	I3	I4	I5	I6
Clustering coefficient	0.238s	0	0.11	0	0.13	0
Diameter	11	6	6	2	5	5
Radius	6	3	3	1	3	3
Characteristic path length	5.162	2.636	2.949	1.5	2.618	2.356
Average node degree	3	2.167	2.154	1.5	2	2

Table 4.7: *Characteristics of islands created by modified Bloom method for the 118-node network*

	I1	I2	I3	I4	I5
Clustering coefficient	0.154s	0.205	0.208	0.208	0.123
Diameter	8	3	6	5	10
Radius	4	5	3	3	5
Characteristic path length	3.436	2	2.705	2.487	5.138
Average node degree	2.154	2.2	2.308	2.615	2.912

As seen from the tables, the general observation for all islands created by each of the two methods is that the clustering coefficient of all the islands by the modified Bloom method

is higher than the clustering coefficient of the islands created by the modified Fast Greedy method. In some of the islands by Fast Greedy, the clustering coefficient is 0, indicating that the nodes of the islands created by the modified Bloom method are better connected to each other. The diameters and radii of the individual islands of the modified Bloom are smaller than the individual islands of the modified Fast Greedy. This indicates that the nodes in the modified Bloom type islands are closer to each other. The most important of the properties is the characteristic path length. A shorter characteristic path length indicates that it is easier to reach the distant nodes. As far as the characteristic path length is concerned, the results are mixed for the two methods. There is no consistency as such, some of the modified Bloom islands have a shorter characteristic path length, while some of the modified Fast Greedy islands have a shorter characteristic path length. As observed, the modified Bloom islands seem to have a more robust structure than that of the modified Fast Greedy due to the closeness of the nodes in the former method, but it is not easy to say which of the two methods is better without performing the vulnerability analysis to test the efficiency of the schemes.

4.6 Discussion

Intentional islanding in power systems has become an important subject of research because there is a need to find efficient solutions for the increasing frequency of blackouts. We explored two different schemes for intentional islanding in power grid - 1) Modified Bloom and 2) Modified Fast Greedy approaches, both based on modularity, and compared their results with that of an optimal islanding scheme. The optimization formulation considers two parts of the system - the island and its topological complement - and works towards minimizing the load shedding in both parts of the system. It is capable of forming multiple islands and is a very efficient scheme for small networks, maintaining about 80-90% of the load after islanding. However, due to its exponential complexity, this method cannot be used for large networks.

We developed two approaches based on modularity, with the DC power flow model incorporated into them, for islanding in medium and large networks. The Bloom type and the Fast Greedy type methods were tested for the 57-, 118- and the 247-node networks, in addition to the 14- and the 30-node networks. These approaches also had the objective of minimizing load shedding, both in the island and the complement. They, in general, performed efficiently for all these systems, maintaining, at an average, at least 50% of the total load in the network.

It was imposed that every island must have at least one generator for independent survival. With more distributed generation, there would be better islanding opportunities and these methods will be well suited for the power grid of the future.

The characterization of islands obtained using the two methods does not throw much light on the quality of the islands, and do not give an indication of whether the islands formed by one method are more robust than the islands formed by another method. Vulnerability analysis of the grid, with island formation based on both the methods must be performed to understand which of the two methods gives more robust islands.

Chapter 5

Mitigation Strategies - Controlled Distributed Generator Placement in Transmission Grid based on Electrical Measures

5.1 Introduction

According to¹³², distributed generation refers to small electric power generators, typically ranging in capacity from 15 to 10,000 kW, which can be located on the utility system, at the customer site, or at a location not connected to the grid. Distributed generation can be conventional, such as combined cycle turbines, small diesel generators, combustion turbines, or renewable, such as wind turbines, and solar generation. In this chapter, we propose the use of distributed generators (DGs) in the transmission system as a strategy to mitigate cascading failures. While the use of DGs is common in the distribution system, little research has been conducted in the field of complex networks regarding the use of DGs in the transmission system and the mitigation of cascading failures.

Although distributed generators present their own challenges, their importance continuously increases because of their advantages, such as providing local power, thus preventing power transport over long distances, which, in turn, also improves grid reliability. This work focuses on placement of conventional distributed generators in the transmission system. Re-

newable energy sources can be treated as a separate area of study. The placement and sizing of DGs is done based on the relative importance of nodes in the system, obtained using two electrical measures: electrical centrality and electrical node significance.

5.2 Related Work

A lot of work has been done in the area of DG placement in the distribution network^{51, 116, 78, 5, 109}. Among the few studies on the placement of DGs in the transmission system,⁴⁰ discusses the impact on grid dynamics if the grid is powered using DGs. The authors, in this work, assert that different dynamics can be seen on the grid by varying the fractions and distributions of DGs in the transmission system. They use a dynamic model of the power transmission grid, called the OPA model²², to perform this analysis. They also mention that improper distribution and sizing of the DGs may lead to increased vulnerability of the grid instead of increased robustness. In¹¹², the authors discuss that the stability and reliability of the grid improves with the use of conventional DGs close to the loads, but if an increasing penetration of stochastic renewable energy sources is present in the grid, these energy sources introduce erratic power inputs into the grid, thereby causing it to fail with a sharp transition.

The authors of⁸¹ use a topological approach to discuss how the interconnection of several DGs in the transmission system causes a structural change in the grid and, therefore, how properties of the system would change. The authors used indices, such as characteristic path length, degree and degree distribution, clustering coefficient, and betweenness to decide how the interconnection of DGs affects topological characteristics of the grid. They have also used weighted graph indices and have suggested new indices based on structure and operational conditions of the grid for the evaluation of structural properties of the grid with incorporated DGs. Similar analysis, based on certain indices, is conducted by the authors of²¹. They proposed three vulnerability indices, Structural Vulnerability Index (SVI), Contingency Vulnerability Index (CVI), and Operational Vulnerability Index (OVI), which were used to evaluate topological vulnerability, in order to identify the vulnerable

component in the grid and determine operational states of the network, respectively.

The main contribution of the work described in this chapter is to propose a simple yet effective method for the placement of DGs in the transmission system, based on two electrical measures, electrical centrality and node significance, and show that this placement of distributed generators enhances the robustness of the power grid network and prevents cascading failures. Vulnerability analysis is performed before and after the placement of the DGs using the DC Power Flow model⁴⁹ and the Overload Cascade model⁹⁵. Results of our method are also compared with results of an existing method, called Method II here, for simplicity. Our method gives better results than Method II, for robustness improvement in terms of load retained in the network after a link failure, for all possible cases.

5.3 Topological and Electrical Structure of Power Grids

As discussed previously, extensive research has been conducted in vulnerability analysis of power grids in the field of complex networks. However, most work in this area has considered only topological properties of the network. While analyzing a complex network, such as a power grid, it is important to consider flow dynamics of the network. Topological measures, such as, node degree and betweenness cannot capture all properties of the electrical network. However, the field of complex networks and topological analysis provide useful insights into network structure. Hence, topological measures, combined with electrical measures and power flow models, can be used for the study of power grid networks.

Previous studies on power grid have described it as a scale-free network, while other studies have claimed that it is a small-world network⁹. However, these claims are based on topological properties. In reality, structure of a power grid does not fit into any particular category of network models exactly, as is the case with most real-world networks. In⁵⁸, the authors distinguished between the topological and electrical structure of power grids, by means of a measure called electrical centrality. Additional information on electrical centrality is given in the following subsection.

5.3.1 Electrical Centrality

Electrical centrality is a measure used in topological analysis of power grid networks, which differentiates electrical structure of the grid from its topological structure. Electrical centrality uses the impedance matrix, or the Z_{bus} matrix of the transmission system, to determine which nodes are more electrically central to the system and indicates them as candidate locations for the placement of DGs. The measure was introduced in⁵⁸. Several discussions have occurred regarding physical topology of the power grid. However, the electrical topology of the grid indicates that power grids possess “electrical hubs”, thus, indicating that some nodes in the power grid have strong electrical connections with other parts of the network. This phenomenon is very different from the physical topology of power grids as their average degree is usually between 2 and 5, indicating the absence of hubs. As mentioned, electrical centrality is calculated using the Z_{bus} matrix, which in this dissertation is computed as the inverse of the Y_{bus} matrix or the admittance matrix of the system. The Y_{bus} matrix is usually sparse, and, hence, the Z_{bus} matrix is obtained as a dense matrix. Every element in the matrix represents an equivalent electrical distance between two nodes. Figures 5.1 and 5.2 show the physical and electrical topology of the 57-node network, and Figures 5.3 and 5.4 show the physical and electrical topology of the 118-node network, respectively³¹. In Figures 5.2 and 5.4, the size and color of the nodes indicate their relative importance in the network, with electrical centrality decreasing as the size decreases. In Figure 5.2, the large green nodes represent nodes with the highest centrality, or the highest number of electrical connections in the network. Similarly, for Figure 5.4, the largest green nodes represent the highest centrality nodes, followed by the cyan and the purple nodes. The small red nodes are the nodes with very small electrical centrality.

Since the Z_{bus} matrix is a non-sparse, dense matrix, there are $\frac{N(N-1)}{2}$ different electrical connections possible. However these figures show the most important L connections to match with the number of connections in the physical topology. For example, the 57-node network has 78 links in the physical topology. There are 1596 different electrical connections

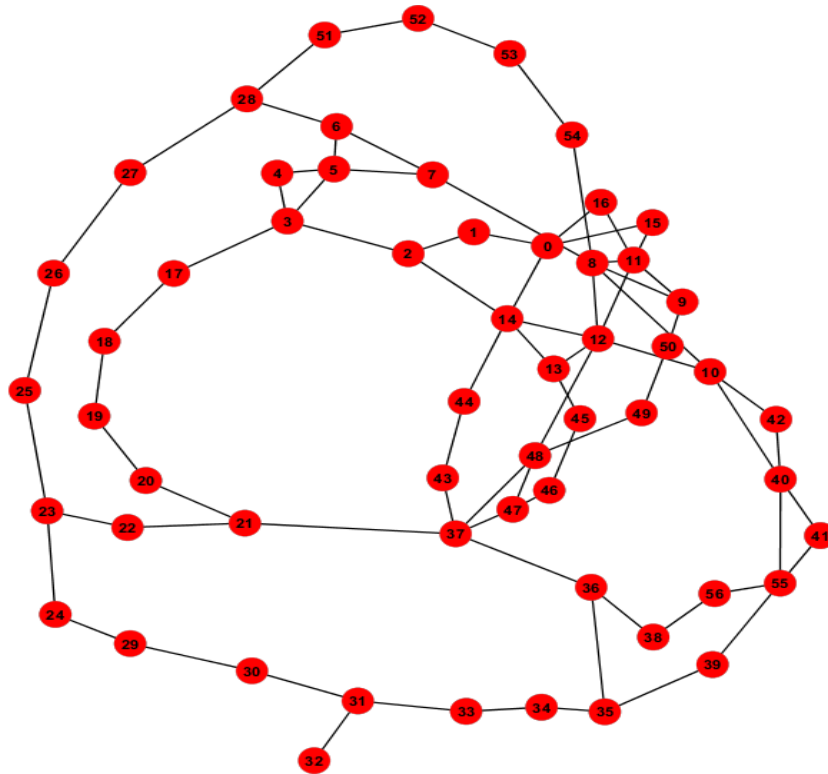


Figure 5.1: *This figure represents the physical structure of the 57-node network, showing the physical connections between the nodes. This is the actual topology of the 57-node network and the average node degree for this network is between 2 and 3. There are no “hub” nodes present in the network.*

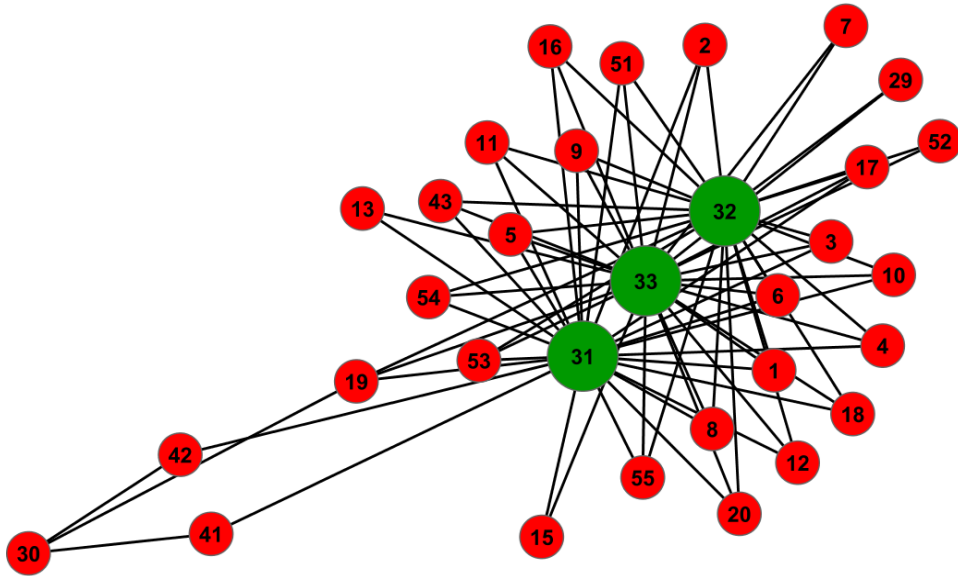


Figure 5.2: *The electrical topology of the 57-node network is represented in this figure. The relative electrical importance of the nodes is shown by their size and color. The big nodes in green are the most electrically central nodes having the maximum electrical connections. The remaining small nodes in red are much less connected, electrically, to the rest of the network. The Z_{bus} matrix, from which the electrical centrality is derived, is a non-sparse matrix and the possible number of electrical connections is $\frac{N(N-1)}{2} = 1596$, for the 57-node network. Only $L = 78$ strongest connections are shown in this picture, where L is the number of links in the physical topology, and this picture shows the existence of “electrical hubs” in the network.*

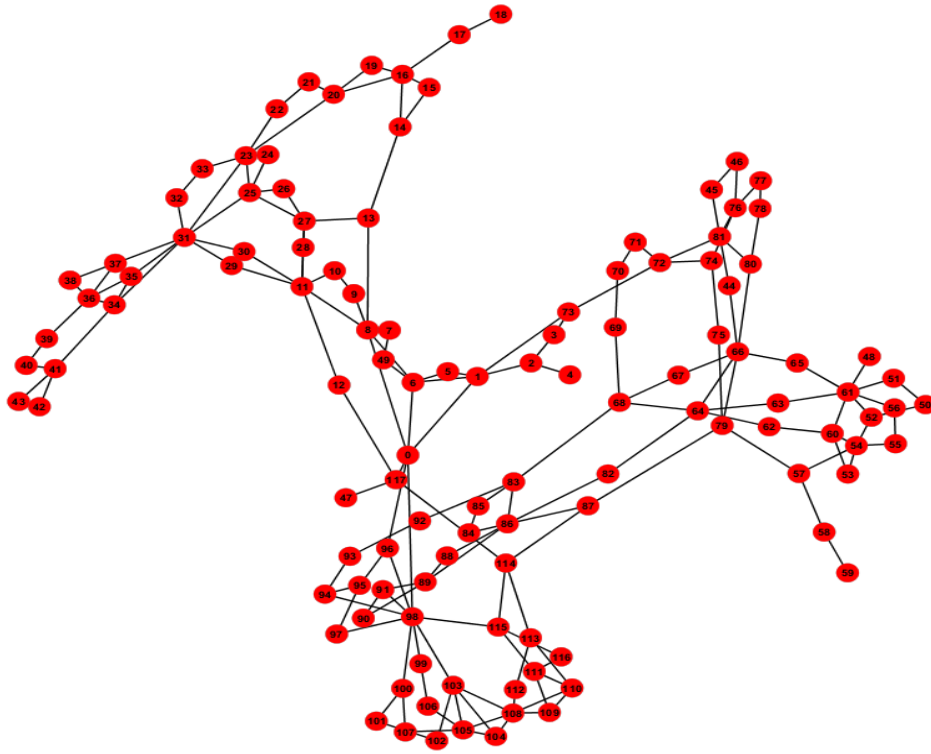


Figure 5.3: *This figure represents the physical structure of the 118-node network, showing the physical connections between the nodes. This is the actual topology of the 118-node network and the average node degree for this network is between 2 and 3. There are no “hub” nodes present in the network.*

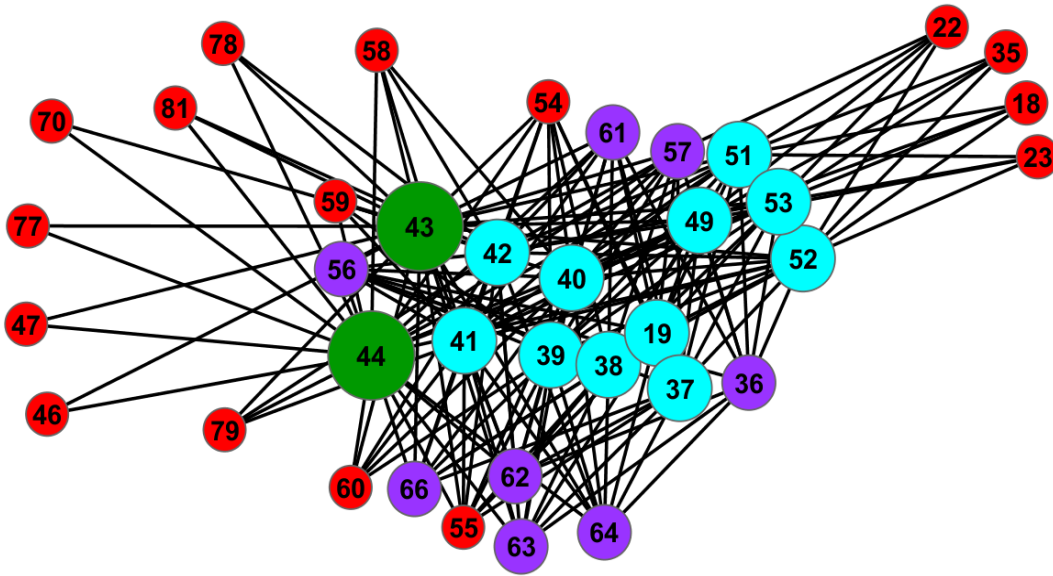


Figure 5.4: *The electrical topology of the 118-node network is represented in this figure. The relative electrical importance of the nodes is shown by their size and color. The big nodes in green are the most electrically central nodes, followed by the slightly smaller nodes in cyan, and then in purple. The remaining small nodes in red are much less connected, electrically, to the rest of the network. The Z_{bus} matrix, from which the electrical centrality is derived, is a non-sparse matrix and the possible number of electrical connections is $\frac{N(N-1)}{2} = 6903$ for the 118-node network. Only $L = 179$ strongest connections are shown in this picture, where L is the number of links in the physical topology, and this picture shows the existence of “electrical hubs” in the network.*

possible. However, the strongest 78 electrical connections are shown in order to match with the number of connections of the physical topology.

5.3.2 Electrical Node Significance

The authors of¹³⁵ have proposed a metric to quantify the robustness of power grid networks with respect to cascading failures by targeted attacks. This robustness metric is a product of different values, one of which is electrical node significance. The concept of electrical node significance ranks nodes as more or less significant, depending on the quantity of power that is distributed by them to the rest of the network. In terms of power systems, electrical node significance is defined as follows:

$$\delta_i = \frac{P_i}{\sum_{j=1}^N P_j}$$

where P_i is the total power distributed by node i and N is the number of nodes in the network. This equation indicates that if node i distributes a large quantity of power and a link which carries power out of this node is disconnected, a portion of the large quantity of power being delivered by node i must be redistributed to other parts of the network, thus leading to further failures. Consequently, node i is electrically significant. Significant nodes for the 57- and the 118-node networks are shown in Figures 5.5 and 5.6.

5.3.3 Method for Placement of DG in the Transmission System

Correct placement of DG in the transmission system is of strategic importance to improve robustness of the grid. Incorrect placement may make the grid more vulnerable to failures or attacks. Two measures were utilized, electrical centrality and electrical node significance, in order to locate nodes where DGs can be placed. The size of the DGs depends on the relative importance of the nodes. Our experiments suggest that the use of electrical centrality or node significance alone does not fulfill the purpose of the analysis. However, when both metrics are used together, significant improvement is noted in the results.

The first step of the procedure is to calculate electrical centrality and node significance

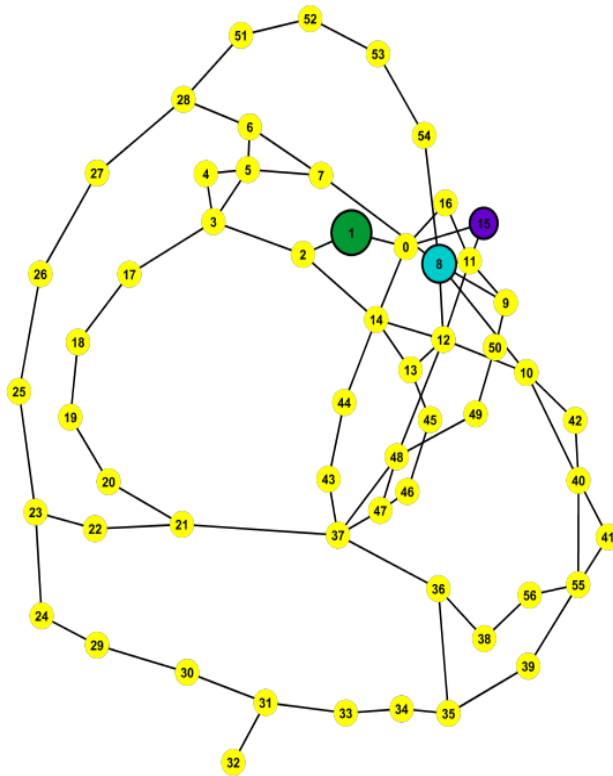


Figure 5.5: *The electrical significance of nodes for the 57-node network is shown in this figure. The relative importance of the nodes is shown by their size and color. The biggest node in green is the most significant node, followed by the slightly smaller node in cyan, and then purple. All the other small yellow nodes are the common nodes of the network, with very small values of electrical significance.*

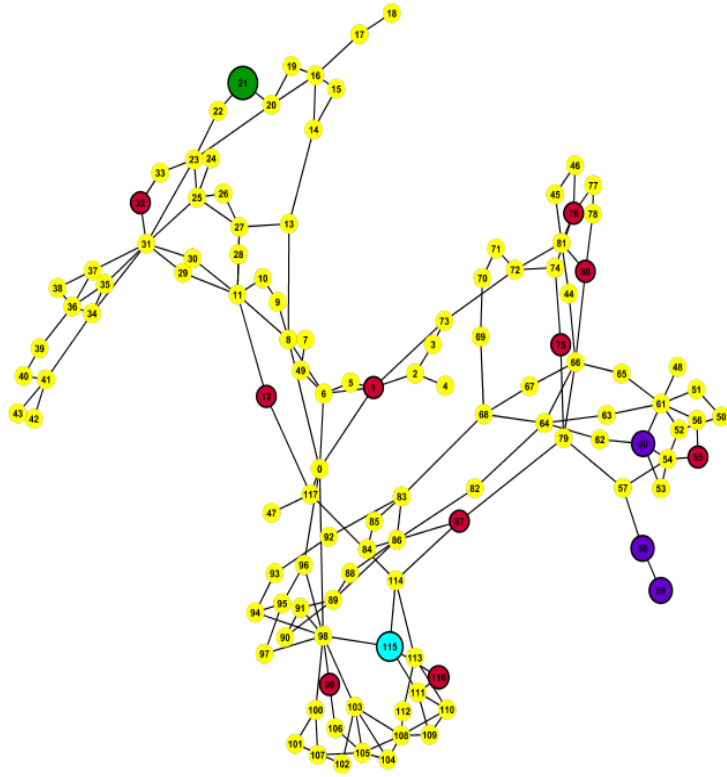


Figure 5.6: *The electrical significance of nodes for the 118-node network is shown in this figure. The relative importance of the nodes is shown by their size and color. The biggest node in green is the most significant node, followed by the cyan node, purple nodes, and red nodes. All the other small yellow nodes are the common nodes of the network with small values of electrical significance.*

of every node in the network. This calculation gives a clear indication of which nodes are more important nodes in the network and offers a candidate set of locations where DGs can be placed. We observed that for all the test networks, most nodes indicated by electrical centrality differed from those indicated by electrical node significance. This shows that different methods can indicate multiple possibilities of locations for DG placement. Individually, they can produce slightly satisfactory results, but with a combination of these methods, the quality of results can be enhanced. The electrically central nodes occur together in groups. For small networks such as the 30- and the 57-node networks, all electrically central nodes were found in a single group of adjacent nodes. For large networks, few distinct groups of electrically central nodes were obtained, as indicated by Fig. 5.4. However, electrically significant nodes were spread throughout the networks.

In this work, we consider that all generation is obtained through DGs. For small networks, we selected only the most central node from the set of electrically central nodes since placing excess generation in one area can actually make the grid more vulnerable rather than robust. Remaining generators were selected from among different electrically significant nodes. Generators which were a part of the original network always appeared in the set of candidate locations for DG, either as electrically central nodes or as electrically significant nodes. However, depending on the relative importance of these nodes as compared to all other nodes in the candidate set, their generation was either increased or decreased. Deciding the size of the DGs in terms of percentage of total generation was an exhaustive process within the final set of locations selected from the candidate set. The final set consisted of 4-20 locations for DG placement, depending on the size of the network.

Vulnerability analysis was performed using the DC Power Flow model and the Overload Cascade model. Results showed that the placement of DGs obtained by the above procedure significantly improved the robustness of the power grid against cascading failures and more load could be saved as compared to the original network. In order to show the effectiveness of this method, results of this method were compared with results of another method proposed

in¹⁴⁰, referred to as Method II for simplicity. The method and results are explained in the following sections.

5.4 Comparison with Method II

The authors of¹⁴⁰ have recently proposed a method based on complex networks theory, to place DGs in the transmission grid and then assess vulnerability of the power grid network. This work discusses the placement of DG in the transmission grid using complex networks theory, for the purpose of improving robustness of the grid. One primary difference between this work and our method is that the authors of¹⁴⁰ consider the power grid to be a weightless graph, indicating that they do not make use of the impedances/admittances of the transmission lines. The other significant difference is the absence of a power flow model in Method II.

In Method II, the authors make use of efficiency and global efficiency metrics, slightly modified to include load and generation information for analysis of the power grid. They use the following definition of efficiency:

$$e_i = \frac{1}{P_{D_i} n_G} \sum_{j \in V_G} \frac{P_{G_j}}{2^{d_{ij}-1}} \quad (5.1)$$

where e_i is the power supplying efficiency of the entire network to the load node i , P_{D_i} is the active load of node i , P_{G_j} is the active capacity of generation node j , d_{ij} is the length of the shortest path between the load node i and the generation node j , V_G is the set of generators, and n_G is the total number of generation nodes in the network. This equation indicates that if the shortest path between a node and a generator is long, the power supplying efficiency to that node will be reduced. The authors used the IEEE 57-node network to test their method, and they calculated the shortest path lengths between all load nodes and all generators, followed by the calculation of power supplying efficiencies of each load node using the above equation. They selected five nodes with the lowest power supplying efficiencies to be locations for DG placement. The locations and sizes of the

already-existing generators was kept the same and five new DGs of a fixed size were added to the network. They also used complex networks based methods for vulnerability analysis. However, as compared to our method, we used the locations for DGs indicated by Method II and performed vulnerability analysis with the power flow and cascade model. Comparison shows that for the 57-node network, our method saves an overall of 8.7% more load than Method II. Detailed analysis of results are given in the next section.

5.5 Results

The results of the vulnerability analysis of the 57-node network without DGs, with DGs placed using the electrical measures, and with DGs placed using Method II are shown in Figures 5.7, 5.8, 5.9. The X-axis of each figure represents the link id from 1-78, and the Y-axis represents the total load of the system as a per unit (p.u) quantity. The figures are divided into four parts horizontally. The first partition is created at the 25% mark of the total load on the Y-axis. The second partition is created at the 50% mark, and the third partition is created at the 75% mark. These partitions allow to specify the range in which the load can be retained when a particular link is disconnected from the network. The same results are also represented in the form of histograms in Figures 5.10, 5.12, ?? for more clarity and finer information. The X-axis on the histograms represent the total load remaining in the network (pu) and the Y-axis represents the frequency of links in a particular load range. Thus, the histograms give an information about how many links in the network retain the amount of load in a given load range on being the initial failure.

Vulnerability analysis is performed using Overload Cascade model⁹⁶, in which every link is characterized by a finite capacity. The capacity of each link is proportional to the power the link carries when the system is in a stable state. Whenever the power in a link exceeds the capacity of the link, the link is considered failed and is disconnected from the network. Then, the power carried by this link is distributed among other links in the network, depending on the flow dynamics, which are based on the power flow model.

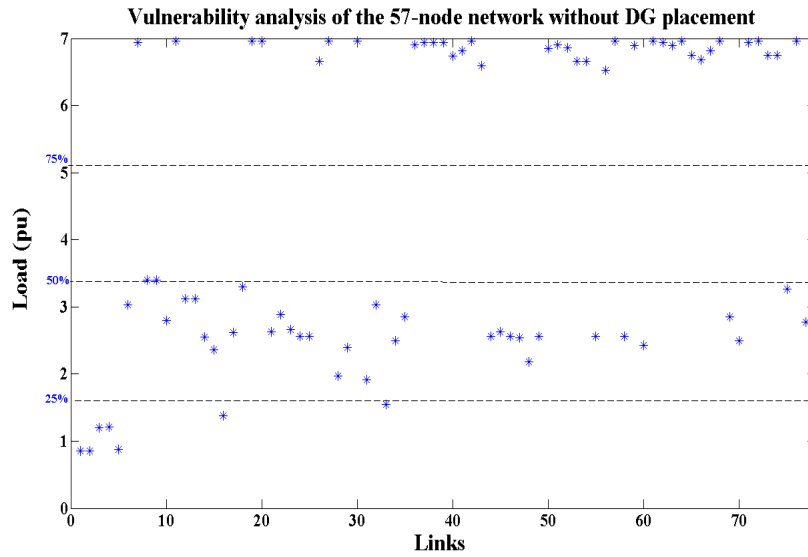


Figure 5.7: This figure represents the results of vulnerability analysis for the 57-node network in the absence of distributed generation. The x-axis represents the link id and the y-axis represents the load remaining in the network, in p.u., when the corresponding link on the x-axis fails. The y-axis is divided into 4 parts: The first partition is created at the 25% mark of the total load, the second partition is marked at 50% load, and the third partition is created at the 75% load level. These partitions help to understand the range in which the load can be retained when a particular link fails. From this figure, it is seen that the load remaining on the network for the vulnerable links is, in general, in the 25-50% range, and for some links, it is also in the 0-25% range. For the non-vulnerable links, failure does not spread across the network and close to 100% of the load can be retained.

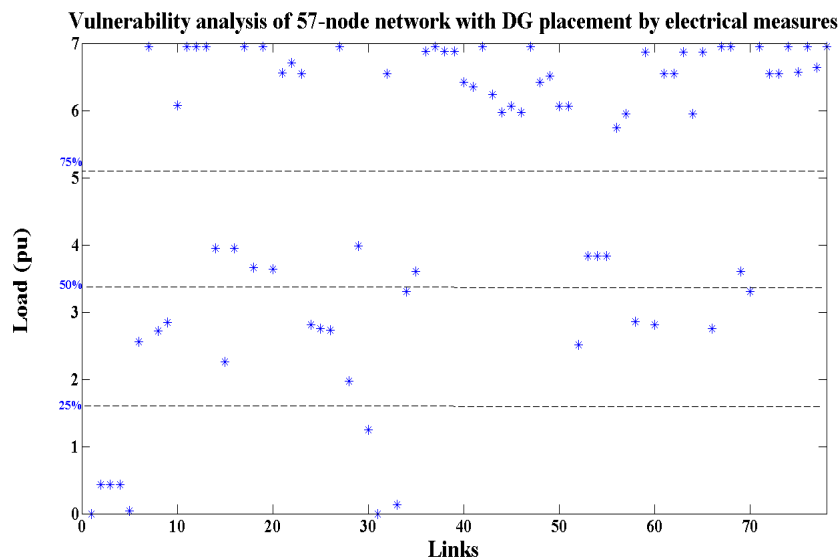


Figure 5.8: This figure represents the results of vulnerability analysis for the 57-node network with DGs placed using the two electrical measures. The x-axis represents the link id and the y-axis represents the load remaining in the network, in p.u., when the corresponding link on the x-axis fails. The y-axis is divided into 4 parts: The first partition is created at the 25% mark of the total load, the second partition is marked at 50% load, and the third partition is created at the 75% load level. These partitions help to understand the range in which the load can be retained when a particular link fails. From this figure, it can be observed that there is a considerable increase in the amount of load that can be retained even due to the failure of vulnerable links. More number of points move into the 75-100% range, few points move into the 50-75% range as compared to no points in this range for the original network without DGs, and some points also move up into the 25-50% range from the 0-25% range, indicating an overall increase in the robustness of the grid. A few points have shifted into the lower-most partition, but this number is not significant as compared to the gain in the overall load.

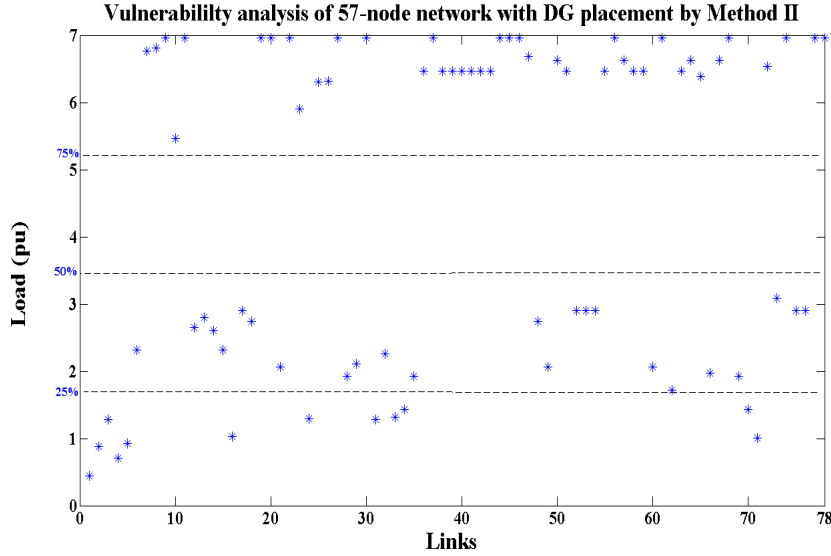


Figure 5.9: This figure represents the results of vulnerability analysis for the 57-node network with DGs placed using Method II. The x-axis represents the link id and the y-axis represents the load remaining in the network, in p.u, when the corresponding link on the x-axis fails. The y-axis is divided into 4 parts: The first partition is created at the 25% mark of the total load, the second partition is marked at 50% load, and the third partition is created at the 75% load level. These partitions help to understand the range in which the load can be retained when a particular link fails. From this figure, it can be seen that the state of the system does not change much as compared to the original network, without DGs. Few points move up into the 75-100% load range, but at the same time, few points move down in the 0-25% range as well. Just as in the case of the original network without DGs, there are no points in the 50-75% load range. This performance of Method II can be attributed to the fact that, although the method considers the presence of loads and generation, it does not consider the presence of a power flow model. The flow distribution is performed using the concept of shortest path, and hence, the results are different from those predicted by this method, when used with a power flow model.

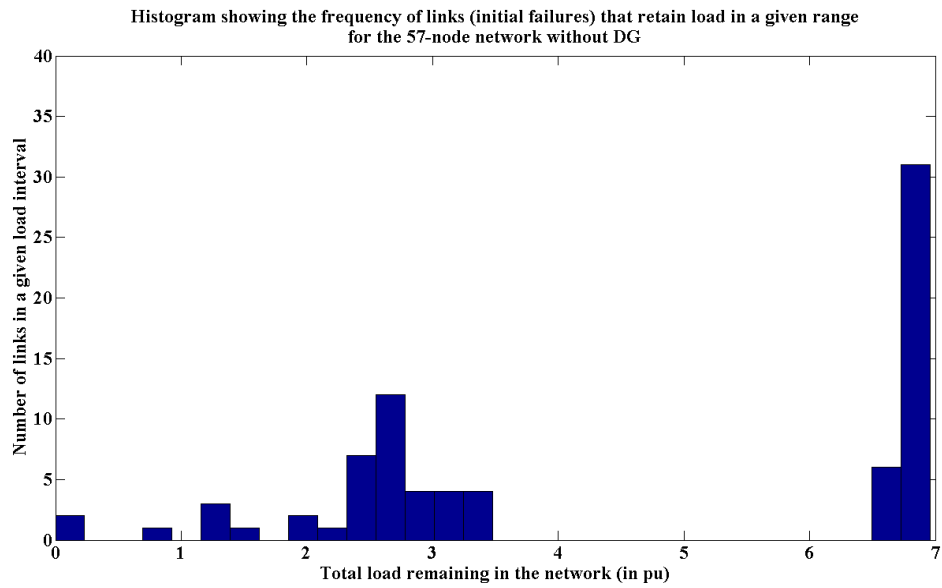


Figure 5.10: *This figure represents the distribution of links that retain load in a given load range in the 57-node network without DG. On the X-axis, the total load remaining in the network as a result of an initial failure is represented in pu. The number of links falling in a given load range represents the number of links that retain the amount of load in that load range when they are the initial failure.*

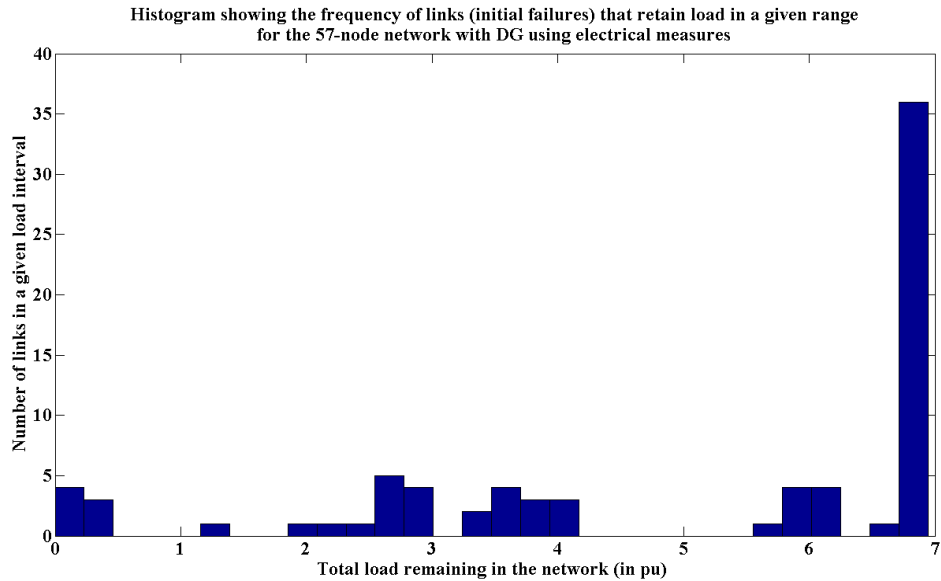


Figure 5.11: *This figure represents the distribution of links that retain load in a given load range in the 57-node network with DG placed in the network using electrical measures. On the X-axis, the total load remaining in the network as a result of an initial failure is represented in pu. The number of links falling in a given load range represents the number of links that retain the amount of load in that load range when they are the initial failure. It is seen that there is an increase in the number of links in the last load range in this network as compared to the network without DG. As represented by the vulnerability analysis graphs, there is a shift from the left to the right side of the histogram.*

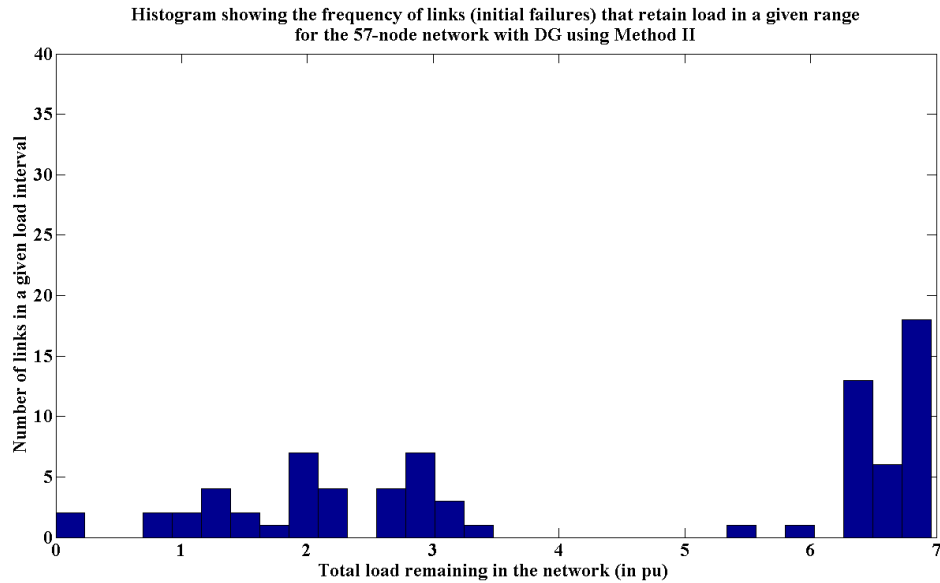


Figure 5.12: *This figure represents the distribution of links that retain load in a given load range in the 57-node network with DG placed in the network using Method II. On the X-axis, the total load remaining in the network as a result of an initial failure is represented in pu. The number of links falling in a given load range represents the number of links that retain the amount of load in that load range when they are the initial failure. It can be seen that although the number of links in the 75-100% load range in the vulnerability analysis is seen for MII as compared with the system without DG, this number is split into the last 3 bins of the histogram and represents an overall increase in the range.*

The range in which the load is saved for different links by various methods for the 57-node network is shown in Table 5.1.

The results of vulnerability analysis of the 118-node network are also shown in Figures 5.13 and 5.14 and these results are not available for Method II. The histograms for the 118-node network without and with DG using electrical measures are shown in Figures 5.15 and 5.16. The range in which the load is saved for different links with and without the presence of the long link for the 118-node network are shown in Table 5.2.

Table 5.1: *Comparison of the results of vulnerability assessment of the 57-node network without DGs, with DGs based on electrical measures, and with DGs based on Method II*

Load range (Percent)	Frequency of links in a load range		
	No DG	DG based on Elec. Meas.	DG based on M II
0 – 25	7	8	13
25 – 50	34	14	26
50 – 75	0	10	0
75 – 100	37	46	39

Table 5.2: *Comparison of the results of vulnerability assessment of the 118-node network without DGs, and with DG placement based on electrical measures*

Load range Percent	Frequency of links in a range	
	No DGs	DGs based on electrical measures
0 – 25	101	44
25 – 50	0	5
50 – 75	1	41
75 – 100	77	89

As shown in Table 5.1, the number of links, the removal of which retains only 0-25% of the load is quite high for Method II as compared to the size of the network. For the 25-50% of the load range, our method has fewer number of links than Method II and the original network. However, the number of links in the 50-75% range is 0 for both, the original network and Method II. Our methods improves the load level for certain links which were in the 25-50% range in the original network, up to the 50-75% range, clearly showing that the system performs significantly better in the case where DGs are placed on nodes that

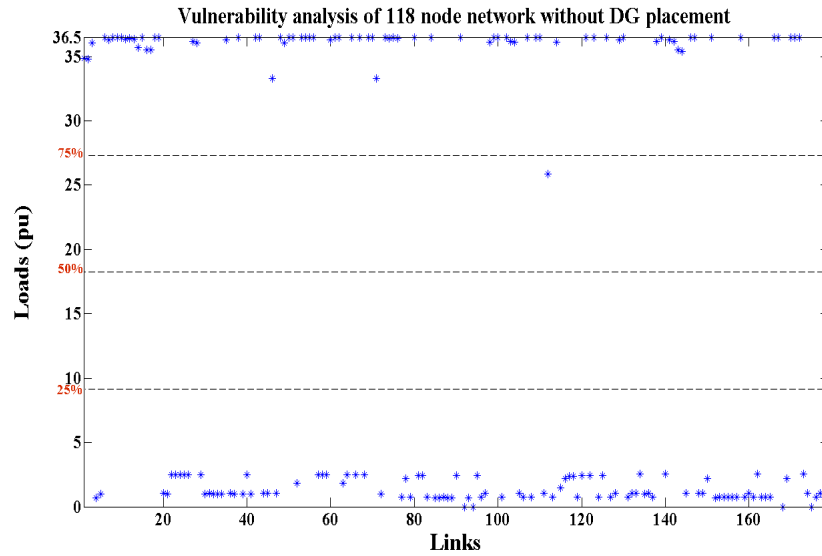


Figure 5.13: This figure represents the results of vulnerability analysis for the 118-node network in the absence of distributed generation. The x-axis represents the link id and the y-axis represents the load remaining in the network, in p.u., when the corresponding link on the x-axis fails, with partitions at 25%, 50%, and 75% of total load. From this figure, it is seen that all the points are either in the 0-25% range or in the 75-100% range, indicating that a vulnerable link causes a complete breakdown of the 118-node network and a non-vulnerable link retains almost all the load in the network.

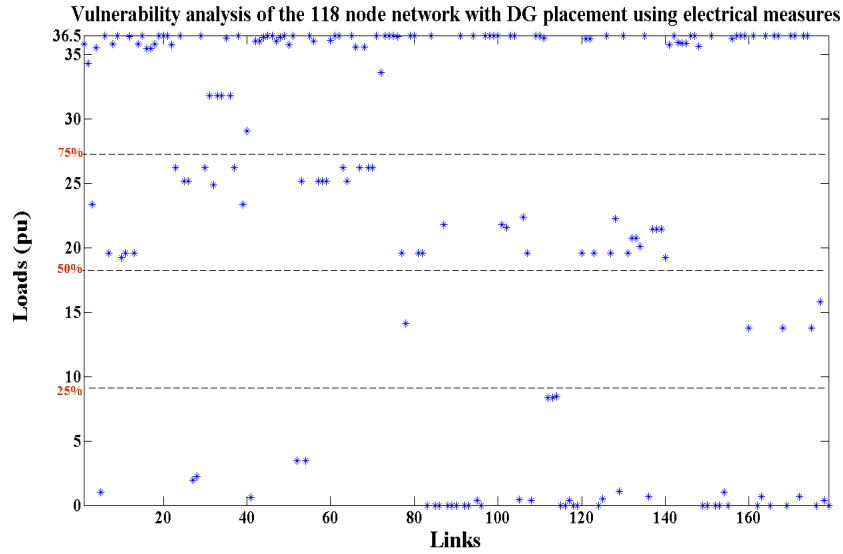


Figure 5.14: This figure represents the results of vulnerability analysis for the 118-node network with DGs placed using the two electrical measures. The x-axis represents the link id and the y-axis represents the load remaining in the network, in p.u., when the corresponding link on the x-axis fails, with partitions at 25%, 50%, and 75% of total load. In this figure, it is easily noticeable that many points from the 0-25% load range move up into the 50-75% load range, with a few points also moving into the 75-100% and in the 25-50% load range. This indicates that a substantial reduction in the level of vulnerability of the network occurs due to the placements of DGs in the network, using the electrical measures.

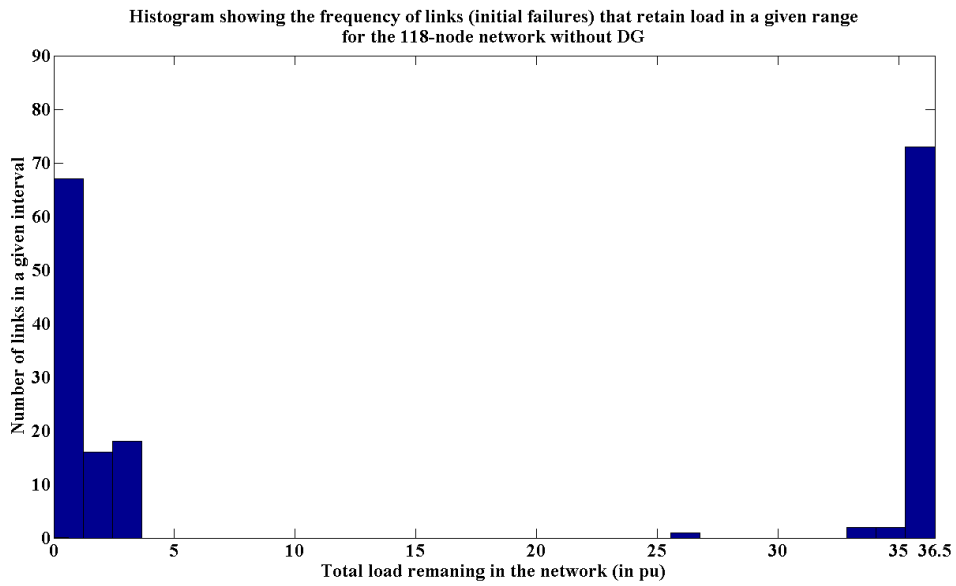


Figure 5.15: *This figure represents the distribution of links that retain load in a given load range in the 118-node network without DG. On the X-axis, the total load remaining in the network as a result of an initial failure is represented in pu. The number of links falling in a given load range represents the number of links that retain the amount of load in that load range when they are the initial failure.*

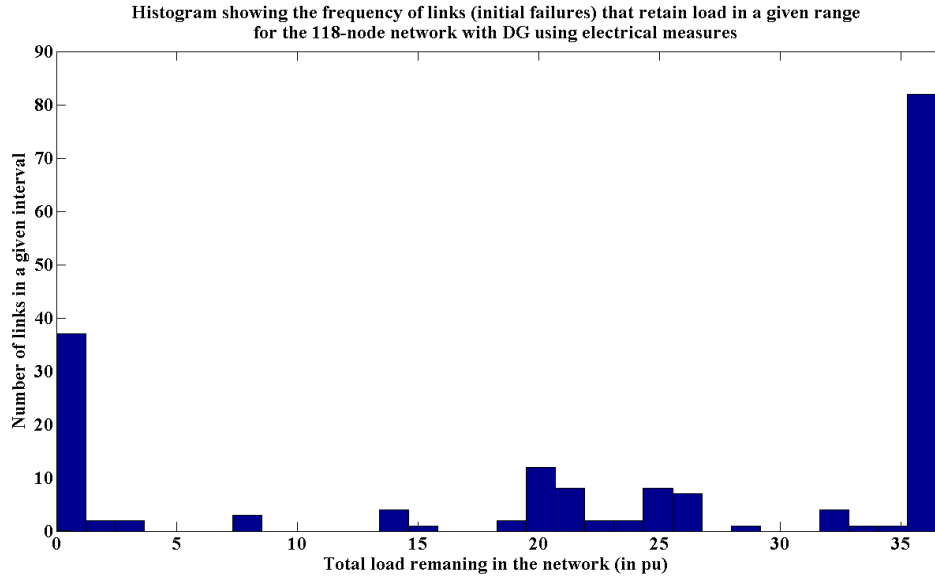


Figure 5.16: *This figure represents the distribution of links that retain load in a given load range in the 118-node network with DG placed in the network using electrical measures. On the X-axis, the total load remaining in the network as a result of an initial failure is represented in pu. The number of links falling in a given load range represents the number of links that retain the amount of load in that load range when they are the initial failure. It is seen that there is an increase in the number of links in the last load range in this network as compared to the network without DG. As represented by the vulnerability analysis graphs, there is a shift from the left to the right side of the histogram.*

are selected based on electrical measures. Similarly, Figures 5.10 and 5.12, and Table 5.2 demonstrate that the robustness of the 118-node network with DGs is much higher than the network without DGs. Table 5.2 shows a significant change in the number of links whose removal brings the load in the 0-25% range. Also, a significant increase in the number of cases where the remaining load on the network is in the 50-75% or in the 75-100% range is present. We observed that an overall improvement of 19.69% in robustness is achieved by placement of DGs for the 118-node network. Results for this network by Method II are not available.

5.6 Discussion

In this chapter, we have proposed a simple yet effective method based on electrical measures in order to place DGs in the transmission system as a strategy to prevent cascading failures. The presence of DGs enables power supply to the loads locally, without the need to supply power over long distances, thereby improving reliability, reducing transmission and distribution costs, and reducing system losses. The DGs are placed using two measures, electrical centrality and electrical node significance. Electrical centrality differentiates between the topological and electrical structure of the power grid, highlighting “electrical hubs” in the system which are the high electrical centrality nodes. Node significance selects more significant nodes in the system by their power distribution ability in the system. The method involves choosing a correct combination of the most important nodes in the network and placing DGs with sizes according to the relative importance of those nodes. Results indicate that the placement of DGs by this method improves the robustness of the 30-node network by 5%, that of the 57-node network by 9%, and improvement in the 118-node network is approximately 20%. The method also performs better than Method II in all cases for the 57-node network. Results for other networks by this method are not available.

Chapter 6

Mitigation Strategies - Addition of a Link in the Transmission Grid based on Spectral Distance Method

6.1 Introduction

As can be seen from the discussion before, even a small change in the structure of the network causes the properties of the network to change. Besides the physical properties of a network, another set of properties exist, called the spectral properties of the network. The spectrum of a network is the entire range of eigenvalues that are obtained from the matrices of the network, such as the adjacency matrix and the Laplacian matrix. Just like the physical properties of the networks, spectral properties also hold a lot of useful information about the network. There is a set of eigenvectors associated with the spectrum of any network, one eigenvector corresponding to each eigenvalue. Sometimes, it is more useful to look at the spectral properties of the network for certain kinds of analyses, including robustness analysis. The second smallest eigenvalue of the Laplacian matrix is called algebraic connectivity and it is used a lot in the robustness analysis of complex networks, due to its close connection to the node and link connectivity metrics. In this chapter, we describe the utilization of the spectral properties of the power grid network to devise a method to find the location where a link must be placed in the network, in order to enhance the robustness of the network. The idea is to check if the reduction in the average spectral distance of the network helps

to make it more robust, and provide a method for the reduction of the average spectral distance by means of strategic placement of an additional link in the network.

6.2 Related Work

Topological characteristics of complex networks have often been linked to the robustness of the network, with respect to random failures as well as intentional attack. Several researchers have shown that by adding long range links in the network, the robustness of the network to attacks can be improved^{131, 98, 85}. The main property of the networks considered in all of these works is long range links. Long range links contribute to a shorter average path length, also known as the characteristic path length, which in turn contributes to the robustness of the networks.

The topology of real networks like power grids traditionally did not include long links. This was partially because of the power losses that were caused if the length of the transmission line was increased beyond a certain threshold, and partially because the topology of the grid was decided based on geographical, cost, and other constraints. However, with the deregulation of the power industry, and the need to supply power over longer distances, there has been progress in the direction of adding long AC and DC transmission lines in power systems^{79, 80}.

In the complex networks domain, several researchers have proposed methods to improve the robustness of networks by slight topological modifications to the network. One of the significant works in this direction is presented in¹²¹ in which the authors try to maximize the algebraic connectivity of the network by link addition. Algebraic connectivity, which is the second smallest eigenvalue of the Laplacian matrix of a network, has been studied extensively because of its importance for connectivity, a crucial measure for network robustness^{127, 126, 72}. The authors of¹²¹ have demonstrated two ways of adding a link to the network to optimize the algebraic connectivity, one based on topological metrics and the other based on the spectral metrics of the Laplacian. The first method to increase the algebraic connectivity

is to add the link between a minimum degree node and a random other node, which is not connected to the minimum degree node because the algebraic connectivity is limited by the lowest degree nodes. In the second method, they use the Fiedler vector, which is the eigenvector corresponding to the second smallest eigenvalue of the Laplacian and select nodes such that the absolute difference between two of its elements is maximized. These two elements correspond to the nodes between which the link should be connected. The authors test these strategies on random and scale free network models.

In⁴, the authors try to optimize the algebraic connectivity by link rewiring instead of addition of a new link. In fact they extend the analysis to rewiring of multiple edges to obtain the maximum increase in the algebraic connectivity, or in other words, to obtain an optimal value for the algebraic connectivity. This rewiring procedure is carried out in two steps: first, to add a link which would increase the algebraic connectivity the most, and second, to remove a link which would reduce the algebraic connectivity the least.

Another link rewiring technique is described in¹¹⁹. The authors use the example of the World Transportation Network and propose a strategy to improve the robustness of the network by a small number of interventions considering the cost constraints. They have devised a smart method to simply swap the link connections, based on node degree of the node and its neighbors. They do so in order to keep the node degrees of all nodes the same before and after rewiring. A series of such successive swaps lead to an improvement in the robustness of the network.

The authors of¹²⁰ use link addition as a means to obtain optimal controllability of the network. They find the set of links to be added with their locations using the concept of maximal matching. Besides achieving their objective of optimizing controllability of the network, they also show how addition of links affect the properties of the complex network such as clustering coefficient, degree-degree correlation, and network heterogeneity. Similarly, the authors of⁷¹ use link addition as a method to enhance controllability of networks. They achieve this by calculating the degree ratio, which is calculated using the out-degree

and the in-degree of nodes. They calculate the node degree ratio of every node and connect the lowest ratio node to the highest ratio node.

The main contribution of this chapter is to determine the location of addition of a link in the transmission system, using the spectral characteristics of the Y_{bus} matrix of a power grid network, in order to enhance the robustness of the power grid network. We consider the eigenvectors corresponding to the second, third, and fourth smallest eigenvalues. We consider the addition of a single link in the network, since there is a cost associated with every additional element in the network. The advantage of using more than one eigenvalue is that it gives a very clear picture about the nodes which are spectrally distant from most of the nodes in the network. This gives us a candidate set of links, one out of which is selected as the link to be added to the network. We compare our results with those obtained by adding a link using algebraic connectivity, as well as by random addition of links, and find that the spectral distance method performs the best out of the three methods of link addition, for improving the robustness of the grid.

6.3 Y_{bus} matrix and Laplacian

A power grid is a real network with electrical properties such as load or demand on the nodes, the impedances of the links, and the power flow in the network, and it is important to consider these characteristics, even when performing an analysis from another perspective. The spectral properties of the Laplacian matrix, combined with the DC power flow model, effectively capture all the properties necessary to make it a realistic mitigation strategy for cascading failures in power grids. In fact, the impact of the complex power flow dynamics of the power grid are apparent in the results of this work.

The Laplacian matrix of a general complex network is equivalent to the Y_{bus} matrix of the power grid. The Laplacian matrix L of a network is an $N \times N$ matrix, where N is the number of nodes in the network, and is defined as:

$$L = D - A \tag{6.1}$$

where, D is the diagonal matrix of the node strengths and A is the adjacency matrix of the network. The diagonal matrix D consists of the total node degree of the node for an unweighted network on the diagonals, with all other elements being 0. For a weighted network, the diagonal elements are the total strength of the nodes, depending on the type of network and weight. In general, the diagonal elements are the sum of their corresponding rows in the adjacency matrix. For an unweighted network, the adjacency matrix A has an entry of 1 if the link exists and 0 if the link does not exist. If the network is weighted, the 1's are replaced by the respective weights on the existing links.

For a power grid, the Y_{bus} matrix is formed in a similar way. The Y matrix is like the adjacency matrix. Whenever a link exists, the corresponding entry in the Y matrix is the impedance of that link. If a link does not exist, the corresponding entry is 0. Thus, the Y matrix may also be called as the admittance matrix of the power grid. The Y_{bus} matrix is formed by placing the negative sum of the rows of the Y matrix as the corresponding diagonal element.

Thus, the Y_{bus} matrix can be written as:

$$\begin{aligned} Y_{bus}^{kl} &= G^{kl} + jB^{kl}, k \neq l \\ &= - \sum_{k \neq l} (G^{kl} + jB^{kl}), k = l \end{aligned}$$

The Y_{bus} matrix can be computed by a standard procedure given in⁴⁹. The use of this matrix ensures that Kirchoff's laws are properly taken into account. The inverse of this matrix is called the impedance matrix or the Z_{bus} matrix. However, the Y_{bus} matrix as it is, is a singular matrix and cannot be inverted. For this purpose, a very small admittance of the order of 10^{-2} is added to each of the diagonal elements of the Y_{bus} matrix. In the sense of power systems, it accounts for a small admittance from the node to the ground. Thus, the Laplacian matrix for the power system is slightly different from that of the normal definition of a Laplacian matrix. The impact of this is seen on some of spectral properties of the Laplacian, such as the smallest eigenvalue of the Y_{bus} matrix is not 0 but a very small number. However, the final results of the location of the long link are not affected by this

change. In order to keep the system realistic, we have considered the presence of the ground admittances in this dissertation.

6.4 Procedure to Find the Location of the New Link

As mentioned above, the spectral properties of the Y_{bus} matrix are utilized to determine the location of placement of the long link in the power grid network. The difference in this work from the previous work is the use of eigenvectors corresponding to the second, third, and the fourth smallest eigenvalues, instead of only the second smallest eigenvalue, better known as the algebraic connectivity. This was done in order to get finer information about the location where the link might be placed. In this method, we calculate the spectral distance between nodes in 3 dimensions, consisting of the second, third, and the fourth smallest eigenvectors. If there are N nodes in the network, the spectral distance is calculated as:

$$spectral\ distance = \sqrt{(x_i - x_j)^2 + (y_i - y_j)^2 + (z_i - z_j)^2} \quad i, j = 1, 2, \dots, N; i \neq j$$

where x , y , and z are the elements of the eigenvectors corresponding to the second, third, and the fourth smallest eigenvalues of the Y_{bus} matrix, respectively. The spectral distance is calculated between every pair of nodes, i and j , in the network to give $N + (N - 1) + (N - 2) + \dots + 1 = \sum_{i=1}^N i$ distances. These distances are then arranged in the ascending order of magnitude. When this ordering of distances takes place, it can be easily observed that, in particular, there are one or two nodes that have longer spectral distances to the rest of the network. This is very useful information that is obtained by the use of three eigenvectors, instead of one. One advantage of this information is that it gives a small subset of links, of size $N - 1$, that must be tested to select one link that gives a substantial improvement in robustness of the network against link failures. The second advantage is that it is very easy to select locations for the addition of more than one links, if desired. However, as mentioned before, in this chapter, we have considered the addition of only one long link, due to the cost constraint

Once we know which node is spectrally the most distant node in the network, we select the subset of the links which have the spectrally distant node as one of the extreme nodes, and perform the vulnerability analysis of the network. This is done by removing one link at a time and estimating the damage to the network in terms of loss of load. The vulnerability analysis is done using the DC Power Flow model⁴⁹ and the Overload Cascade model⁹⁶. The results of the vulnerability analysis after link addition are compared with the results of the vulnerability analysis of the original network, without any additional link. All the links in the candidate set improve the robustness of the network as compared to the original, but the one that gives maximum benefit, in terms of load retention after failures, among these candidate links, is selected as the additional link in the network. The results of vulnerability analysis with the selected link are also compared with the vulnerability analysis by link addition through algebraic connectivity and by random link addition method.

We also compared the properties of the networks before and after link addition, both by spectral distance method and by algebraic connectivity method. The results of this comparison are summarized in Tables 6.2 and 6.3. We observed that the selected link did not give the shortest possible characteristic path length, but it was between that of the original network and the network with the shortest characteristic path length. The link, the addition of which, gives the shortest characteristic path length, did not improve the robustness of the network as much as the addition of the selected link with the spectrally distant node as one of its extremes did, and this can be attributed to the complex power flow dynamics of the power grid network. The numerical results and analysis are discussed in more detail in the next section.

6.5 Results

The results of this chapter are presented in two parts: The vulnerability analysis and the structural properties. The vulnerability analysis gives a numerical evaluation of the robustness of the different tested networks and the structural analysis shows how the change in

the properties of the network before and after addition of the long link.

We used the DC Power Flow model to consider the flow dynamics of the networks and the Overload Cascade model for the vulnerability analysis. The main focus is on link failures, where every link is characterized by a finite capacity. Whenever a link goes beyond its capacity, it is considered as a failed link and removed from the network, with its power being shifted to the other links in the network. The power carrying capacity of a link is mainly a function of the inverse of its impedance. Lower the impedance, higher is the power carrying capacity.

After the new link obtained by spectral distance method was added to the network, the results were obtained by removing each link from the new network, one at a time, and performing the vulnerability analysis. The same analysis was performed after link addition by algebraic connectivity method. There can be $R = \frac{N(N-1)}{2} - L - (N - 1) - 1$ possibilities for connecting a random link in the network, where $\frac{N(N-1)}{2}$ is the total number of links for a fully connected network, L is the number of links already present in the original network, $N - 1$ is the size of the candidate set of links tested using the spectral distance method and 1 link is suggested by algebraic connectivity. Thus, the number of random link connections possible is given by R . This set can be very big, especially as the network size increases. Hence, we selected 10% of the links from R , which have a high spectral distance. Figures 6.1 and 6.2 show the location of addition of the long link on the physical topology of the 57- and the 118-node networks, respectively. These networks have links represented in two colors, red and green. The green links indicate the non-vulnerable links and the red links represent the vulnerable links, before the new link is added to the network. Vulnerable links are those the failure of which cause more than 10% loss in the total load of the system.

The results of the vulnerability analysis of the 118-node network are shown in Figures 6.3, 6.4, and 6.5, each of these figures showing the vulnerability analysis without the additional link, with the link based on spectral distance method, and with the link placed by algebraic connectivity method, respectively. The x-axis shows the link ids of the differ-

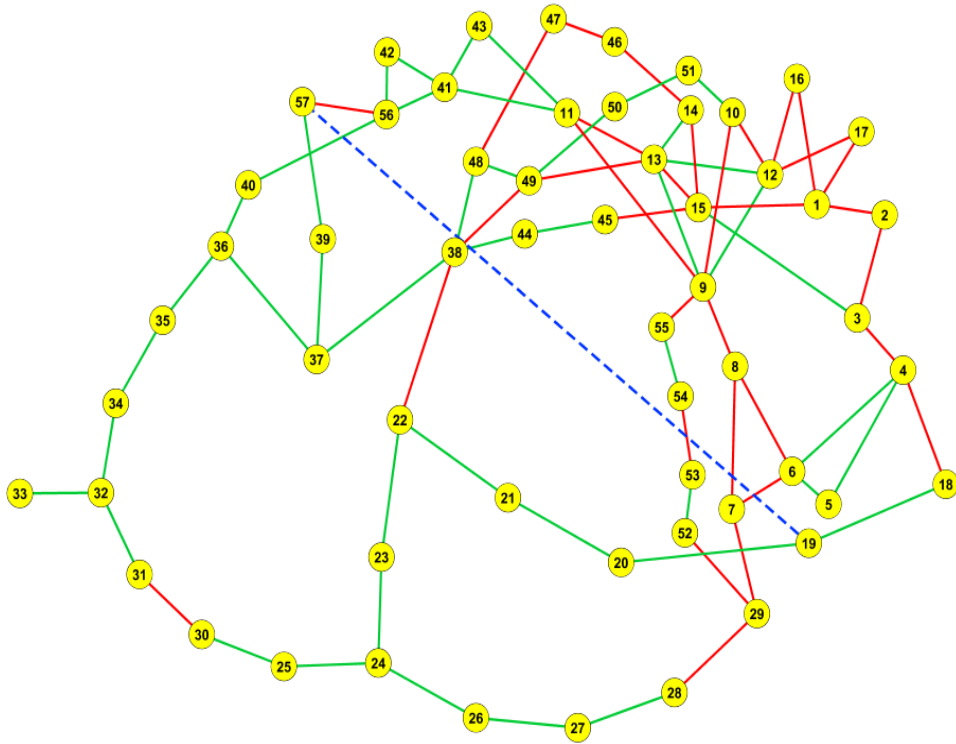


Figure 6.1: *This figure shows the location of the additional link in the 57-node network. The additional link is shown as the dotted blue line. The addition of this link reduces the average spectral distance of the network, which, in turn, improves the robustness of the network. The red and green links represent the vulnerable and the non-vulnerable links, respectively, before the link is added. Vulnerable links are those the failure of which cause more than 10% loss of total load in the network.*

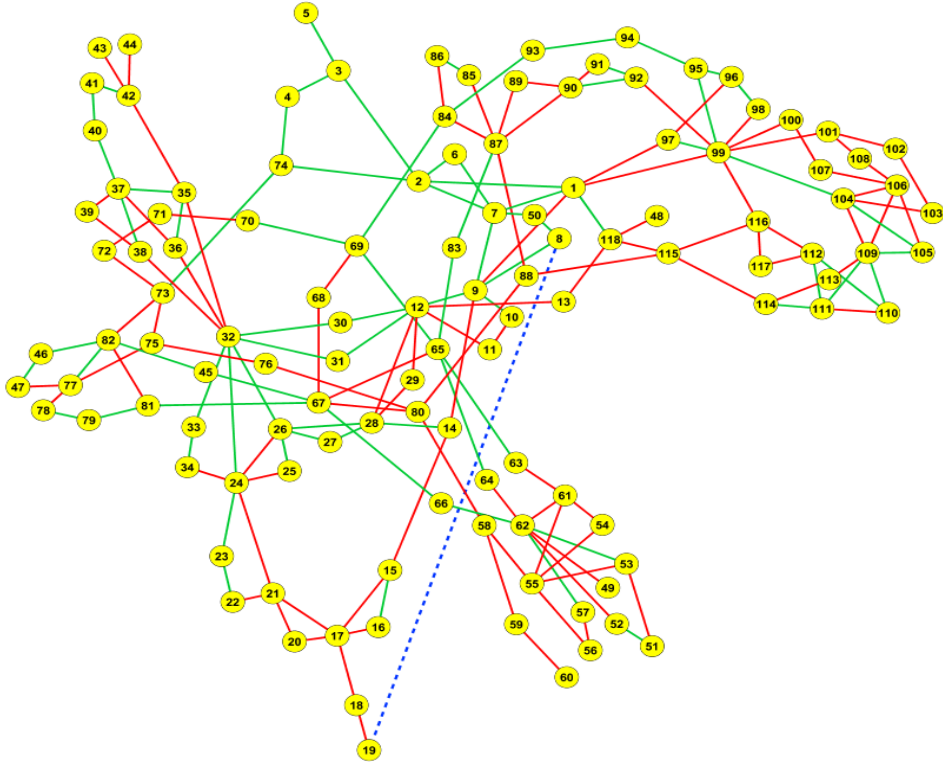


Figure 6.2: *This figure shows the location of the additional link in the 118-node network. The additional link is shown as the dotted blue line. The addition of this link reduces the average spectral distance of the network, which, in turn, improves the robustness of the network. The red and green links represent the vulnerable and the non-vulnerable links, respectively, before the link is added. Vulnerable links are those the failure of which cause more than 10% loss of total load in the network.*

ent links in the network, and the y-axis represents the total load remaining on the network (in p.u.) when a corresponding link on the x-axis is disconnected. The first observation is that the average load remaining on the network increases by approximately 10% after the addition of the long link by the spectral distance method. The figures show that the long link added to the network using the spectral distance method improves the robustness of the network more than both, the link added by algebraic connectivity, as well as the random additions. For the 30 node network, we see that the robustness of the network with link addition by spectral distance was 8% higher than that of the original network, and it was 3.67% higher than the algebraic connectivity method. Similarly, we see that for the 57 node network, the robustness by the spectral distance method was 10.46% higher than the original, whereas it was only about 1.66% better than the algebraic connectivity method. Similarly, for the 118-node network, the improvement in robustness of the spectral distance method was about 16% as compared to the original network as well as the algebraic connectivity method. Figures 6.6, 6.7, 6.8 represent the histograms for the link distribution in different load ranges for 118-node network without additional link, with link addition using Spectral Distance method and with link addition using Algebraic Connectivity method, respectively.

Table 6.1 shows the characteristics of the 57-node network before and after the addition of the long link, both using our method and using algebraic connectivity. Table 6.2 shows the characteristics of the 118 node network.

Table 6.1: *Characteristics of the 57-node network before and after the addition of long link*

	Original	Spectral distance	Algebraic Connectivity
Characteristic path length	4.954	4.853	4.726
Diameter	12	11	10
Average degree	2.737	2.772	2.772
Clustering Coefficient	0.122	0.122	0.122

For the 57-node network, we observe that the addition of the long link slightly reduces the characteristic path length of the network from that of the original. For the 118-node

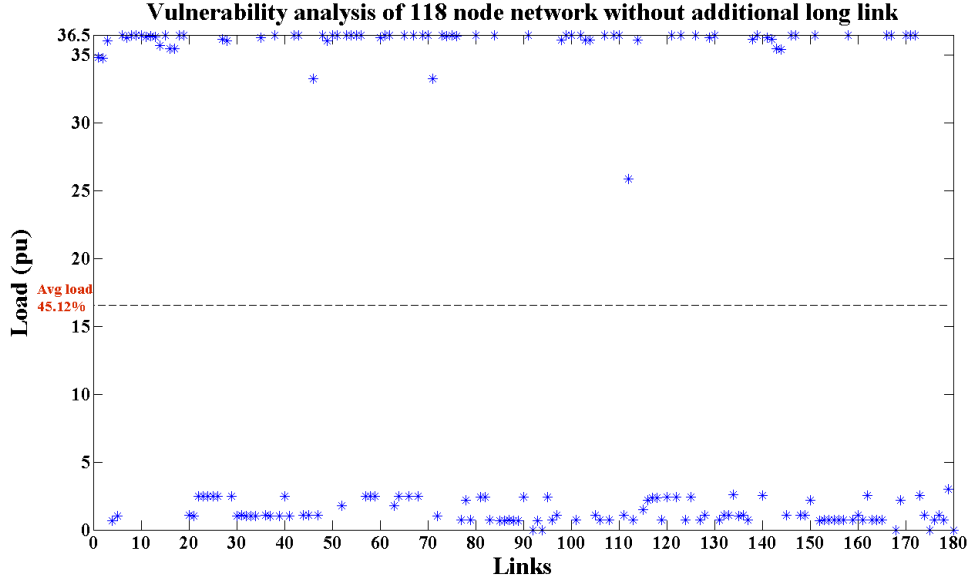


Figure 6.3: This figure shows the results of vulnerability analysis of the 118-node network without the additional link. The vulnerability analysis is performed by removal of each link, on the x-axis, one at a time, and running the Overload Cascade model to record the final percentage of load remaining at the end of the failure. The average load retained on the network when the link failure simulation is done for every link in the network, is 45.12% and it is indicated by the partition on the y-axis. It can be seen that the vulnerable links in the network lead to a complete breakdown of the network

Table 6.2: Characteristics of the 118-node network before and after the addition of long link

	Original	Spectral distance	Algebraic Connectivity
Characteristic path length	6.309	6.156	6.261
Diameter	14	14	14
Average degree	3.034	3.051	3.051
Clustering Coefficient	0.165	0.164	0.165

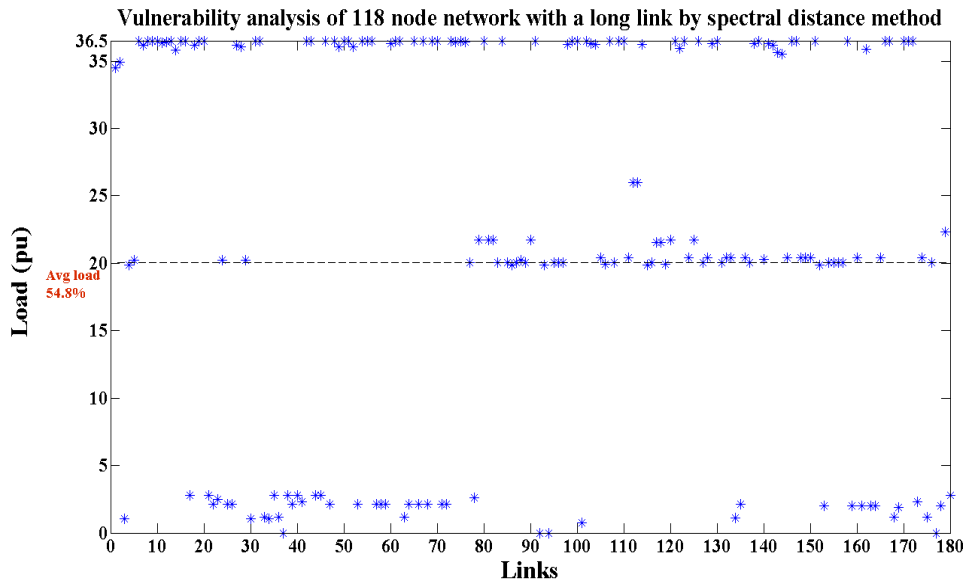


Figure 6.4: This figure shows the results of vulnerability analysis of the 118-node network with the addition of a link, using spectral distance method. It can be seen that the average load retained on the network increases to 54.8%, an increase of approximately 10% from the network without the additional link. Also, a number of points move up, at a position closer to the average load, and some points move up closer to the 100% load level.

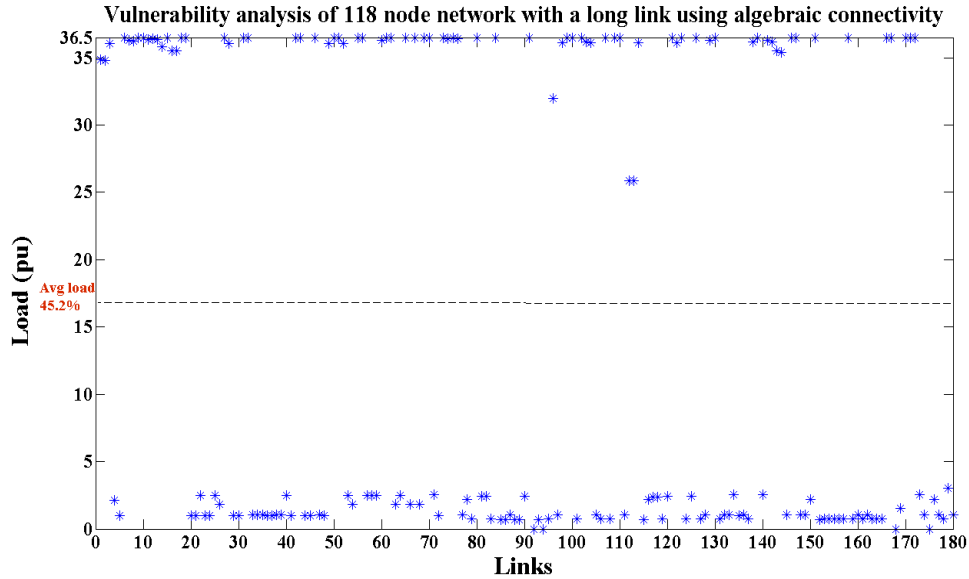


Figure 6.5: This figure shows the results of vulnerability analysis of the 118-node network with the addition of a link, using algebraic connectivity method. The figure indicates that the results do not differ much from the results of the original network, without the additional link. Also, the average load retained by the network by adding a link using algebraic connectivity is 45.2%, close to the average load retention of the original network. This can be attributed to the fact that the vulnerability analysis previously done in literature does not account for the complex power flow dynamics of the network. When a power flow model is used, the results are different, as indicated by this figure, from those mentioned in literature.

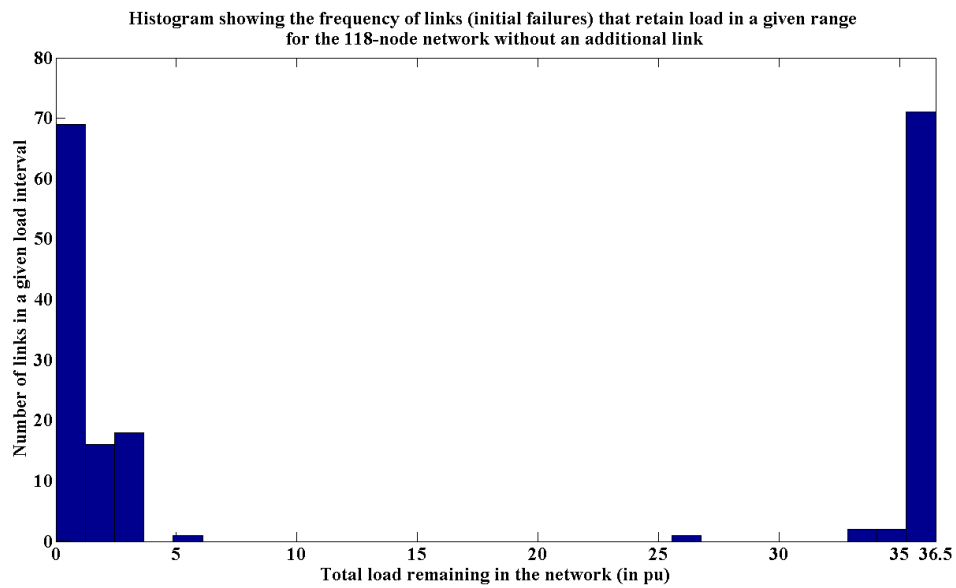


Figure 6.6: *This figure represents the distribution of links that retain load in a given load range in the 118-node network without the additional link. On the X-axis, the total load remaining in the network as a result of an initial failure is represented in pu. The number of links falling in a given load range represents the number of links that retain the amount of load in that load range when they are the initial failure.*

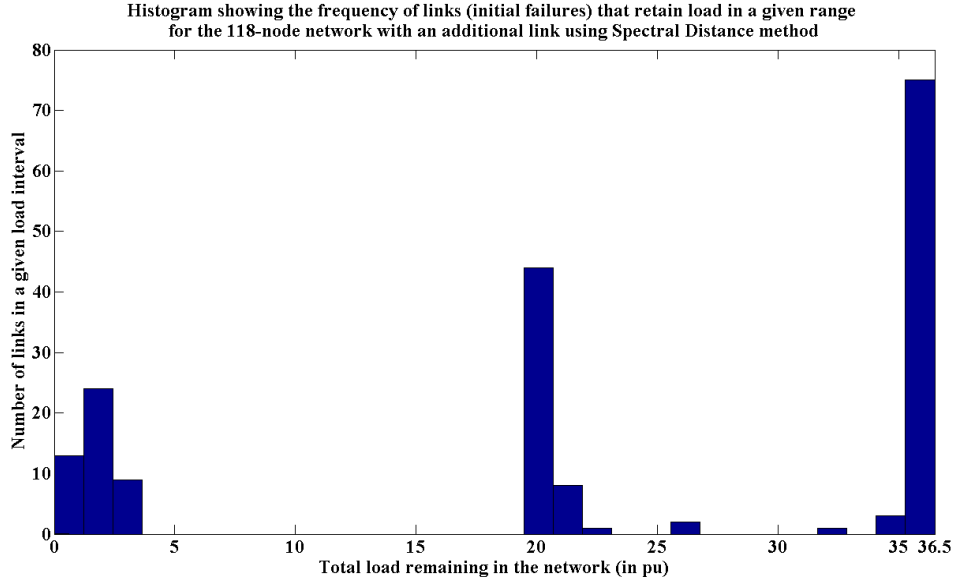


Figure 6.7: *This figure represents the distribution of links that retain load in a given load range in the 118-node network with additional link placed in the network using Spectral Distance method. On the X-axis, the total load remaining in the network as a result of an initial failure is represented in pu. The number of links falling in a given load range represents the number of links that retain the amount of load in that load range when they are the initial failure. It is seen that there is an increase in the number of links in the last load range in this network as compared to the network without the additional link. As represented by the vulnerability analysis graphs, there is a shift from the lower load ranges to the middle and the higher ranges, indicating that some of the vulnerable links have become less vulnerable due to the presence of the new link which provides alternate path for power to flow from one node to the other.*

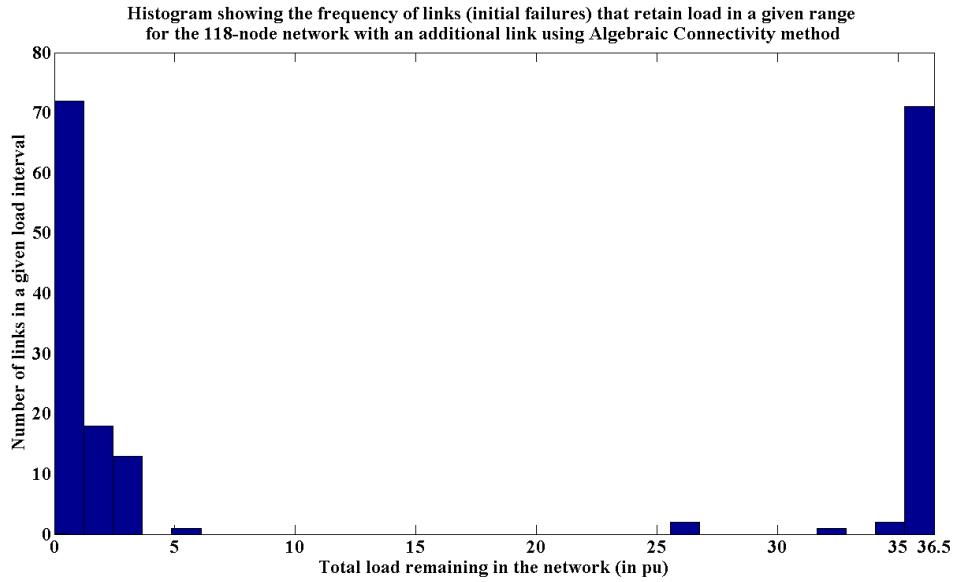


Figure 6.8: *This figure represents the distribution of links that retain load in a given load range in the 118-node network with additional link placed in the network using Algebraic Connectivity method. On the X-axis, the total load remaining in the network as a result of an initial failure is represented in pu. The number of links falling in a given load range represents the number of links that retain the amount of load in that load range when they are the initial failure. It is seen that there is not much difference in the state of the network from the original network. This is because the original method, in literature, was implemented without the inclusion of the power flow model. In the present work in this dissertation, the Algebraic Connectivity method was used with the power flow model and results indicate that the system remains close to the original system in this case.*

network, there is hardly any change in the network characteristics from the original with either of the two methods. We also observe that the algebraic connectivity method or random addition of a link may give us a shorter characteristic path length than obtained by the spectral distance method, but this is attributed to the complex flow dynamics of the power system. These selected links give a marginal decrease in the characteristic path length but increase the robustness of the grid by a substantial amount. Some other links which would give a much shorter characteristic path length might not be able to improve the robustness as much.

Table 6.3 gives the average percentage of the load remaining on the network when there is no additional link, with a link addition based on spectral methods, with a link addition based on algebraic connectivity, and with many random link additions, for the 57- and the 118-node networks.

Table 6.3: *Average load remaining on the 57- and 118-node network (in %) by link addition based on different methods*

Network	No additional link	Spectral distance	Algebraic Connectivity	Random
57	65.09	71.64	70.99	66.95
118	45.12	54.8	45.2	43.6

Figures 6.9 and 6.10 represent the comparison of the vulnerability of the original network with the new network (with an additional link by the spectral distance and the algebraic connectivity methods) using the case of a single failure, for the 118-node network. Figure 6.9 represents the results for failure of link number 20 and Figure 6.10 represents the results for link number 113 of the 118-node network, respectively.

6.6 Discussion

In this chapter, we propose a simple method based on spectral properties of the Y_{bus} matrix to improve the robustness of the power transmission grid against cascading failures. The eigenvalues and eigenvectors of the Laplacian or the Y_{bus} matrix hold a lot of important information about the properties of the network. We use this information to our advantage

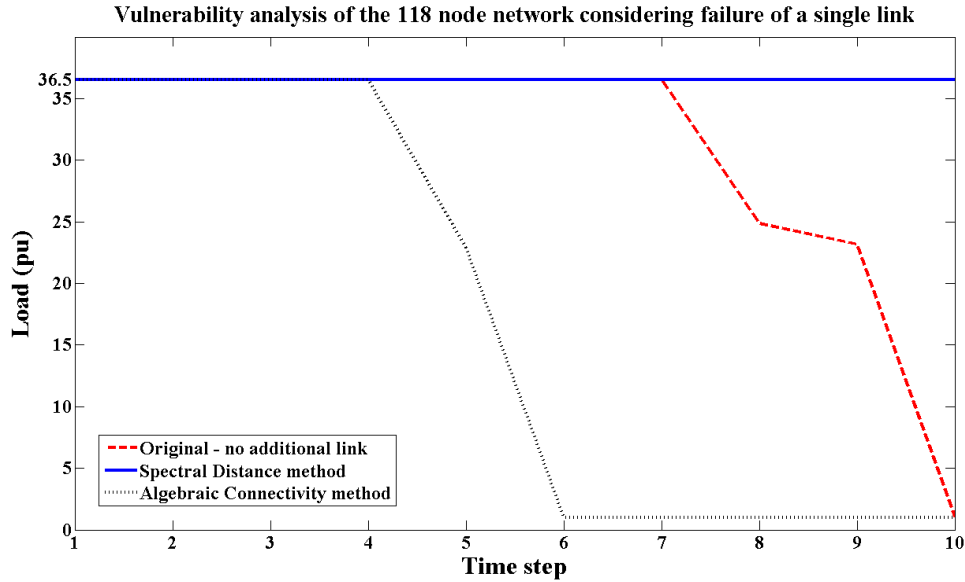


Figure 6.9: This figure represents the simulation for a single link failure considering the original 118-node network without an additional link, and the new 118-node networks, with an additional link, placed using the spectral distance method and the algebraic connectivity method. The link used for simulation is link 20. This is a vulnerable link, as it causes the complete breakdown of the original network, when it fails. The different stages of cascade that the original network goes through, are indicated by the dashed red line in the figure. The x-axis represents the different stages, in terms of times steps, and the y-axis represents the load remaining in p.u. The results of vulnerability analysis for the network with additional link placed using algebraic connectivity is shown in the dotted black line. This network performs equal to the original network, in terms of load retention for the first few steps, but then it breaks down completely. The results of the network with the link addition by spectral distance method are shown in the solid blue line. This new network is able to retain all the load in the network, in spite of the failure of link 20, which was a vulnerable link in the original network.

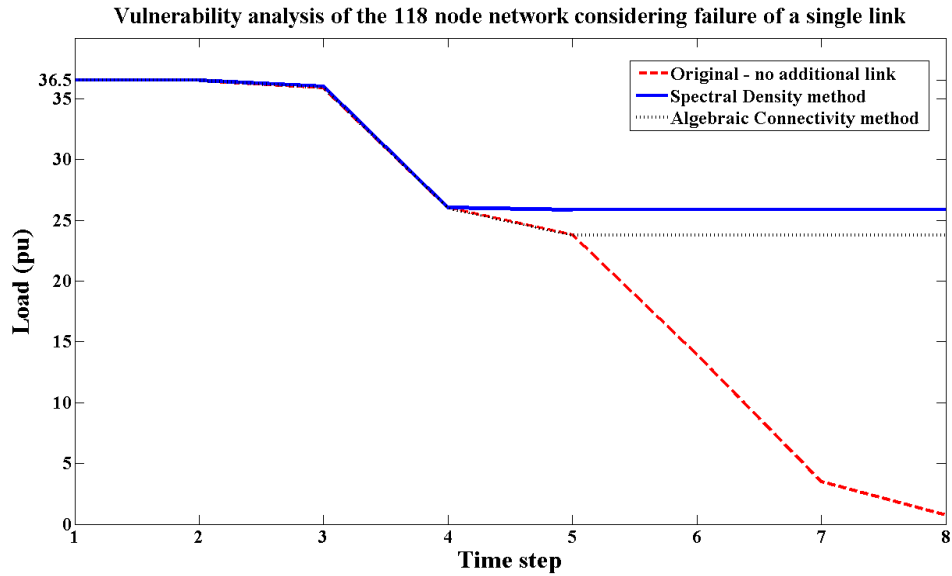


Figure 6.10: This figure represents the simulation for a single link failure considering the original 118-node network without an additional link, and the new 118-node networks, with an additional link, placed using the spectral distance method and the algebraic connectivity method. The link used for simulation is link 20. This is a vulnerable link in the original network. The result of vulnerability analysis of the original network, new network with link addition by algebraic connectivity, and new network with link addition by spectral distance are shown in the dashed red, dotted black, and solid blue lines, respectively. In this case, it is observed that algebraic connectivity performs almost equally as good as the spectral distance method.

and propose a method that involves addition of a link in the network, the location of which is determined based on the spectral distance between the nodes of the network. We use the second, third, and fourth smallest eigenvalues of the Y_{bus} matrix to obtain information about the nodes which are spectrally distant from most other nodes in the network, and then select a link from the set of candidate links.

Algebraic connectivity, which is the second smallest eigenvalue of the Laplacian matrix, and the eigenvector corresponding to it have been extensively used in the past for robustness analysis since it is directly related to the connectivity of the graph. However, with the use of higher order eigenvalues and eigenvectors, we show that the other components of the spectrum also provide information, such as the spectral distance of a node from the other nodes in the network.

The results indicate that the link introduced in the network by this method substantially improves the robustness of the network as compared to the original network without the new link. The method also produces better results from vulnerability analysis as compared to the link addition by algebraic connectivity and random link addition. Even though the location of the link placement may not be optimal, the improvement in robustness of power grid networks is substantial. Thus, we achieve a proper balance between the simplicity of the method and the effectiveness of the results.

Chapter 7

Conclusions and Future Work

In this chapter, we finally discuss the conclusions of all the work that has been done as a part of this dissertation, and discuss the scope for future work.

7.1 Conclusions

The operation of the power grid, which was designed almost a century ago, has changed a lot in recent years due to increased demand, interconnections, increased power flow in the system, and incorporation of intermittent distributed generators. We examined the state of the power grid under two scenarios: Load growth causing the grid to reach its capacity, and the incorporation of random fluctuations in the grid. Through simulations on the real, realistic, and synthetic networks, we observed that in the load growth scenario, there comes a critical point at which the grid breaks down with an abrupt transition. This critical point is the threshold of load after which the network approaches a breakdown state. Depending on the size and topology of the grid, it either goes to a complete breakdown immediately or goes through an intermediate state in which a fraction of the links of the network is disconnected, and it approaches a complete breakdown if load is increased any further. The breakdown is smoother in the case of random fluctuations. There is no clear transition point and the presence of a threshold is not apparent. Moreover, the IEEE and synthetic grids do not reach a point of complete breakdown in the examined range of fluctuations. The graphs show an increasing trend and if the range of fluctuations is expanded, it is possible to see

a complete breakdown of the networks. However, as the size of the system increases, the sensitivity of the system to both load increase and random fluctuations may increase. The presence of a threshold is evident in both the scenarios for the Polish grid. This indicates that the fragility of the grid may increase with increasing size. Also, the 2746-node Polish grid is the only real network used in the analysis. Further analysis and test scenarios are needed to gain more insights and reach any conclusions on the dynamics of the power grid network.

Considering the current status of the grid, preparation to reduce the effects of a cascading failure is important. Intentional islanding can be a practical method to isolate faults during times of emergency, thus mitigating cascading failures. Complex networks based algorithms for community detection, Bloom and Fast Greedy, are utilized for island formation in this dissertation. These algorithms have been modified to make them suitable for the power grid. The results have been compared with an optimal strategy for island formation. The complexity of the optimal islanding method is very high, and it can solve IEEE systems up to 30 nodes only. Modified Bloom and Modified Fast Greedy algorithms give sub-optimal results for islanding but can give islanding solution for networks up to thousands of nodes within seconds or a few minutes, depending on the network size and number of islands required. Modified Bloom performs better than Modified Fast Greedy, both in terms of time of execution (complexity) as well as load shedding. Both techniques achieve their best results with different number of islands, indicating the importance of island structure in determining the amount of load shedding. Island characterization reveals that, while the islands created by the Modified Bloom method appear to be more robust, due to shorter characteristic path length ensuring better connectivity of nodes, a vulnerability analysis of islands formed by both methods will actually reveal the true efficiency of both the islanding methods.

A method to prevent the spread of cascades due to generator failure is to provide the load nodes access to multiple generators located close to the nodes. This is possible by the

introduction of DGs in the transmission system. However, the locations where the DGs are placed must be carefully selected, and also the size of DGs. Improper locations and sizes can lead to more damage to the system than improving its robustness. In this dissertation, DGs refer to conventional DGs, and their placement was done based on electrical centrality and node significance measures. Electrical centrality differentiates between the electrical and physical structure of the power grid showing that the grid actually contains “electrical hubs”. Node significance decides the more significant node in the network by the node’s ability to distribute power. Any single method did not bring significant improvement in the system robustness. However, when the two methods were combined and used for DG placement, there was a considerable improvement in the robustness, in terms of the amount of load that could be retained in the network in the event of a failure, as compared to the case without DGs. Results obtained by comparison with another method clearly shows the merits of our method.

The properties of a network can be significantly changed by introducing a small change in the structure of the network. Strategic placement of an additional link, using the spectral characteristics of the Y_{bus} matrix of the transmission grid, was used as a method to reduce the vulnerability of the grid. Eigenvectors corresponding to the second, third, and fourth eigenvalues were chosen to determine the spectral distances between all node pairs in the network. The sorting and arranging of links by spectral distance indicate that there exists at least one node in the network that has much longer spectral distances to the other nodes in the network. The hypothesis was, that by bringing this spectrally distant node closer to the other nodes in the network, and thereby reducing the average spectral distance of the network, the robustness of the grid can be enhanced. We select a link with one of the extreme nodes of the link as the spectrally distant node, with the help of an algorithm, as the additional link in the network. Vulnerability analysis of the network is performed before and after link placement, and the results of the spectral distance method are compared with the results of algebraic connectivity method and random link placement method. In the

random link placement method, 10% from the set of possible random links are selected and added to the network, one at a time, and the vulnerability analysis is performed. Our results indicate that the spectral distance method performs better than the algebraic connectivity method and the random link placement method.

7.2 Future Work

The following points discuss the scope of future research, related to the work discussed in this dissertation:

1. More analysis of different methods by which the grid can be stressed up to the critical point should be done. Such analysis could give substantial information about the behavior of the grid under stress. Additionally, large real networks should be used for the analysis to study the behavior that would be exhibited by large interconnected systems when subject to undesirable effects.
2. The optimal islanding technique could be simplified using semi-definite programming or other linearization technique. This would enable the use of the optimal islanding technique for large networks, for different number of islands.
3. Refinements could be proposed for the modularity based islanding methods, to enable them to reverse a previously taken decision, if the decision does not prove to be advantageous to the system in the long term. In this case, advantage would mean minimization of load shedding.
4. Vulnerability analysis of the grid using the islanding scenarios would help to determine the quality and efficiency of the two islanding techniques, and the actual amount of load shedding taking place as a result of the islanding. Island characterization gives an idea that the Modified Bloom technique provides more robust islands than the Modified Bloom technique, but this can only be confirmed by simulating failure scenarios after island creation and performing the vulnerability analysis.

5. Other spectral methods such as the spectral gap method must be explored to obtain a location for the placement of the additional link in the transmission grid. This method would involve reducing the spectral gap of the adjacency matrix. The spectral gap has a close relation with algebraic connectivity and plays an important role in determining the robustness of networks. It would be interesting to see if these graph properties also prove to be true for a real network such as the power grid, with its capacity constraints and complex flow dynamics. Comparison of results with the spectral distance method could reveal the merits and demerits of the respective strategies.

Bibliography

- [1] European offshore supergrid proposal - vision and executive summary, 2006.
- [2] Desertec foundation: Milestones, September 2012. <http://www.desertec.org/en/global-mission/milestones/>.
- [3] M. E. J. Newman A. Clauset and C. Moore. Finding community structure in very large networks. *Phys Rev E*, 70.
- [4] C. Scoglio A. Sydney and D. Gruenbacher. Optimizing algebraic connectivity by edge rewiring. *Appl. Math. Comput.*, 219:5465–5479, 2013.
- [5] M. Afzalan and M. A. Taghikhani. Dg placement and sizing in radial distribution network using pso&hmbo algorithms. *Energy and Power*, 2:61–66, 2012.
- [6] R. K. Ahuja, T. L. Magnati, and J. B. Orlin. Network flows: Theory, algorithms and application. 1993.
- [7] R. Albert, I. Albert, and G. L. Nakarado. Structural vulnerability of the north american power grid. *Phys. Rev. E*, 69:025103, 2004.
- [8] R. Albert and A. Barabasi. Statistical mechanics of complex networks. *Rev. of Mod. Phys.*, 74:47–97, 2002.
- [9] L. A. N. Amaral, A. Scala, M. Barthelemy, and H. E. Stanley. Classes of small-world networks. *PNAS*, 97:11149, 2000.
- [10] E. E. Aponte and J. K. Nelson. Time optimal load shedding for distributed power systems. *IEEE T Power Syst*, 21.

- [11] S. Arianos, E. Bompard, A. Carbone, and F. Xue. Power grid vulnerability: A complex network approach. *CHAOS*, 19:013119, 2009.
- [12] L. Aurora. Massive blackout hits java, bali. The Jakarta Post, 2005. <http://www.thejakartapost.com/news/2005/08/19/massive-blackout-hits-java-bali.html>.
- [13] I. Dobson B. A. Carreras, V. E. Lynch and D. E. Newman. Critical points and transitions in an electric power transmission model for cascading failure blackouts. *CHAOS*, 12.
- [14] K. Bae and J. S. Thorp. A stochastic study of hidden failures in power system protection. *Decision Support Systems*, 24:259–268, 1999.
- [15] P. Bak, C. Tang, and K. Wiesenfeld. Self-organized criticality: An explanation of 1/f noise. *Phys. Rev. Lett.*, 59:381–384, 1987.
- [16] A. L. Barabasi and R. Albert. Emergence of scaling in random networks. *Science*, 286:509–512, 1999.
- [17] D. Beinstock. Optimal control of cascading power grid failures. In *Proceedings of the 50th IEEE Conference on Decision and Control and European Control Conference (CDC-ECC), Orlando, FLA*, pages 2166–2173, December 2011.
- [18] E. Bompard, R. Napoli, and F. Xue. Analysis of structural vulnerabilities in power transmission grids. *International Journal of Critical Infrastructure Protection*, 2:5–12, 2009.
- [19] C. D. Brummitt, R. M. D’Souza, and A. E. Leicht. Suppressing cascades of load in interdependent networks. *PNAS*, 109.
- [20] S. V. Buldyrev, R. Parshani, G. Paul, H. E. Stanley, and S. Havlin. Catastrophic cascade of failures in interdependent networks. *Nature*, 464.

- [21] Z. Chen C. Liu, Q. Xu and C. L. Bak. Vulnerability evaluation of power system integrated with large-scale distributed generation based on complex network theory. In *Proceedings of the 47th IEEE International Universities Power Engineering Conference, Middlesex, United Kingdom*, pages 1–5, September 2012.
- [22] B. A. Carreras, V. E. Lynch, I. Dobson, and D. E. Newman. Critical points and transitions in an electric power transmission model for cascading failure blackouts. *CHAOS*, 12:985–994, 2002.
- [23] B. A. Carreras, V. E. Lynch, D. E. Newman, and I. Dobson. Blackout mitigation assessment in power transmission systems. In *Proceedings of the 36th Hawaii International Conference in System Sciences, Big Island, Hawaii*, page 65.2, January 2003.
- [24] B. A. Carreras, D. E. Newman, I. Dobson, and A. B. Poole. Initial evidence for self-organized criticality in electric power system blackouts. In *Proceedings of the 33rd Hawaii International Conference on System Sciences, Maui, Hawaii*, page 4038, January 2000.
- [25] B. A. Carreras, D. E. Newman, I. Dobson, and A. B. Poole. Evidence for self-organized criticality in a time series of electric power system blackouts. *IEEE Transactions on Circuits and Systems - I : Regular Papers*, 51:1733–1740, 2004.
- [26] D. P. Chassin and C. Posse. Evaluating north american electric grid reliability using the barabasi-albert network model. *Physica A*, 355.
- [27] G. Chen, Z. Y. Dong, D. J. Hill, G. H. Zhang, and K. Q. Hua. Attack structural vulnerability of power grids: A hybrid approach based on complex networks. *Physica A*, 389:595–603, 2010.
- [28] J. Chen and J. S. Thorp. A reliability study of transmission system protection via a hidden failure dc load flow model. In *Proceedings of the 5th IEEE International Conference on Power System Management and Control*, pages 384–389, April 2002.

- [29] J. Chen, J. S. Thorp, and I. Dobson. Cascading dynamics and mitigation assessment in power system disturbances via a hidden failure model. *Int. J. Elec. Power*, 27:318–326, 2005.
- [30] X. Chen, K. Sun, Y. Cao, and S. Wang. Identification of vulnerable lines in power grid based on complex network theory. In *Proceedings of the IEEE Power Engineering Society General Meeting, Tampa, FLA*, pages 1–6, June 2007.
- [31] R. D. Christie. Power systems test case archive. University of Washington, 1961-1993. <http://www.ee.washington.edu/research/pstca/>.
- [32] Investigation Committee. Final report of the investigation committee on the 28th september 2003 blackout in italy. Union for the Coordination of the Transmission of Electricity, 2004. http://www.rae.gr/old/cases/C13/italy/UCTE_rept.pdf.
- [33] The Enquiry Committee. Report of the enquiry committee on grid disturbance in northern region on 30th july, 2012 and in northern, eastern and north-eastern region on 31st july, 2012. Ministry of Power, 2012. http://www.powermin.nic.in/pdf/GRID_ENQ_REP_16_8_12.pdf.
- [34] North American Electric Reliability Corporation. Evaluation of criteria, methods, and practices used for system design, planning, and analysis response to nerc blackout recommendation 13c, 2005. <http://www.nerc.com/docs/pc/tis/>.
- [35] World Energy Council. Blackouts.
- [36] World Energy Council. Interconnectivity: Benefits and challenges, 2010. <http://www.worldenergy.org/documents/interconexsum.pdf>.
- [37] World Energy Council. Smart grids: Best practice fundamentals for a modern energy society, 2012. http://www.worldenergy.org/documents/20121006_smart_grids_best_practice_fundamentals_for_a_modern_energy_system.pdf.

- [38] P. Crucitti, V. Latora, and M. Marchiori. Model for cascading failures in complex networks. *Phys. Rev. E*, 69:045104, 2004.
- [39] P. Crucitti, V. Latora, and M. Marchiori. A topological analysis of the italian electric power grid. *Physica A*, 338:92–97, 2004.
- [40] M. Kirchner D. E. Newman, B. A. Carreras and I. Dobson. The impact of distributed generation on power transmission grid dynamics. In *Proceedings of the 44th Hawaii International Conference on System Sciences, Kauai, HI*, pages 1–8, January 2011.
- [41] I. Dobson, B. A. Carreras, V. E. Lynch, and D. E. Newman. Complex systems analysis of series of blackouts: Cascading failure, critical points, and self-organization. *CHAOS*, 17:026103, 2007.
- [42] P. Erdos and A. Renyi. On the evolution of random graphs. *Publications of the Mathematical Institute of the Hungarian Academy of Sciences*, 5:17–61, 1960.
- [43] P. Fairley. The unruly power grid. *IEEE Spectrum*, vol. 41, no. 8, pp.22-27.
- [44] N. Fan, D. Izraelevitz, F. Pan, P. M. Pardalos, and J. Wang. A mixed integer programming approach for optimal power grid intentional islanding. *Energy Systems*, 3.
- [45] European Regulators’ Group for Electricity and Gas. Ergeg final report - the lessons to be learned from the large disturbance in the european power system on the 4th of november 2006. Council of European Energy Regulators, 2007. http://www.energy-regulators.eu/portal/page/portal/EER_HOME/EER_PUBLICATIONS/CEER_PAPERS/Electricity/2007/E06-BAG-01-06_Blackout-FinalReport_2007-02-06.pdf.
- [46] U.S.-Canada Power System Outage Task Force. Final report on the august 14, 2003 blackout in the united states and canada: Causes and recommendations.

U.S. Department of Energy, 2004. <http://energy.gov/sites/prod/files/oeprod/DocumentsandMedia/BlackoutFinal-Web.pdf>.

- [47] S. Fortunato. Community detection in graphs. *Physics Reports*, 486:75–174, 2010.
- [48] J. Gao, S. V. Buldyrev, H. E. Stanley, and S. Havlin. Networks formed from interdependent networks. *Nature Physics*, 8.
- [49] B. R. Gungor. *Power Systems - Chapter 6*. Technology Publications.
- [50] A. G. Tikdari H. Bevrani and T. Hiyama. An intelligent based power system load shedding design using voltage and frequency information. July 2010.
- [51] S. A. Nabaviniyaki H. Hedayati and A. Akbarimajd. A method for placement of dg units in distribution networks. *IEEE T. on Power Deliver*, 23:1620–1628, 2008.
- [52] V. Vittal H. You and X. Wang. Self-healing in power systems: an approach using islanding and rate of frequency decline-based load shedding. *IEEE T Power Syst*, 18:174–181, 2003.
- [53] V. Vittal H. You and X. Wang. Slow coherency-based islanding. *IEEE T Power Syst*, 19:183–491, 2004.
- [54] N. HadjSaid, C. Tranchita, B. Rozel, M. Viziteu, and R. Caire. Modeling cyber and physical interdependencies - application in ict and power grids. In *Proceedings of the IEEE PES Power Systems Conference and Exposition, Seattle, WA*, pages 1–6, March 2009.
- [55] I. A. Hamad, B. Israels, P. A. Rikvold, and S. V. Poroseva. Spectral matrix methods for partitioning power grids: Applications to the italian and floridian high-voltage networks. *Physics Procedia*, 4.

- [56] I. A. Hamad, P. A. Rikvold, and S. V. Poroseva. Floridian high-voltage power-grid network partitioning and cluster optimization using simulated annealing. *Physics Procedia*, 15.
- [57] The Hindu. Tripping of taramani substation causes blackout.
- [58] P. Hines and S. Blumsack. A centrality measure for electrical networks. In *Proceedings of the 41st Annual Hawaii International Conference on System Sciences, Big Island, Hawaii*, page 185, January 2008.
- [59] P. Hines, E. Cotilla-Sanchez, and S. Blumsack. Do topological models provide good information about electricity infrastructure vulnerability? *CHAOS*, 20:033122, 2010.
- [60] P. Hines and S. Talukdar. Reciprocally altruistic agents for the mitigation of cascading failures in electrical power networks. In *Proceedings of the International Conference on Infrastructure Systems, Rotterdam, Netherlands*, pages 1–6, November 2008.
- [61] P. Holme and B. J. Kim. Vertex overload breakdown in evolving networks. *Phys. Rev. E*, 65:066109, 2002.
- [62] A. J. Holmgren. Using graph models to analyze the vulnerability of electric power networks. *Risk Anal.*, 26:955–968, 2006.
- [63] Mitigation IEEE PES CAMS Task Force on Understanding, Prediction and Restoration of Cascading Failures. Initial review of methods for cascading failure analysis in electric power transmission systems. In *Proceedings of the IEEE Power Engineering Society General Meeting, Pittsburgh, PA*, pages 1–8, July 2008.
- [64] J.S Thorp J. Chen and I. Dobson. Cascading dynamics and mitigation assessment in power system disturbances via a hidden failure model. *Int J Elec Power*, 27:318–326, 2005.

- [65] C. W. Johnson. Analysing the causes of the italian and swiss blackout, 28th september, 2003. In *Proceedings of the 12th Australian Workshop on Safety Critical Systems and Software-Related Programmable Systems, Adelaide, Australia*, pages 21–30, August 2007.
- [66] D. Zheng K. Sun and Q. Lu. Splitting strategies for islanding operation of large-scale power systems using obdd-based methods. *IEEE T Power Syst*, 18:912–923, 2003.
- [67] J. Kim and I. Dobson. Propagation of load shed in cascading line outages simulated by opa. In *Proceedings of the IEEE Workshop on Complexity in Engineering (COM-PENG), Rome, Italy*, pages 1–6, February 2010.
- [68] S. Kim. Heatwave causes massive power outages. The Huffington Post, 2011. http://www.huffingtonpost.com/2011/09/15/south-korea-heat-wave_n_963922.html.
- [69] S. Kubler, S. Pahwa, N. Schulz, and C. Scoglio. A simulative analysis of the robustness of smart grid communication networks. In *Proceedings of the 43rd North American Power Symposium, Boston, MA*, pages 1–7, August 2011.
- [70] P. Kundur. *Power System Stability and Control, Chapter 1: General Characteristics of Modern Power Systems*. McGraw-Hill, Inc.
- [71] L. Hou L. Bai and S. Lao. A method for enhancing controllability with adding links in directed networks. In *Proceedings of the International Conference on Systems and Informatics, Yantai, China*, pages 13–15, May 2012.
- [72] F. Neri L. Donnetti and M. A. Munoz. Optimal network topologies: Expanders, cages, ramanujan graphs, entangled networks and all that. *J. Stat. Mech.*, 2006:P08007, 2006.
- [73] S. Larsson and E. Ek. The blackout in southern sweden and eastern denmark, september 23, 2003.

- [74] V. Latora and M. Marchiori. Efficient behavior of small-world networks. *Phys. Rev. Lett.*, 87:198701, 2001.
- [75] W. Liu, L. Liu, D. A. Cartes, and G. K. Venayagamoorthy. Binary particle swarm optimization based defensive islanding of large scale power systems. *Int J Comput Sci Applications*, 4:69–83, 2007.
- [76] J. Lyons. Brazil blackout sparks infrastructure concerns. *The Wall Street Journal*, 2009. <http://online.wsj.com/article/SB125798817743744475.html>.
- [77] J. Brooks M. El-werfelli and R. Dunn. Controlled islanding scheme for power systems. In *Proceedings of the 43rd International Universities Power Engineering Conference*, pages 1–6, September 2008.
- [78] H. Ghasemi M. Etehad and S. Vaez-Zadeh. Voltage stability-based dg placement in distribution networks. *IEEE T. Power Deliver.*, 28:171–178, 2012.
- [79] M. Z. Mostafa M. H. Okba, M. H. Saied and T. M. Abdel-Moneim. High voltage direct current transmission - a review, part i. In *Proceedings of EnergyTech 2012, Cleveland, OH*, pages 1–7, May 2012.
- [80] M. Z. Mostafa M. H. Okba, M. H. Saied and T. M. Abdel-Moneim. High voltage direct current transmission - a review, part ii - converter technologies. In *Proceedings of EnergyTech 2012, Cleveland, OH*, pages 1–7, May 2012.
- [81] L. Feng M. Yanbin and M. Shengwei. On the topological characteristics of power grids with distributed generation. In *Proceedings of the 29th Chinese Control Conference, Beijing, China*, pages 4714 – 4720, July 2010.
- [82] R. Moreno and A. Torres. Security of the power system based on the separation into islands. October 2011.

- [83] A. E. Motter. Cascade control and defense in complex networks. *Phys. Rev. Lett.*, 93:098701–1–098701–4, 2004.
- [84] A. E. Motter and Y. C. Lai. Cascade-based attacks on complex networks. *Phys. Rev. E*, 66:065102, 2002.
- [85] A. E. Motter, T. Nishikawa, and Y. C. Lai. Range-based attacks on links in scale-free networks: Are long-range links responsible for the small-world phenomenon? *Phys. Rev. E*, 66:065103, 2002.
- [86] M. E. J. Newman. Fast algorithm for detecting community structure in networks. *Phys Rev E*, 69.
- [87] M. E. J. Newman. The structure and function of complex networks. *SIAM Rev.*, 45:167256, 2003.
- [88] M. E. J. Newman. A measure of betweenness centrality based on random walks. *Social Networks*, 27:39–54, 2005.
- [89] M. E. J. Newman. Modularity and community structure in networks. *PNAS*, 103:8577–8582, 2006.
- [90] M. E. J. Newman and M. Girvan. Finding and evaluating community structure in networks. *Physical Review E*, 69:026113, 2004.
- [91] BBC News. Fire cuts power to thousands of portsmouth homes.
- [92] BBC News. Melting in zanzibar’s blackout.
- [93] NERC Board of Trustees. Glossary of terms used in nerc reliability standards. North American Electric Reliability Corporation, 2013. http://www.nerc.com/files/glossary_of_terms.pdf.

- [94] T. J. Overbye, X. Cheng, and Y. Sun. A comparison of the ac and dc power flow models for lmp calculations. In *Proceedings of the 37th Hawaii International Conference on System Sciences*, pages 1–9, January 2004.
- [95] S. Pahwa, A. Hodges, C. Scoglio, and S. Wood. Topological analysis of the power grid and mitigation strategies against cascading failures. In *Proceedings of the 4th Annual International IEEE Systems Conference*, pages 272–276, April 2010.
- [96] S. Pahwa, C. Scoglio, and N. Schulz. Enhancing the robustness of power grid by network restructuring.
- [97] S. Pahwa, M. Youssef, P. Schumm, C. Scoglio, and N. Schulz. Optimal intentional islanding to enhance the robustness of power grid networks. *Physica A*, 392.
- [98] S. A. Pandit and R. E. Amritkar. Characterization and control of small-world networks. *Phys. Rev. E*, 60:R1119–22, 1999.
- [99] R. Parshani, S. V. Buldyrev, and S. Havlin. Interdependent networks: Reducing the coupling strength leads to a change from a first to second order percolation transition. *Physical Review Letters*, 105.
- [100] A. Peiravi and R. Ildarabadi. A fast algorithm for intentional islanding of power systems using the multilevel kernel k-means approach. *Journal of Applied Sciences*, 9.
- [101] A. Pinar, J. Meza, V. Donde, and B. Lesieutre. Optimization strategies for the vulnerability analysis of the electric power grid.
- [102] National Grid Company PLC. Investigation report into the loss of supply incident affecting parts of south london at 18:20 on thursday, 28 august 2003. National Grid Transco, 2003. http://www.g4jnt.com/Hams_Hall_Investigation_Report.pdf.
- [103] K. Purchala, L. Meeus, D. Van Dommelen, and R. Belmans. Usefulness of dc power

- flow for active power flow analysis. In *Proceedings of IEEE Power Engineering Society General Meeting*, pages 454–459, June 2005.
- [104] D. Zheng, J. Ma, Q. Zhao, K. Sun and Q. Lu. A study of system splitting strategies for island operation of power system: a two-phase method based on obdds. *IEEE T Power Syst*, 18:1556, 2003.
- [105] H. Ren, I. Dobson, and B. A. Carreras. Long-term effect of the n-1 criterion on cascading line outages in an evolving power transmission grid. *IEEE Transactions on Power Systems*, 23:1217–1225, 2008.
- [106] V. Rosato, S. Bologna, and F. Tiriticco. Topological properties of high-voltage electrical transmission networks. *Electr Pow Syst Res*, 77:99–105, 2007.
- [107] B. Rozel, R. Caire, N. Hadjsaid, and J-P. Rognon. Complex network theory and graph partitioning: Application to large interconnected networks. In *Proceedings of the IEEE Bucharest Power Tech Conference, Bucharest, Romania*, pages 1–6, June 2009.
- [108] M. Vrakopoulou, S. Koch, S. Chatzivasileiadis and G. Andersson. Mitigation of cascading failures by real-time controlled islanding and graceful load shedding. In *2010 IREP Symposium - Bulk Power System Dynamics and Control - VIII (IREP)*, pages 1–19, August 2010.
- [109] C. Scoglio, S. Pahwa, D. Weerasinghe and R. Miller. A complex networks approach for sizing and siting of distributed generators in the distribution system. September 2013.
- [110] M. L. Sachtjen, B. A. Carreras, and V. E. Lynch. Disturbances in a power transmission system. *Phys. Rev. E*, 61.

- [111] A. Scala, S. Pahwa, and C. Scoglio. Cascade failures from distributed generation in power grids. *Accepted for publication in International Journal of Critical Infrastructure*.
- [112] A. Scala, S. Pahwa, and C. Scoglio. Cascade failures from distributed generation in power grids, 2013. <http://arxiv.org/pdf/1209.3733v2.pdf>.
- [113] P. Schumm and C. Scoglio. Bloom: A stochastic growth-based fast method of community detection. *JoCS*, 3:356–366, 2012.
- [114] R. V. Sole, M. Rosas-Calas, B. Corominas-Murtra, and S. Valverde. Robustness of the european power grids under intentional attack. *Phys. Rev. E*, 77:026102–26109, 2008.
- [115] A. Swarankar, N. Gupta, and K. R. Niazi. Efficient reconfiguration of distribution systems using ant colony optimization adapted by graph theory. In *Proceedings of the IEEE Power and Energy Society General Meeting, Detroit, MI*, pages 1–8, July 2011.
- [116] C. Tautiva and A. Cadena. Optimal placement of distributed generation on distribution networks. In *Proceedings of the IEEE PES T&D Conference and Exposition, Bogota, Latin America*, pages 1–5, August 2008.
- [117] S. Tomranglak, S. H. Horowitz, A. G. Phadke, and J. S. Thorp. Anatomy of power system disturbances: Preventive relaying strategies. *IEEE Transactions on Power Delivery*, 11:708–715, 1996.
- [118] P. A. Trodden, W. A. Bukhsh, A. Grothey, and K. I. M. McKinnon. Milp formulation for controlled islanding of power networks. *International Journal of Electric Power and Energy Systems*, 45:501–508, 2013.
- [119] H. J. Herrmann V. H. P. Louzada, F. Daolio and M. Tomassini. Smart rewiring for network robustness, 2013. <http://arxiv.org/abs/1303.5269>.

- [120] Y.-C. Lai W.-X. Wang, X. Ni and C. Grebogi. Optimizing controllability of complex networks by minimum structural perturbations. *Phys. Rev. E*, 85:026115, 2012.
- [121] H. Wang and P. Van Meighem. Algebraic connectivity optimization via link addition. November 2008.
- [122] H. Wang and J. S. Thorp. Enhancing reliability of power protection systems economically in the post-restructuring era. In *Proceedings of the 32nd North American Power Symposium, Ontario, Canada*, page 2000, October 6-29-6-35.
- [123] W.-J. Wang and L.-L. Rong. Cascade-based attack vulnerability on the us power grid. *Safety Science*, 47:1332 – 1336, 2009.
- [124] W.-J. Wang and L.-L. Rong. Robustness of the western united states power grid under edge attack strategies due to cascading failures. *Safety Science*, 49:807 – 812, 2011.
- [125] X. Wang and V. Vittal. System islanding using minimal cutsets with minimal net flow. In *Proceedings of the IEEE PES Power Systems Conference and Exposition, New York City, NY*, pages 379–384 vol.1, October 204.
- [126] X. F. Wang and G. Chen. Synchronization in scale-free dynamical networks: Robustness and fragility. *IEEE Trans. Circ. Syst. I*, 49:54–62, 2002.
- [127] X. F. Wang and G. Chen. Synchronization in small world dynamical networks. *Int. J. Bifurcation Chaos*, 12:187–192, 2002.
- [128] Y. Wang, J. Zhao, F. Zhang, and B. Lei. Study of structural vulnerabilities of power grids based on the electrical distance. In *Proceedings of the IEEE PES Innovative Smart Grid Technologies - Asia, Tianjin, China*, pages 1–5, May 2012.
- [129] Z. Wang, A. Scoglione, and R. J. Thomas. Electrical centrality measures for electric power grid vulnerability analysis. In *Proceedings of the 49th IEEE Conference on Decision and Control, Atlanta, GA*, pages 5792–5797, December 2010.

- [130] I. Watson and Y. Comert. Istanbul blackout leaves millions in dark. CNN, 2012. <http://edition.cnn.com/2012/01/14/world/meast/turkey-blackout/>.
- [131] D. J. Watts and S. H. Strogatz. Collective dynamics of small world networks. *Nature*, 393.
- [132] H. L. Willis and W. G. Scott. *Distributed Power Generation - Planning and Evaluation*. CRC Press, 2000.
- [133] CNN World. Widespread power blackout hits chile.
- [134] D. Xu and A. A. Girgis. Optimal load shedding strategy in power systems with distributed generation. January 2001.
- [135] R. E. Kooij Y. Koc, M. Warnier and F. M. T. Brazier. An entropy-based metric to quantify the robustness of power grids against cascading failures. *Safety Science*, 59:126–134, 2013.
- [136] B. Yang, V. Vittal, and G. T. Heydt. Slow-coherency-based controlled islanding - a demonstration of the approach on the august 14, 2003 blackout scenario. *IEEE Transactions on Power Systems*, 21.
- [137] M. Youssef. *Measure of Robustness for Complex Networks*. PhD thesis, Kansas State University, 2012.
- [138] M. Youssef, C. Scoglio, and S. Pahwa. Robustness measure for power grids with respect to cascading failures. In *Proceedings of the International Workshop on Modeling, Analysis, and Control of Complex Networks, San Fransisco, CA*, pages 45–49, September 2011.
- [139] S. Zhao Z. Li J. Xu X. Li Z. Zhou, X. Bai and W. Zhao. A new islanding boundary searching approach based on slow coherency and graph theoretic. October 2008.

- [140] Y. Zhang and S. Chen. Complex networks theory based vulnerability analysis of power grid with distributed generation. January 2013.
- [141] R. D. Zimmerman, C.-E. Murillo-Sanchez, and R. J. Thomas. Matpower: Steady-state operations, planning, and analysis tools for power systems research and education. *IEEE Transactions on Power Systems*, 26:12–19, 2011.

Appendix A

Power Flow Models

Two different power flow models are widely used for power systems - the complete AC model and the simplified linearized DC model. Both the models are explained in detail below:

A.1 AC Power Flow Model

The AC power flow model comprises of the complete set of equations representing the non-linear dynamics of the power grid. Standard methods and algorithms such as Newton-Raphson method or Gauss-Seidel technique⁴⁹ are used to analyze the power grid using the AC power flow model. To find the power flowing through each link in the power grid, we first apply Kirchhoff's Current Law (KCL) at each node. We obtain a group of equations representing the relationship between the voltages and currents, which can be written in a matrix form as follows

$$\begin{bmatrix} \mathbf{Y}_{11} & \mathbf{Y}_{12} & \dots & \mathbf{Y}_{1N} \\ \mathbf{Y}_{21} & \mathbf{Y}_{22} & \dots & \mathbf{Y}_{2N} \\ \dots & \dots & \dots & \dots \\ \dots & \dots & \dots & \dots \\ \mathbf{Y}_{N1} & \dots & \mathbf{Y}_{N(N-1)} & \mathbf{Y}_{NN} \end{bmatrix} \begin{bmatrix} \mathbf{V}_1 \\ \mathbf{V}_2 \\ \cdot \\ \cdot \\ \mathbf{V}_N \end{bmatrix} = \begin{bmatrix} \mathbf{I}_1 \\ \mathbf{I}_2 \\ \cdot \\ \cdot \\ \mathbf{I}_N \end{bmatrix} \quad (\text{A.1})$$

Where I_k is the current that enters the node from the generator/load side. The first matrix is called the admittance matrix or the \mathbf{Y}_{bus} matrix. Each diagonal element \mathbf{Y}_{kk} equals the sum of the admittances of all branches connected to bus k . Every off-diagonal

element \mathbf{Y}_{jk} where $j \neq k$ is the sum of admittances of all branches between bus j and bus k multiplied by -1. Using Eq.(A.1), we obtain the following equation at node k

$$\mathbf{V}_1 \mathbf{Y}_{k1} + \mathbf{V}_2 \mathbf{Y}_{k2} + \cdots + \mathbf{V}_k \mathbf{Y}_{kk} + \cdots + \mathbf{V}_N \mathbf{Y}_{kN} = \mathbf{I}_k = \frac{P_k - jQ_k}{\mathbf{V}_k^*}. \quad (\text{A.2})$$

To find all unknown active power, reactive power, voltage magnitudes, voltage angles, different numerical techniques such as Gauss-Seidel or Newton-Raphson methods may be used.

The AC power flow model takes a longer time to converge and adds to the complexity of the islanding problem. Since the DC power flow model is linear, it does not add much to the complexity of the different islanding techniques we have discussed in this paper. Below we describe the fundamentals of the DC power flow model.

A.2 DC Power Flow Model

The DC power flow model represents a linearization of the full AC model. In the AC model, let V_i and V_j represent the voltage at the buses i and j , respectively. In addition, let Y_{ij} represent the admittance of the transmission line between buses i and j . the relation between real power, complex voltages and line impedance is expressed through the following equation which describes the amount of real power flowing through a transmission line

$$P_{ij} = |V_i||V_j||Y_{ij}|\cos(\delta_i - \delta_j + \theta_{ij}) \quad (\text{A.3})$$

where θ_{ij} is the phasor angle of the admittance Y_{ij} . To obtain the DC power flow model, the following assumptions are applied to Eq.(A.3) as follows

- Voltage angle differences are small, i.e. $\sin(\delta_{ij}) \approx \delta_{ij}$.
- Flat Voltage profile: All voltage magnitudes are considered to be 1 *p.u.*

- Line resistance is neglected since $R \ll X$.

Applying Taylor expansion on Eq.(A.3) around the operating voltage, and neglect the coupling between the power flow and the voltage, we obtain

$$P_{ij} = \frac{\delta_{ij}}{x_{ij}} \quad (\text{A.4})$$

where δ_{ij} is the difference in phase shift angle between the voltages at the sending and receiving buses, and x_{ij} is the reactance of the transmission line. The DC power flow equation (A.4) can be written in matrix form where P is the $N \times N$ matrix of power flows between each node i and j in the network, δ is the $N \times 1$ vector of phase angles and X is the $N \times N$ weighted adjacency matrix, each element of which represents the reactance of a transmission line. It is a real number if a line is present between two nodes, and 0 otherwise. In matrix form,

$$[P] = [b][\delta] \quad (\text{A.5})$$

The matrix $[b]$ represents the imaginary part of the Y_{bus} matrix of the power grid, where $b_{ij} = -\frac{1}{x_{ij}}$ and $b_{ii} = \sum_{i \in N} -b_{ij}$ for $i \neq j$. We usually assume that there is a reference node with voltage angle equals 0 (which is the same node as the slack generator, in the most general sense). The power handled by each node is the net sum of all the ingoing and outgoing power flows at that node as follows:

$$P_i = \sum_{j=1}^N P_{ij} = \sum_{j=1}^N (-b_{ij}\delta_{ij}) \quad (\text{A.6})$$

The total load at each node is given, while the phase angles are computed using the following equation:

$$[\delta] = [b]^{-1}[P] \quad (\text{A.7})$$

Appendix B

Optimal Islanding Algorithm

The optimal islanding scheme can be studied in detail at¹³⁷. This optimization formulation has two sets of constraints: Topological constraints to ensure proper physical implementation of the islanding scenario, and power flow constraints describing the DC power flow model, which directs the flow of power through the power grid network. The optimization formulation and the constraints are given and described in detail below:

B.1 Given:

Number of islands: n_{isl}

Island index: k

Power grid topology: G , island topology: g_k

The group of links that interconnects the island with its topological complement: l_k

Topological complement of the island: $T_k = G \setminus \{l_k \cup g_k\}$

Index that separates the two parts due to existence of an island: s ,

for eg: for island k , $s = 1$ denotes the island topology (g_k) and $s = 2$ denotes the island topological complement (T_k)

Number of nodes: N

Original load: $power_i$

B.2 Objective function:

$$\begin{aligned} \text{Minimize } & A \sum_{i=1}^{i=N} \sum_{k=1}^{k=n_{isl}} |power_i - d_i^k| \\ & + B \sum_{i=1}^{i=N} \sum_{j=1}^{j=N} \sum_{k=1}^{k=n_{isl}} \mu_{i,j}^{k,1} \end{aligned} \quad (\text{B.1})$$

B.3 To Find:

New load after islanding: d_i^k

Size of the island: μ

B.4 Constraints:

B.4.1 Topological constraints

$$\sum_{k=1}^{k=n_{isl}} \mu_{i,j}^{k,1} \leq a_{i,j} \quad \forall i, j = 1 \dots N \quad (\text{B.2})$$

$$\mu_{i,j}^{k,1} + \mu_{i,j}^{k,2} \leq 1 \quad \forall i, j = 1 \dots N, k = 1 \dots n_{isl} \quad (\text{B.3})$$

$$\sum_{i=1}^{i=N} \sum_{j=1}^{j=N} \mu_{i,j}^{k,s} \geq 4 \quad \forall k = 1 \dots n_{isl}, s = 1, 2 \quad (\text{B.4})$$

$$\sum_{j=1}^{j=N} (\mu_{i,j}^{k,1} + \mu_{i,j}^{k,2}) \geq 1 \quad \forall i = 1 \dots N, k = 1 \dots n_{isl} \quad (\text{B.5})$$

$$\sum_{k=1}^{k=n_{isl}} (\mu_{i,j}^{k,1} + \mu_{i,j}^{k,2}) \leq a_{i,j} n_{isl} \quad \forall i, j = 1 \dots N \quad (\text{B.6})$$

$$\sum_{j=1}^{j=N} \sum_{k=1}^{k=n_{isl}} \mu_{i,j}^{k,1} \geq 1 \quad \forall i = 1 \dots N \quad (\text{B.7})$$

$$\begin{aligned}
& \left(\sum_{j=1}^{j=N} (\mu_{i,j}^{k,1} + \mu_{j,i}^{k,1}) \geq 1 \right) \\
\Rightarrow & \left(\sum_{j=1}^{j=N} (\mu_{i,j}^{k,2} + \mu_{j,i}^{k,2}) = 0 \right) \quad \forall i = 1 \dots N, k = 1 \dots n_{isl} \tag{B.8}
\end{aligned}$$

$$\begin{aligned}
& \left(\sum_{j=1}^{j=N} (\mu_{i,j}^{k,2} + \mu_{j,i}^{k,2}) \geq 1 \right) \\
\Rightarrow & \left(\sum_{j=1}^{j=N} (\mu_{i,j}^{k,1} + \mu_{j,i}^{k,1}) = 0 \right) \quad \forall i = 1 \dots N, k = 1 \dots n_{isl} \tag{B.9}
\end{aligned}$$

$$\begin{aligned}
& \left(\sum_{j=1}^{j=N} \mu_{i,j}^{k,1} \geq 1 \right) \\
\Rightarrow & \left(\sum_{j=1}^{j=N} \sum_{k'=1, k' \neq k}^{k'=n_{isl}} \mu_{i,j}^{k',1} = 0 \right) \quad \forall i = 1 \dots N, k = 1 \dots n_{isl} \tag{B.10}
\end{aligned}$$

$$\mu_{i,j}^{k,s} = \mu_{j,i}^{k,s} \quad \forall i, j = 1 \dots N, k = 1 \dots n_{isl}, s = 1, 2 \tag{B.11}$$

$$\mu_{i,i}^{k,s} = 0 \quad \forall i = 1 \dots N, k = 1 \dots n_{isl}, s = 1, 2 \tag{B.12}$$

The group of inequalities in [B.2](#) - [B.12](#) describes the topological constraints for creating the islands.

Inequality [B.2](#) imposes that the decision variable $\mu_{i,j}^{k,1}$ can equal 1 only if the transmission line (i, j) exists in the power grid i.e. $a_{i,j} = 1$. In other words, if transmission line (i, j) does not exist in the power grid ($a_{i,j} = 0$), the decision variable $\mu_{i,j}^{k,1}$ equals 0 for all the islands $k = 1 \dots n_{isl}$. Also this inequality guarantees that the transmission line (i, j) can belong to at most one island $k, s = 1$.

In inequality [B.3](#), a transmission line (i, j) can either be a part of the island $\mu_{i,j}^{k,s=1} = 1$ or its complement $\mu_{i,j}^{k,s=2} = 1$, or an interconnecting line between two islands. In the latter case, the transmission line does not belong to any island and the decision variables $\mu_{i,j}^{k,s=1}$

and $\mu_{i,j}^{k,s=2}$ equal 0 for all k . This ensures that the interconnecting transmission lines do not carry power flow.

Inequality [B.4](#) ensures that the number of transmission lines in every island and its topological complement is at least 2. Notice that the transmission lines are undirected (even though the power flowing through the lines is directional). Hence the decision variables $\mu_{i,j}^{k,s}$ and $\mu_{j,i}^{k,s}$ are equal and the right-hand side of this inequality is 4.

Inequality [B.5](#) ensures that every node i in the power grid is assigned to either an island or to its topological complement and there is at least one transmission line that connects node i with another node that belongs to the same island component. In addition, in inequality [B.6](#), every line (i, j) can belong to an island or its topological complement, and it can belong to any combination of them at most n_{isl} times.

Inequality [B.7](#) guarantees that every node i is assigned to an island. In other words, for every node i , there is at least one transmission line (i, j) that connects node i with another node j in island $k, s = 1$. Notice that inequalities [B.7](#) and [B.6](#) together ensure that each node belongs to an island.

Constraints [B.8](#), [B.9](#) and [B.10](#) are formulated using the logical constraints. Each constraint has two parts, the conditional constraint (left-hand side), and the actual constraint (right-hand side). If the conditional constraint is true, the actual constraint is applied to the problem. As shown in constraint [B.8](#), if there is at least a transmission line that is connected to node i in island $k, s = 1$ imposing that node i belongs to island $k, s = 1$, it implies that there is no transmission line that is connected to node i in the topological complement $k, s = 2$ imposing that node i does not belong to the topological complement $k, s = 2$. Constraint [B.9](#) shows the case for the topological complement in the conditional constraint such that if there is at least one transmission line that is connected to node i in the topological complement $k, s = 2$, it implies that node i does not belong to island $k, s = 1$. Constraint [B.10](#) ensures that if node i has at least one transmission line in island $k, s = 1$, node i does not have any link in other islands $k' \neq k$. This constraint implies that node i can only

belong to one island $k, s = 1$ and it does not belong to other islands.

Inequality [B.11](#) says that the line is symmetric or $i - j$ is the same as $j - i$, and inequality [B.12](#) avoids self connecting nodes or self-loops.

B.4.2 Power flow model constraints

All the power flow calculations are based on the DC power flow model[?]. The DC model is linear and it does not add significantly to the complexity of the optimization formulation. The use of the DC model allows the optimization to easily converge for a few test cases in spite of its complexity. The DC model has been used in the recent works^{44,?} for islanding using MIP.

$$\delta_{generator(1)}^k = 0 \quad \forall k = 1 \dots n_{isl} \quad (\text{B.13})$$

$$\begin{aligned} & \left(\mu_{i,j}^{k,1} + \mu_{i,j}^{k,2} = 1 \right) \\ \Rightarrow & \left(|b_{i,j}(\delta_i^k - \delta_j^k)| \leq c_{i,j} \right) \quad \forall i, j = 1 \dots N, k = 1 \dots n_{isl} \end{aligned} \quad (\text{B.14})$$

$$d_{gen(g)}^k \leq 0 \quad \forall g = 1 \dots n_{gen}, k = 1 \dots n_{isl} \quad (\text{B.15})$$

$$d_{gen(g)}^k \geq 1.05 * power_{gen(g)} \quad \forall g = 1 \dots n_{gen}, k = 1 \dots n_{isl} \quad (\text{B.16})$$

$$d_{load(l)}^k \leq power_{load(l)} \quad \forall l = 1 \dots n_{loads}, k = 1 \dots n_{isl} \quad (\text{B.17})$$

$$d_{load(l)}^k \geq \alpha power_{load(l)} \quad \forall l = 1 \dots n_{loads}, k = 1 \dots n_{isl} \quad (\text{B.18})$$

The group of constraints [B.13 - B.18](#) represents the DC power flow model equations, the upper bounds, and the lower bounds of the generated power and loads. For DC power flow model, we assume that node 1 is the slack generator with voltage angle equals 0 as shown in equation [B.13](#). The logical constraint [B.14](#) indicates that whether a line (i, j) belongs

to an island or to the complement, the amount of power it can carry is always restricted by a finite capacity of the transmission line, given by $c_{i,j}$. The second part of this logical constraint is the main equation of the DC power flow model which computes the amount of power flowing through a link. Inequalities [B.15](#) and [B.16](#) represent the bounds on the amount of generated power from each generator $gen(g)$ for each island scheme k . Thus, the generation is made flexible so that any fluctuations in the load can be accounted for. The inequalities [B.17](#) and [B.18](#) represent the bounds on the delivered loads. We impose the lower bound on the delivered power at each node to be a fraction α of the total load, where α is a real number between 0 and 1. Thus, we allow load shedding in the network but at the same time a minimum fraction α of the load must be satisfied in each node.

In addition to the topological constraints and power flow model constraints, the author has used the network flow model⁶ to ensure that every island is a single component in which all buses are interconnected by transmission lines.

Appendix C

Algorithms for Modularity Based Islanding Methods - Modified Fast Greedy and Modified Bloom

The common objective of the two algorithms is stated below and the algorithms are described one after the other:

Objective:

$$J = \text{Minimize} \sum_{i=1}^N \sum_{k=1}^{n_{isl}} | \text{power}_i - d_i^k | \quad (\text{C.1})$$

Algorithm 1 Modified Fast Greedy algorithm for intentional islanding, adapted from⁸⁶ and³

Given: A power grid with N nodes, L transmission lines

n_{gen} is the number of generator nodes in the system

$n_{isl}(n'_{isl})$ is the required (current) number of islands

Initialize: $P \leftarrow$ A partitioning of N islands with 1 node in each

$n'_{isl} \leftarrow N$

$\Delta J \leftarrow$ The $N \times N$ benefit matrix for J by merging any pair of islands Isl_r and Isl_s

while ($n'_{isl} > n_{gen}$) **do**

Find Isl_r and Isl_s such that $\Delta J_{Isl_r, Isl_s}$ is the minimum element in the matrix ΔJ and they are not both generators

Merge islands Isl_r and Isl_s (This is the update for P)

$n'_{isl} \leftarrow n'_{isl} - 1$

Update $\Delta J_{n'_{isl} \times n'_{isl}}$ using the linear programming load shedding scheme for optimal load shedding

end while

Superislanding

while ($n_{isl} < n'_{isl}$) **do**

Find islands Isl_r and Isl_s from the n'_{isl} islands such that $\Delta J_{r,s}$ is the minimum element in the matrix ΔJ

Merge islands Isl_r and Isl_s (This is the update for P)

$n'_{isl} \leftarrow n'_{isl} - 1$

Update ΔJ using the linear programming load shedding scheme for optimal load shedding.

end while

Algorithm 2 Modified Bloom algorithm for intentional islanding, adapted from [113](#)

Given: A power grid with N nodes, L transmission lines
 n_{gen} is the number of generators nodes in the system
 $n_{isl}(n'_{isl})$ is the required (current) number of islands
Initialize: $P \leftarrow$ A partition of n_{gen} islands (these are the island seeds).
 $covered \leftarrow$ The set of n_{gen} seed nodes
 $uncovered \leftarrow$ The set of all nodes except the seed nodes
 $boundary \leftarrow$ The set of nodes $\in uncovered$ which are neighbors of the seeds
 $\Delta J \leftarrow$ The $N \times n_{gen}$ benefit matrix
while ($uncovered \neq \emptyset$) **do**
 Select node p and island Isl_k such that $p \in boundary$ and $\Delta J_{p, Isl_k}$ is minimal (for largest decrease in J)
 Copy any uncovered neighbors of p to $boundary$
 $boundary \leftarrow boundary \setminus \{p\}$
 $covered \leftarrow covered \cup \{p\}$,
 $uncovered \leftarrow uncovered \setminus \{p\}$
 Add p to island Isl_k (This is the update for P)
 Update ΔJ using the linear programming load shedding scheme for optimal load shedding
end while
Superislanding
while ($n_{isl} < n'_{isl}$) **do**
 Find islands Isl_r and Isl_s from the n_{gen} islands such that $\Delta J_{r,s}$ is the minimum element in the matrix ΔJ
 Merge islands Isl_r and Isl_s (This is the update for P)
 $n'_{isl} \leftarrow n'_{isl} - 1$
 Update ΔJ using the linear programming load shedding scheme for optimal load shedding.
end while
